This item was submitted to Loughborough's Research Repository by the author.
Items in Figshare are protected by copyright, with all rights reserved, unless otherwise indicated.

New formats for affinity selection of human cells

PLEASE CITE THE PUBLISHED VERSION

PUBLISHER

© Tina Sutar

PUBLISHER STATEMENT

This work is made available according to the conditions of the Creative Commons Attribution-NonCommercial-NoDerivatives 4.0 International (CC BY-NC-ND 4.0) licence. Full details of this licence are available at: https://creativecommons.org/licenses/by-nc-nd/4.0/

LICENCE

CC BY-NC-ND 4.0

REPOSITORY RECORD

Sutar, Tina. 2015. “New Formats for Affinity Selection of Human Cells”. figshare. https://hdl.handle.net/2134/17735.

NEW FORMATS FOR AFFINITY SELECTION OF HUMAN CELLS

by

Tina Šutar

June 2015

A Doctoral Thesis submitted in partial fulfilment of the requirements for the award of the degree of Doctor of Philosophy of Loughborough University

© Tina Šutar (2015)

Abstract

Despite recent advances in stem cell biology, immunotherapy and transplantation, substantial barriers still exist in the large-scale specific separation of a discrete population of human therapeutic cells from a cell suspension. The ideal purification technique should combine high cell purity, yield and function, with fast processing and affordability. Currently, fluorescence-activated cell sorting with flow cytometry (FACS) and magnetic activated cell sorting (MACS®) are the most used methods for cell separation and purification and have been employed extensively in molecular biology, diagnostic and cell sorting applications, because they are considered to be gentle, fast and scalable. However, these methods have several key disadvantages; they are invariably expensive, yield low log cell reduction (LCR) rates, and suffer from drawbacks when applied to niche cell populations, such as those requiring multiple tandem separation steps and/or involving combined positive and negative cell selection steps. To address this challenge, a new cell affinity selection system was developed. The selectivity is based on the reversible monomeric avidin – biotin interaction and it is primary designed for positive selection. The initial studies were performed on flat, nonporous, glass coverslips and the technology was then successfully transferred on high grade smooth non-porous glass beads (with a diameter of 79.12 to 118.59 μm). The multi-step 'layer-by-layer' deposition procedure culminating in dextran-coated supports bearing monomeric avidin was rigorously characterized and subsequently employed in packed bed chromatography experiments with human erythrocytes isolated from cord blood and B lymphocytes from cell lines. The developed affinity selection platform was highly selective, efficient and, most importantly, resulted in high yields, cell purity and viability comparable with MACS® technology. Additionally scale up is possible and could be easily transferred to another chromatographic matrix with the appropriate structure.

Key words: Affinity separation, human therapeutic cells, red blood cells, B lymphocytes, T lymphocytes, dextran, monomeric avidin, D- biotin, competitive displacement, glass coverslips, non-porous glass beads, MACS®

Acknowledgements

I would like to acknowledge and thank a number of people for the help and support that I received throughout my PhD.

Firstly to my supervisor, Dr Eirini Theodosiou, I am grateful for your guidance and support, which enabled me to get to the end of this PhD, while providing the constructive criticism which made this thesis what it is. I would like to say thank you as well to the Dr Aleš Podgornik, my industrial supervisor, who introduced me to the world of chromatography and always encouraged me to think critically and believe in myself. Thank you for everything.

I would like to thank COBIK, Centre of Excellence for Biosensors, Instrumentation and Process control (Solkan, Slovenia), and Loughborough University for providing the funding and support. Thank you for the offered opportunity to go and taste the research work and life abroad.

The Loughborough University technical staff, Dave, Rob, Monika, Kim, Sean and Tony, for helping me and sharing your knowledge and experience which helped my work run as smoothly as possible. I especially appreciate all the support from Dave in the Biolab. Thank you. A special mention also needs to go to Paul Izzard for all the discussions and IT support.

I am grateful to the Centre for Biological Engineering for allowing me to use the Guava flow cytometer and helping with the setup, method development and data analysis. In particular, I would like to recognise Dr Andy Picken, Dr Pete Mitchell and Kirstie Marrow.

Many thanks also go to Dr Nuno Reis and his group who helped me with the setup of confocal microscopy.

Miltenyi Biotech, UK subsidiary, for lending me LS magnet and stand. Special thanks go to Dr Aimee Tyler and Dr Susan Barton for their help with the MACS® technology.

To Dr Christine Müller, for the constant debates about my work and putting up with me for the past two years. Her endless support and contribution to this thesis were vital.

I want to acknowledge Claire Pretty, who is an amazing person and she was always there to give me advice and listen to me. Thank you for all the time you spent proofreading my thesis. I hope one day I will reciprocate the favour.

I am especially grateful to my friends for your encouragement along the way; I cannot express how much your support has meant to me. Thank you for being on hand for discussions both work-related and just to keep me sane. Thank you for your time and for all the great moments we spent together. There are too many of you to list individually, but thank you all. I will always keep you close to my heart.

Last but certainly not least I would like to mention my family, particularly my parents and sisters, who have been there for me no matter what.

Table of Contents

Abstract _______ i
Acknowledgements _______ ii
Table of Contents _______ iv
List of Figures _______ viii
List of Tables _______ x
List of Abbreviations _______ xi

1. INTRODUCTION _______ **1**

- **1.1 CELL THERAPHY** _______ **1**
  - 1.1.1 CELL SOURCES FOR CELL THERAPIES _______ 3
    - 1.1.1.1 Stem cells _______ 3
    - 1.1.1.2 Progenitor cells _______ 8
    - 1.1.1.3 Blood products _______ 9
- **1.2 DOWNSTREAM PROCESSING OF CELLS FOR CELL THERAPY** _______ **12**
  - 1.2.1 CELL SEPARATION TECHNIQUES _______ 13
    - 1.2.1.1 Physicochemical-based methods _______ 13
    - 1.2.1.2 Affinity-based methods _______ 15
    - 1.2.1.3 Label-free methods _______ 25
    - 1.2.1.4 Combined methods _______ 26
    - 1.2.1.5 Cell separation methods – current status and future trends _______ 28
- **1.3 CELL SEPARATION PROCESS DESIGN CONSIDERATIONS** _______ **35**
- **1.4 RESEARCH AIMS AND SCOPE** _______ **41**
- **1.5 STRUCTURE OF THESIS** _______ **42**
- **1.6 REFERENCES** _______ **44**

2. TAILORED SURFACES FOR AFFINITY SELECTION OF HUMAN THERAPEUTIC CELLS _______ **57**

- **2.1 INTRODUCTION** _______ **57**
- **2.2 MATERIALS AND METHODS** _______ **61**
  - 2.2.1 MATERIALS _______ 61
  - 2.2.2 METHODS _______ 63
    - 2.2.2.1 Surface modification _______ 63

2.2.2.2 Purification of anti-glycophorin A monoclonal antibody from cell culture supernatant 67
2.2.2.3 Biotinylation of antibodies 68
2.2.2.4 Surface functionalization 68
2.2.2.5 Cell culture 69
2.2.2.6 Isolation of red blood cells from umbilical cord blood 70
2.2.2.7 Cell labelling with antibody 71
2.2.2.8 Static binding studies 71
2.2.2.9 Flow-based assay 73
2.2.2.10 Analytical methods 75

2.3 RESULTS AND DISCUSSION 79

2.3.1 PREPARATION AND CHARACTERIZATION OF GLASS SUPPORTS 79
2.3.2 STATIC BINDING KINETIC TESTS 84
2.3.2.1 The impact of free biotin on cells 84
2.3.2.2 Kinetics of binding of biotinylated antibody to immobilized avidin 86
2.3.2.3 Binding capacities of functionalized glass surfaces 87
2.3.2.4 Kinetics of cell binding to functionalized glass surfaces 89
2.3.2.5 Kinetics of cell elution from functionalized glass surfaces 91
2.3.3 FLOW-BASED ASSAY 95

2.4 CONCLUDING REMARKS 98

2.5 REFERENCES 99

3. PREPARATION, CHARACTERIZATION AND APPLICATION OF NON-POROUS GLASS BEADS FOR THE POSITIVE SELECTION OF HUMAN RED BLOOD CELLS 103

3.1 INTRODUCTION 103

3.2 MATERIALS AND METHODS 105

3.2.1 MATERIALS 105
3.2.2 METHODS 107
3.2.2.1 Surface modification 107
3.2.2.2 Surface functionalization 107
3.2.2.3 Isolation of red blood cells from the umbilical cord blood 107
3.2.2.4 Labelling beads with biotinylated anti-glycopherin A antibody 107
3.2.2.5 Analytical methods 108
3.2.2.6 Affinity chromatography 110

3.3 RESULTS AND DISCUSSION ____ 113
3.3.1 PREPARATION AND CHARACTERIZATION OF GLASS BEADS ____ 113
3.3.2 APPLICATION OF PREPARED GASS BEADS IN AFFINITY CHROMATOGRAPHY ____ 120
3.4 CONCLUDING REMARKS ____ 131
3.5 REFERENCES ____ 132
4. APPLICATION OF GLASS BEAD CHROMATOGRAPHY FOR THE POSITIVE SELECTION OF HUMAN WHITE BLOOD CELLS ____ 136
4.1 INTRODUCTION ____ 136
4.2 MATERIALS AND METHODS ____ 138
4.2.1 MATERIALS ____ 138
4.2.2 METHODS ____ 139
4.2.2.1 Preparation of antibodies and cells ____ 139
4.2.2.2 Preparation of affinity support ____ 140
4.2.2.3 Coupling of biotinylated antibody to the beads ____ 140
4.2.2.4 Binding of biotinylated antibody to cells ____ 140
4.2.2.5 Affinity chromatography ____ 141
4.2.2.6 Immunophenotypic analysis of cells ____ 141
4.3 RESULTS AND DISCUSSION ____ 143
4.4 CONCLUDING REMARKS ____ 156
4.5 REFERENCES ____ 157
5. GLASS BEAD CHROMATOGRAPHY VERSUS MACS® MICROBEADS: A FIRST PRINCIPLE COMPARISON ____ 159
5.1 INTRODUCTION ____ 159
5.2 MATERIALS AND METHODS ____ 163
5.2.1 MATERIALS ____ 163
5.2.2 METHODS ____ 164
5.2.2.1 Preparation of affinity matrix ____ 164
5.2.2.2 Chromatography-based cell enrichments ____ 164
5.2.2.3 Immunophenotypic analysis of cell suspensions ____ 165
5.2.2.4 MACS® enrichment of selected cell populations ____ 165

5.3 RESULTS AND DISCUSSION 167

5.4 CONCLUDING REMARKS 173

5.5 REFERENCES 174

6. CONCLUSIONS AND FUTURE WORK RECOMMENDATIONS 177

6.1 CONCLUSIONS 177

6.2 FUTURE WORK RECOMMENDATIONS 179

6.2.1 THE SELECTION OF THE CHROMATOGRAPHIC SUPPORT 179
6.2.2 OPTIMIZATION OF THE SURFACE MODIFICATION AND FUNCTIONALIZATION 180
6.2.3 SCALE-UP 180
6.2.4 THE SELECTION OF AFFINITY LIGANDS 180
6.2.5 THE EVALUATION OF THE SELECTIVITY AND EFFICIENCY OF THE DEVELOPED AFFINITY METHOD WITH VARIOUS FEEDSTOCKS 181
6.2.6 ADDITIONAL ASSESSMENT OF CELLS AFTER COMPLETED SEPARATION 181
6.2.7 CLOSED SYSTEM SEPARATION 182

6.3 REFERENCES 183

7. APPENDICES 185

APPENDIX A: STANDARD CURVE FOR TNBS (PICRYLSULFONIC ACID) ASSAY 185

APPENDIX B: STANDARD CURVE FOR BCA (BICINCHONINIC ACID) PROTEIN ASSAY 186

APPENDIX C: STANDARD CURVE FOR THE DETERMINATION OF FREE BIOTIN 187

APPENDIX D: MEDICAL GRADE BOROSILICATE GLASS SPHERES “GL-0179” DATA SHEET 188

APPENDIX E: GLASS BEADS SIZE DISTRIBUTION – ANALYSIS REPORT 189

APPENDIX F: CERTIFICATE OF ANALYSIS FOR AVIDIN, EGG WHITE 190

APPENDIX G: PUBLICATIONS 191

List of Figures

Figure 1.1: Schematic view of haematopoiesis ______ 9
Figure 1.2: Direct and indirect immunoadsorption techniques ______ 20
Figure 1.3: Challenges associated with cell separation of cellular therapies ______ 36
Figure 1.4: Antibody structure and antibody fragments made by antibody engineering 39

Figure 2.1: Reaction scheme for the surface modification of aminosilane derived glass surfaces ______ 65
Figure 2.2: Two schematic representations of antibody coupling to glass surfaces ______ 69
Figure 2.3: Schematic representation of the flow based assay set up ______ 74
Figure 2.4: Immobilized forms of avidin on the surface of aldehyde-derived coverslips analysed by BCA assay ______ 81
Figure 2.5: Avidin egg white structure ______ 82
Figure 2.6: SEM analysis of non-modified and fully functionalized glass coverslis ______ 84
Figure 2.7: Adsorption of biotinylated BB7.2 antibody on glass coverslips, functionalized with tetrameric and monomeric avidin______ 87
Figure 2.8: Binding capacity for the binding of B lymphocytes to the glass coverslips for the biotinylated antibody bound to the cells and bound to the coverslips ______ 88
Figure 2.9: Kinetic static test of cell attachment______ 90
Figure 2.10: Cell detachment studies of Bristol-8 cell line (T-lymphocytes) bound to the glass coverslips through biotinylated BB7.2 antibody______ 92
Figure 2.11: Photographs of bound B lymphocytes (Toledo cell line) and red blood cells on glass coverslips during elution______ 94
Figure 2.12: Video frame sequences of B lymphocytes (Toledo cell line) flowing through mono-avidin coated glass hollow capillary tubes functionalised with the biotinylated anti-CD20 antibody ______ 96

Figure 3.1: Unmodified glass beads (300x magnification) ______ 116
Figure 3.2: Modified and functionalized bead under SEM microscope______ 117
Figure 3.3: Functionalized glass bead analysed by confocal microscopy ______ 117
Figure 3.4: Fluorescence intensity profile of analysed glass bead______ 118
Figure 3.5: 3D AFM images of 10 µm x 10 µm sections of glass bead surfaces ______ 119
Figure 3.6: Pressure drop on the packed column at various flow rates ______ 122
Figure 3.7: Photographs of column and collected fractions during affinity based separation of red blood cells______ 123
Figure 3.8: Chromatography of red blood cells elution flow path strategies______ 124
Figure 3.9: Interactions between red blood cells ______ 127

Figure 3.10: Impact of cell loading on subsequent elution ______________________ 128
Figure 3.11: Affinity chromatography of human red blood cells (4.5*10^6 cells injected) on antibody labelled monomeric avidin coated glass beads _______________________ 129

Figure 4.1: The impact of concentration of injected cell suspension on the binding efficiency (%) on the monomeric avidin packed bed column_____________________ 147
Figure 4.2: The impact of the number of specifically bound cells onto elution efficiency (%) from the monomeric avidin affinity support________________________________ 148
Figure 4.3: The impact of linear flow rate and contact time on the specifically bound cells (%) ____ 149
Figure 4.4: The impact of antibody concentration on the binding and elution efficiency of white blood cells to and from the affinity packed bed with immobilized monomeric avidin ____ 151
Figure 4.5: Affinity chromatography of human CD20 positive cells (challenge = 1x10^7 cells) labelled in advance with biotinlyated monoclonal antibody ________________ 153

Figure 5.1: Comparison of chromatography and MACS® column _______________ 167

Figure App. A: An example of standard curve for TNBS assay__________________ 185
Figure App. B: An example of standard curve for BCA assay___________________ 186
Figure App. C: An example of standard curve for the determination of free biotin in the experimental slurries____ 187

List of Tables

Table 1.1: Cell source considerations 2
Table 1.2: Potency of stem cells 4
Table 1.3: Differences between human adult and embryonic stem cells 8
Table 1.4: Some group-specific ligands and their specifies 19
Table 1.4: Cell separation techniques 29
Table 1.5: Commercially available devices for separation of human therapeutic cells 34

Table 2.1: Dissociation constants for the interactions between various forms of avidin and biotin 60
Table 2.2: Cells and antibodies used in experiments 63
Table 2.3: X-ray photoelectron spectroscopy survey of non-modified, amino- and aldehyde-derived glass coverslips 80
Table 2.4: Expression of CD20 cell surface marker and cell viability of a Toledo cell line after 2 h exposure to D-biotin and DSB-X biotin 85

Table 3.1: Elemental evaluation of surface modification of beads by XPS 114
Table 3.2: Summary of representative data of affinity chromatography of human red blood cells on antibody labelled monoavidin/dextran coated glass beads 126

Table 4.1: Overview of results obtained by challenging the monomeric avidin immobilized in a packed bed column with various number of cells 146
Table 4.2: Theoretical percentage of the occupancy of surface CD20 antigens on the single B lymphocyte from a peripheral blood of a healthy donor by various antibody concentrations 150
Table 4.3: The summary of the positive selection of B lymphocytes from Toledo cell line labelled with biotinylated antibody on the immobilized monomeric avidin in the packed bed column 151
Table 4.4: The overview of the flow cytometry results of injected sample and fractions collected during positive separation of CD20 positive cells on monomeric avidin packed bed column 154

Table 5.1: Comparison of glass bead chromatography and MACS® system for the separation of human B lymphocytes 168
Table 5.2: Evaluation of costs associated with affinity based chromatography and MACS® for the purification of 5 % target cells from the cell population, sufficient for one cell based therapy 171

List of Abbreviations

AFM	Atomic force microscopy
BCA assay	Bicinchoninic acid assay
BET theory	Brunauer, Emmett and Teller theory
B_{max}	Maximum number of adsorbed antibody/eluted cells
BSA	Bovine serum albumine
cGMP	Current good manufacturing practice
CH	Constant heavy chain of antibody
CL	Constant light chain of antibody
CLP	Common lymphoid progenitors
CMP	Common myeloid progenitors
CV	Column volume
EDTA	Ethylenediaminetetraacetic acid
Fab	Fragment antigen-binding
FACS	Fluorescence-activated cell sorting
FBS	Foetal bovine serum
Fc	Fragment crystallizable region of antibody
FDA	Food and Drug Agency
Fv	Variable fragment of antibody
GMP	Granulocyte macrophage precursors
HETP	Height equivalent to theoretical plate
IMAC	Immobilized metal affinity chromatography
IUPAC	International Union of Pure and Applied Chemistry

iPS	Induced pluripotent stem cells
k_A	Binding rate
k_D	Constant of dissociation
k_t	Time needed to reach a half of maximal binding
LCR	Log cell reduction
MACS®	Magnetic activated cell sorting
MEP	Megakaryocyte erythrocyte precursors
NK	Natural killer cells
PEG	Polyethylene glycol
scFv	Single chain Fv antibody region
SEM	Scanning electron microscopy
TCA assay	Trichloroacetic acid protein precipitation
TNBS assay	Picrylsulfonic acid assay
UFLMP	Unfrozen liquid microphase
UV	Ultraviolet light
VH	Variable heavy chain of antibody
VL	Variable light chain of antibody
v/v (%)	Volume/volume percentage
WHO	World Health Organization
XPS	X-ray photoelectron spectroscopy

1. INTRODUCTION

1.1 CELL THERAPHY

Cell therapy, a subtype of regenerative or reparative medicine, has the potential for treating diseases of tissue malformation, degeneration, trauma, and genetic deficiency (Daley, 2010). Every year millions of people suffer and die from serious and largely incurable degenerative diseases of the nervous system, for example Parkinson's disease, multiple sclerosis and strokes, the heart (*e.g*. myocardial infarction), the liver (*e.g*. hepatitis), the pancreas (*e.g*. diabetes) and other organs (McLaren, 2001). The aim of cell therapy is to replace, repair or enhance the biological function of damaged tissue or organs (Gage, 1998) using isolated and characterized stem or mature functional cells from different sources with or without the addition of gene therapy.

For cell therapies two different techniques may be used: i) includes the use of a scaffold and ii) a scaffold free approach. In scaffold-based cell therapies, scaffolds, made from different natural and synthetic materials, act as the extracellular matrix of native tissues and are designed to degrade and to be eventually replaced by regenerated tissues. On the other hand, the scaffold free approach does not require any support material. Scaffold free cell therapies can be implemented using three different methods: i) single cells injection therapy; ii) implantation of cell sheets; or iii) microtissues, cell aggregated gain structure and functionality of the native tissue (Demirbag *et al*., 2011).

The first evidence, that a specific, 'master', cell type might be responsible for reconstituting the bone marrow of people who had been exposed to lethal doses of radiation, was published in 1945 by (Hipp and Atala, 2008). Eleven years later, in 1956, bone marrow transplantation, the first cell-based therapy, was conducted (Thomas *et al.*, 1957). Most types of tissue damage or disease that disrupt cell function override the capacity of the mature body to self-repair.

In such cases, cell therapy could be employed, using cells that can provide the function that is required once they are transplanted back into the body (Gage, 1998).

The choice of the cell source depends on many factors, such as access to cells, their potency, cultivation parameters, and ability to multiply and manipulate cells. The number of cells needed for successful cell therapy is usually a limiting factor, at the same time, some cell types cannot self-renew under *in vitro* conditions (Table 1.1).

Table 1.1: Cell source considerations (adapted from Gage, 1998)

Cell source	Advantages	Disadvantages	Solution
Autologous (same organism)	Immunologically privileged No ethical issues	Limited supply Time constraints for donor and host	Cryopreservation Multiplication *in vitro*
Allogeneic (same species)	Greater supply Fewer time constraints on donor (rapidly gained)	Cellular immunity Ethical issues	Immunosuppress Encapsulation
Xenograft (different species)	Greater supply No time constraints on donor	Cellular and humoral immunity Possible transfer of new viruses across species	Immunosuppression Encapsulation Genetically masked immunity
Cell line (immortalized or tumorigenic)	Infinite supply No time constraints for donor or host Safety test and standardization simplified	Cellular and humoral immunity Tumorigenicity and neoplasia	Immunosuppression Encapsulation Genetically masked immunity

The quantity of cells necessary to achieve an optimal effect depends on application and cell source. For example, in clinical trials of transplantation of autologous mononuclear bone marrow cells, doses between 1 and $4*10^7$ cells were used for efficient treatment (Perin *et al*., 2003). In one of the more recent studies three doses of $2*10^6$ bone marrow mesenchymal stromal cells have been used to treat tissue damage caused after allogenic haematopoietic stem cell transplantation (Yin *et al*., 2014).

From immunogenic prospective, autologous cells (*i.e*. those that are collected directly from the patient) are the preferred option for cell therapy. But due to the ability to collect the cells in a time period that meets the needs of the patients, allogenic cells (*i.e*. those that are collected from the same species), are preferred. The first cells, which were employed successfully in the clinic for cell therapy, were autologous keratinocytes (Gallico *et al.*, 1984) and since then huge advances have been made.

According to the World Health Organisation (WHO) International Clinical Trials Registry Platform, more than 150 cell-based autologous and allogenic therapies are now in different phases of clinical trials.

1.1.1 CELL SOURCES FOR CELL THERAPIES

1.1.1.1 Stem cells

Stem cells are undifferentiated cells, with the ability to divide indefinitely in organism and with the potential to give rise to different cell types. When a stem cell divides asymmetrically, the daughter cells can either enter a path leading to the formation of differentiated specialized cells or self-renew to remain stem cells (Bongso and Richards, 2004). Stem cells are distinguished from other cell types by the following four characteristics:

- *Self-renewal*: stem cells are particularly immortal because of telomerase expression, which allows them to divide repeatedly;
- *Clonality*: a single cell has a capacity to create more stem cells because of asymmetrical cell division;
- *Potency*: capability to differentiate into at least one, and sometimes many, specialized cell types (Table 1.2);
- *Plasticity*: stem cells have the ability to differentiate into cell types from different germ layers (Melton and Cowan, 2004).

Table 1.2: Potency of stem cells (adapted from Stem cell basics, 2009)

Potency	Property
Totipotency	Having the unlimited ability to give rise to all the cell types of the body plus the entire cell types that make up extra-embryonic tissues, such as the placenta. Totipotent cells are found only in an embryo after the first few cell divisions. Once gastrulation begins, the cells are considered pluripotent.
Pluripotency	Having the ability to give rise to several types of all three embryonic germ layers (endoderm, mesoderm and ectoderm), but cannot make extra-embryonic tissues, such as the amnion, chorion, and other components of the placenta.
Multipotency	Having the ability to develop into more than one cell type of the body.

There are four classes of pluripotent stem cells: embryonic stem cells, embryonic germ cells, embryonic carcinoma cells and induced pluripotent stem cells (iPS) (Smith, 2001). The ability of pluripotent stem cells to give rise to a wide array of differentiated derivatives is the reason why they may prove to be extremely useful for cell-based therapy (Donovan and Gearhart, 2001). The discovery that bone marrow and purified haematopoietic stem cells can give rise to non-haematopoietic tissues, suggests that these cells may have greater differentiation potential than was previously assumed (Reya *et al.*, 2001).

Stem cells are present not only in embryos but also in many tissues of adult animals and are important in tissue repair and homeostasis (Donovan and Gearhart, 2001).

Mammalian stem cells are usually classified according to their tissue of origin (Bongso and Richards, 2004). The microenvironment, *i.e*. the region from which stem cells originate, is called a ‘niche’. This is a subset of tissue cells and extracellular substrates that can indefinitely house one or more stem cells and control their self-renewal and progeny production *in vivo* (Spradling *et al.*, 2001).

Some types of stem cells, such as bone marrow and skin, have already been used in cell therapies, and others are being effectively employed in trials for cardiac repair, neurological and immunological application and for a treatment of genetic blood disease (Trounson *et al.*, 2011). Combining stem cell therapy with pharmacological, surgical, and interventional treatment may increase therapeutic options in future (Perin *et al.*, 2003).

Embryonic stem cells are derived from the pluripotent inner cell mass of the pre-implantation, blastocyst-stage embryo (Evans and Kaufman, 1981; Martin, 1981). Outgrowth cultures of blastocysts give rise to different types of colonies of cells, some of which have undifferentiated phenotype (Donovan and Gearhart, 2001). The cells of the inner cell mass are destined to differentiate into tissues of the three primordial germ layers (ectoderm, mesoderm and endoderm) and finally form the complete soma of adult organism. In nature embryonic stem cells are ephemeral, *i.e*. present only at the earliest stages of development, and could be found only in the inner cell mass. However, the continuous *in vitro* subculture and expansion of an isolated inner cell mass on an embryonic human or murine fibroblast feeder layer leads to the development of an embryonic stem cell line (Bongso and Richards, 2004) that appears to be immortal (Donovan and Gearhart, 2001).

Cell types that eventually could develop into the various organs of the body can also be found in the foetus. Research with pluripotent fetal stem cells has been limited to only a few cell types (neural crest stem cells, fetal haematopoietic stem cells, fetal mesenchymal stem cells and pancreatic progenitors). Fetal blood, placenta and umbilical cord are rich sources of fetal haematopoietic stem cells (Bongso and Richards, 2004).

Embryonic stem cells could be the ideal resource for tissue engineering purposes because of their fundamental properties. However, their clinical application is limited because they represent an allogeneic resource and thus have the potential to evoke an immune response. New stem cell technologies, such as somatic cell nuclear transfer and reprogramming, promise to overcome this limitation (Hipp and Atala, 2008). Another disadvantage is pluripotency of undifferentiated embryonic stem cells, demonstrated by spontaneous formation of teratoma-like masses. Although these are classified as benign, the appearance in an anatomically sensitive (such as central nervous system and joint capsules) location could pose a considerable safety concern (Fink Jr., 2009). One study has shown that both, human embryonic stem cell and induced pluripotent stem cells, can induce the formation of teratomas. After subcutaneous or intratesticular injection of $1*10^6$ fully characterized undifferentiated cells in mice, at least 81 % of population developed teratoma within 2 months (Gutierrez-Aranda *et al*., 2010). Earlier Lee *et al*. (2009) reported that minimal number of human embryonic stem cells needed to form teratomas in intramyocardical area is $1*10^5$ cells and $1*10^4$ cells, when cells are injected in the skeletal muscles. A study before reported that even less cells (between 0.5 and $1*10^3$ cells) were sufficient enough to induce teratoma formation in subcutaneous dorsal regions (Cap *et al*., 2007)

Embryonic stem cells themselves cannot be used in cell therapy due to their characteristics, so are expanded *ex-vivo* in the culture, which could lead to spontaneous malignant transformation. Other concerns involve the ability of the embryonic stem cell to migrate from the implantation site and the biologic impact of non-target cellular impurities within the differentiated cell product (Fink Jr., 2009).

Although biological material can be donated, human embryonic stem cell research is ethically and politically controversial because it involves the destruction of embryos, which have the potential to grow into human beings if implanted in women’s uterus (Lo and Parham, 2009).

Adult stem cells, also known as somatic stem cells, can be found in diverse tissues and organs (Bongso and Richards, 2004). They are derived from so-called somatic cells that are no longer capable of making germ cells (Donovan and Gearhart, 2001). The fact that stem cells are also still present in postnatal vertebrates is evident from the observed continuation of tissue growth and differentiation, which is essentially an extension of the latter part of prenatal gestation in mammals (Marshak *et al*., 2001). Currently, we do not have a sufficient understanding of the developmental events that lead to organogenesis from the inner cell mass, to program the production of tissue- and organ-specific stem cells (Weissman, 2000).

Adult stem cells tend to be multipotent, tissue-specific, self-renewing populations of cells which can differentiate into cell types associated with the organ system in which they reside (Spradling *et al.*, 2001). Their isolation has proven quite problematic as they are rare, in the order of 1 in 10,000 cells, within the tissue of interest. Currently, it is known that niche of stem cells exist in many tissues, such as the bone marrow, the brain, the liver, the skin, the skeletal muscle, the gastrointestinal tract, the pancreas, the eye, the blood, and the dental pulp (Hipp and Atala, 2008). Furthermore, experimental results suggest that those adult stem cells are extremely resilient to changes in temperature, pH values, and exposure to toxic substances (Presnell *et al.*, 2002).

The most studied adult stem cells are the haematopoietic stem cells, which have been used widely in clinical settings for over 40 years and form the basis of bone marrow transplantation success (Bongso and Richards, 2004). Haematopoietic stem cells are present in the bone marrow and umbilical cord blood and also in smaller numbers in the blood stream (Gage, 1998). Mesenchymal stem cells are another well-characterized population of adult stem cells. It is thought that they respond to local injury by dividing to produce daughter cells that differentiate into multiple mesodermal tissue types and a variety of other connective tissues (Short *et al.*, 2003).

Adult stem cells were thought originally to have a limited potential for production of differentiated derivates, however later studies have questioned that view (*e.g.* neural stem cells can form blood-forming and muscle tissue (Bjornson *et al.*, 1999)). Such findings have had a significant impact on the debate over the derivation and use of pluripotent stem cells from embryos (Donovan and Gearhart, 2001).

In contrast to embryonic stem cells, isolated adult stem cells can be used for purposes of cell therapy and, at the same time further differentiated in *ex-vivo* culture.

The major differences between human adult and embryonic stem cells are summarised in Table 1.3.

Table 1.3: Differences between human adult and embryonic stem cells (adapted from Bongso and Richards, 2004)

Human adult stem cells	Human embryonic stem cells
Stem cells from organs are scarce and hard to access and purify	Once derived and propagated, stem cells exhibit prolific cell growth and are abundant
Multipotent; low plasticity	Pluripotent; versatile; high plasticity
Maintenance of normal genetic make-up *in vitro* conditions not known	Normal karyotype in late passages in 'cut and paste' protocol; changes in karyotype in late passage in high density bulk culture protocol
Telomerase levels low	Telomerase levels high and consistent; unlimited self-renewal
Shortening of chromosome length with ageing	No shortening of chromosome length with serial passaging
Early apoptosis	Late apoptosis
Customizing stem cells / differentiated tissues not possible	Possible via somatic cell nuclear transfer
No risk of teratoma induction after accidental transplantation	Risk of teratoma induction after transplantation if not purified
Epigenetic genomic changes difficult to reverse	Reversible
No ethical issues	Ethical issues limited to some countries and institutions
Applications: transplantation therapy	Applications: (1) transplantation therapy; (2) pharmaceutical screening; (3) gamete and embryo production; (4) studies on human development, congenital anomalies and infant cancers

1.1.1.2 Progenitor cells

Progenitor cells are the link between adult stem cells and differentiated cells. They have a tendency to differentiate into specific types, but, unlike stem cells, are usually unipotent, and sometimes oligopotent. Their capability to self-renew *in vitro* and *in vivo* is limited, and their growth is slow, probably because of their function in tissues and organs, which is to replace normal cell loss. Similar to stem cells, they have their niches and they can be mobile (Weissman *et al.*, 2001), and they are commonly equated with stem cells.

1.1.1.3 Blood products

The term ‘blood product’ refers to any therapeutic substance that is prepared from human blood. Blood can be separated into a variety of blood components for different clinical applications (McClelland, 2001). Blood cells are continuously produced throughout the human lifespan from rare pluripotent bone marrow stem cells, called haematopoietic stem cells, which are, like other stem cells, endowed with two characteristics: they give rise to additional stem cells during self-renewal and also undergo differentiation (through a process called haematopoiesis) to progenitor cells that become variously committed to different haematopoietic lineages (Orkin, 2001; see Figure 1.1).

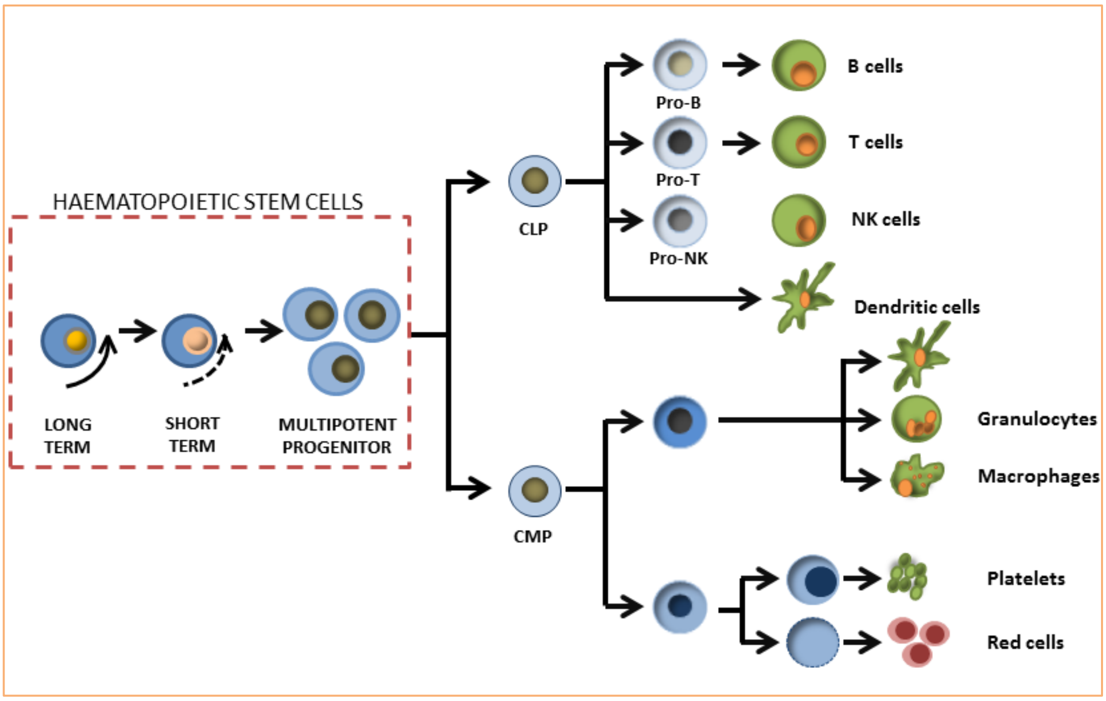
HAEMATOPOIETIC STEM CELLS
LONG TERM
SHORT TERM
MULTIPOTENT PROGENITOR
CLP
CMP
Pro-B
Pro-T
Pro-NK
B cells
T cells
NK cells
Dendritic cells
Granulocytes
Macrophages
Platelets
Red cells

Figure 1.1: Schematic view of haematopoiesis (redrawn from Reya *et al.*, 2001). Haematopoietic stem cells can be subdivided into long-term self-renewing stem cells, short term stem cells or multipotent progenitors. They give rise to common lymphoid progenitors (CLP), which are precursors of all lymphoid cells (B cells, T cells and natural killer (NK) cells); and common myeloid progenitors (CMP), which are precursors of granulocyte macrophage precursors (GMP) and megakaryocyte erythrocyte precursors (MEP). Dendritic cells, granulocytes and macrophages are derived from GMP and MEP give rise to platelets and red blood cells. Besides GMP, CLP as well give are precursors of dendritic cells.

Red blood cells (erythrocytes) are the most abundant cells in the blood. They are biconcave discs and their major component is haemoglobin, a globular protein, which transports oxygen. Red cells are produced in the bone marrow and usually lose their nuclei when they are released into the blood stream. Consequently, mature human red cells do not have a nucleus (Bain, 1996). Red blood cells transfusions are widely used for the treatment of anaemia, for around 40 % of patients' red blood cells transfusions are the only possible treatment (Malcovati, 2009).

White cells are made up of a nucleus and a cytoplasm. They are divided into granulocytes, also known as polymorphonuclear leucocytes, and mononuclear cells. There are three types of granulocytes (neutrophils, eosinophils and basophils) and two types of mononuclear cells (lymphocytes and monocytes). **Neutrophils** have a nucleus which is divided into two to five fragments or lobes. They are produced in the bone marrow and their major function is tissue phagocytosis. They move to the sites of infection or inflammation where they ingest, kill and break down bacteria. **Eosinophils** have a nucleus, which is usually bilobed, and in their cytoplasm they contain granules which take up the acidic dye eosin. Eosinophils are also produced in the bone marrow and are important for the body's defence against tissue parasites, being able to discharge their granule contents extracellularly. Eosinophils are also involved in allergic reactions. **Basophils** have a lobulated nucleus, often obscured by large granules. They are produced in the bone marrow, and play a major role in allergic and inflammatory responses in tissues. **Lymphocytes** are produced in the bone marrow and probably in the thymus. They are divided into three functional types: B cells, T cells and natural killer (NK) cells. B cells differentiate in tissues into plasma cells, which secrete antibodies, thereby providing humoral immunity. T cells function in cell-mediated immunity, as do NK cells. T cells also modulate B cell function. **Monocytes** have lobulated nuclei and voluminous cytoplasm, which may be vacuolated or contain granules. They differentiate in tissues into macrophages and are phagocytic. They also present antigen to lymphocytes. Monocytes differentiate also into Kupffer cells of the liver and microglial cells of the brain (Bain, 1996).

Lymphocytes, especially T cells, have been employed for the purposes of adoptive cell therapies, where cells are isolated, activated and expanded or genetically engineered in order to express chimeric antigen receptors or conventional alpha/beta cell receptors. After sufficient expansion, cells are injected into patients with cancer in an attempt to give their immune system the ability to overwhelm remaining tumour via T cells which can attack and kill cancer cells. Various adoptive cell therapies are currently in I/II stage of clinical trials (Wang and Rivière, 2015).

Platelets (thrombocytes) are cell fragments, produced in the bone marrow by fragmentation of megakaryocytes, large bone marrow cells. Platelets are smaller than red and white cells. They are a natural source of growth factors. They circulate in the blood and are involved in haemostasis, leading to the formation of blood clots. They are also involved in inflammation, phagocytosis and cytokine signalling (Bain, 1996).

1.2 DOWNSTREAM PROCESSING OF CELLS FOR CELL THERAPY

The number of cellular therapies for the treatment of a wide variety of diseases in the development and in the clinical trials is increasing intensively. One of the major challenges facing the translation of whole cell products into not only licensed therapies but further research, drug screening and pharmacological testing, is the development of efficient and scalable purification system. Current devices are expensive, with limited scale-up and they struggle to provide high resolution separations whilst ensuring sufficient cellular recovery (Weil and Veraitch, 2014). At the present, most regenerative treatments based on cell separation are restricted to tissues such as blood and bone marrow, but there is a potential for cell therapies based on cells derived from a variety of tissues, such as adipose tissue and intestine (Tomlinson *et al*., 2012).

The history of cell separation is long, dating back to the 1960s when first physical and biochemical differences between different cell types were identified, such as density and availability of selectable enzymes (Esser, 1998). In 1967, Plotz and Talal reported fractionation of splenic antibody-forming rat cells on glass bead columns. A year after, in 1968, first purification of human blood cells was published (Böyum, 1968). Separation is based on Ficoll – density gradient media. Later on, a tremendous number of methods were developed. Most of them are simple and reliable routine procedures; many have as well the advantage of requiring little equipment (Esser, 1998), therefore are still recognized and widely used as a pre-enrichment step in purification not only on laboratory scale, but as well on preparative scale.

For the purposes of cell therapy it is expected that a single dose for a treatment of a patient will consist of between 10^7 and 10^9 cells of high purity. Current requirement is less than 10^{-1} impurity cells per dose (Schriebl *et al*., 2010).

1.2.1 CELL SEPARATION TECHNIQUES

Nowadays, a large variety of cell separation techniques are commercially available and are predominately based of three methodologies: adherence, density and antibody binding. New procedures that utilise more than one cellular property are being developed and are mostly based on microfluidic technologies but are only available on an experimental scale (Tomlinson *et al*. 2012).

In general, cell separation techniques can be divided in four groups, namely methods based on (i) physicochemical properties; (ii) affinity; (iii) biophysical properties (label-free methods); or (iv) combination of at least two cellular properties.

1.2.1.1 Physicochemical-based methods

Physicochemical-based methods are in generally based on traditional methods such as centrifugation and membrane filtration. These label-free techniques are known by low resolution capacity and are therefore used as pre-enrichment step of very distinct cell types and/or for cell concentration (Diogo *et al*., 2014).

Apheresis is a medical procedure in which patient’s or donor’s whole blood is passed through a medical device and separated by centrifugation. Depending on the application, various processes are employed. For example, device can contain an additional column or filter to selectively remove plasma, plasma components, immuglobulins and/or certain type of cells. To isolate the buffy coat, the blood fraction containing white blood cells and platelets, additional saline washing steps are integrated in the device. At the end, final product is put back in the patient or collected and injected intravenously as a treatment (Schwartz *et al*., 2013).

Density gradient centrifugation is a single batch process. Two immiscible solutions with different densities, usually sucrose and a polymer, are combined. Cells are added on the top and then centrifuged to allow their distribution within the gradient. After centrifugation, cells with lower density will settle down at the interface (Diogo *et al*., 2012). Different polymer solutions are commercially available for this technique, such as Percoll, Ficoll, Lymphoprep and Dextran (Gonzáles-Gonzáles *et al*., 2011).

Density gradient centrifugation is an effective method for the enrichment of haematopoietic stem cells, usually resulting in a two- to five-fold increase. This enrichment is the result of the removal of denser and more mature cell types, such as red blood cells and granulocytes (Wognum *et al*., 2003).

Although it is believed that specify of this method is not large enough, this problem can be overcome by repeated centrifugation steps using different concentrations of working solutions combined with different velocities (Tomlinson *et al*., 2012). However, repeat centrifugation step can be a problem in itself with expected losses of 20-30 % in cell population with each centrifugation step (Lemarie *et al*., 2005).

Membrane filtration is an alternative physiochemical method for cell separation based on cell size and membrane pore size (Diogo *et al*., 2014). It is used for isolation of single cells from mechanically and often enzymatically treated tissues (Tomlinson *et al*., 2012). This technique is label-free, simple to use at relatively low cost, can be run continuously and with a possible scale-up. The biggest disadvantage is clumping (Diogo *et al*., 2014), causing cell loses. Polyurethane foaming membranes modified with carboxyl functional groups and coated with Pluronic F127 or hyaluronic acid have been used for the isolation of CD34+ cells from whole peripheral blood (Higuchi *et al*., 2006; Higuchi *et al*., 2008) and human adipose-derived stem cells (Wu *et al*., 2012).

Cell adhesion is a technique that utilises cellular adherence and is routinely used for the isolation of single cells from digested or explanted primary tissue. It is very simple and relatively cheap method, but is often time consuming and not specific, therefore, nowadays it is only used for applications where cell purity is not a concern and isolation of various cell populations is not required (Tomlinson *et al*., 2012). After cells of interest are bound, contaminant cells, which are usually present in suspension, are simply removed by medium exchange (Lennon and Caplan, 2006). Cell adhesion is usually the first step in the isolation of mesenchymal stem cells from bone marrow, umbilical cord blood or adipose tissue (Kern *et al*., 2006).

1.2.1.2 Affinity-based methods

Affinity-based cell separations relay on the interaction of cell surface-bound molecules and their complementary ligands (*e.g*. monoclonal antibodies, aptamers and lectins). The specificity and diversity of monoclonal antibodies offer enormous possibilities for immunoaffinity-based isolation of cells. Antibodies have been coupled to toxins to obtain selective cell killing, fluorochromes to allow fluorescent activated sorting, and various solid supports such as flasks, beads and magnetic particles to achieve selective cell adherence.

There are two types of cell selection, namely positive and negative. The former is isolation of a target cell population which is labelled with antibodies and then removed from the remaining unlabelled cells. In the latter, the unwanted cells are labelled with antibodies and then removed (Thomas *et al.*, 1999).

Fluorescent activated cell sorting (FACS) allows physical separation of fluorescent labelled sub-populations of target cells from a heterogeneous population and is one of the most widely used high-resolution techniques for purification of cells.

FACS was invented in the late 1960s with a purpose of flow cytometry and cell sorting of viable cells. After the discovery of hybridomas in 1975 and consequently continuous production of monoclonal antibodies, the pool of possible FACS applications has expanded (Herzenberg *et al*., 2002; Battula *et al*., 2009; Jiang *et al*., 2010).

Prior to the separation, cells are labelled with fluorescently-labelled monoclonal antibodies against specific surface antigen markers. When surface markers are absent, reporter construct can be inserted using vectors inside the cells to make fluorescent labels. The downside of this approach is regulatory concerns when genetically modified cells are used in clinical application (Diogo *et al*., 2014).

Sorter has three major components: fluidics, optics and electronics. After analysis and identification of the target population, cells in the liquid stream are separated into small droplets through the use of mechanical vibrations (Brown and Wittwer, 2000), followed by one of the existing sorting mechanism:

- *Mechanical sorting with a mechanical device referred to as 'catcher tube'*: If the cell is identified as a cell of interest, it is captured by the catcher tube and collected into a tube or into a concentration module; otherwise it is dispatched to the waste tank.
- *Electrostatic sorting*: The droplets containing a cell of interest are charged electrically. When a charged droplet passes through a high voltage electrostatic field between deflection plates, it is deflected and collected into the corresponding collection tube (Gasol, 2005).

FACS is a powerful, high-resolution, tool in biomedical research, but with very limited scale-up. However, the equipment is large, very expensive and requires skilled personnel to operate it (Diogo *et al*., 2012).

Magnetic activated cell sorting (MACS®) is a trademark name (Miltenyi Biotec, Bergisch Gladbach, Germany) for magnetic-based cell separation method. Prior to sorting, the cells are labelled with a monoclonal antibody, which is specific to a surface antigen. The antibodies are directly covalently labelled with magnetic particles. The cell suspension is then passed through a column containing a ferromagnetic matrix placed in a strong external magnetic field. The matrix creates a strong magnetic field gradient, which acts as a specific cell filter: magnetically labelled cells are retained on the column, while unlabelled cells flow through (Miltenyi *et al.*, 1990). After washing, the matrix and bound microbeads are demagnetized by removing the column from the magnetic field, and the retained cells are easily eluted without chemical or physical treatment. Both, the enriched and depleted fractions, are suitable for further use (Kantor *et al.*, 1998; Kastrinaki *et al*., 2008). For highly purified cells, the MACS® procedure needs to be repeated and combined with other methods, usually with flow cytometry (Miltenyi and Schmitz, 2000).

Due to the biological and optical inertness, colloidal super-paramagnetic particles ranging from 20 to 100 nm have become the gold standard for magnetic separations. Microbeads are always in suspension, therefore binding kinetics is fast. Due to their size, these particles do not saturate cell epitopes and therefore there is no need to be removed after completed separation (Grützkau and Radbruch, 2010). Microbeads are since recently available as well in column free form (EasySep™, Stem cell technologies, Vancouver, British Columbia, Canada).

Positive selection by EasySep™ is done by labelling with dextran-coated magnetic nanoparticles using bispecific anti-surface antigen-anti-dextran tetrameric complex. Tube containing cell suspension is then placed inside the magnet and unlabelled cells are removed by pouring out the supernatant. Tube is then removed from the magnet and cells of interest are ready to use after several washes with buffer (Wognum *et al*., 2003)

Miltenyi Biotec has launched autoMACS™ in recent years, a multimagnetic device that allows and parallel processing of samples and for clinical applications, and CliniMACS™, closed and sterile system for automated purifications on large scale ($1.2*10^{12}$ cells in total). Both systems are being widely used for enrichment of stem and progenitor cells from bone marrow, umbilical cord blood and mobilized peripheral blood (Diogo *et al*., 2014).

To achieve high purities using MACS® technology, separation step is often repeated and/or combined with other cell separation methods, such as density gradient centrifugation, FACS and selective killing with a specific antibody, conjugated with cytotoxic molecule (Diogo *et al*, 2014).

When compared to other separation methods, MACS® may present undesirable biological effects, due to the use of magnetic particles, which can interfere with cellular properties and further analysis, since cell’s optical properties can change. Overall, MACS® is easy to use, it is faster than FACS and provides with comparable purities and efficacies (Grützkau and Radbruch, 2010).

Since FDA approval of MACS® for clinical purposes, in particular the enrichment of CD34+ cells in neuroblastoma *ex-vivo* therapy, MACS® has been considered as the gold standard for stem cell isolation (Handgretinger *et al.*, 2002).

Affinity chromatography is an example of strong and specific binding, which is based on so called lock and key mechanism (Miller, 2005) and offers a huge potential in cell separation.

Chromatography is one of the most important separation methods and a part of a thermal separation procedure. According to IUPAC definition, chromatography is “a physical method of separation in which the components to be separated are distributed between two phases, one of which is stationary (stationary phase) while the other (the mobile phase) moves in a definite direction” (Ettre, 1993). Chromatographic-like separations are used in industry and research from the industrial revolution in the nineteenth century, but the real breakthrough occurred in 1931, when Lederer and co-workers separated lutein and zeaxanthine in carbon disulphide and the xanthophylls from egg yolk on a column of calcium carbonate powder (Braithwaite and Smith, 1996). Nowadays, chromatography is still the unit operation of choice for the majority of high value biotherapeutics, because it can achieve high purity, combined with flexibility of operation.

Affinity chromatography is “the particular variant of chromatography in which the unique biological specificity of the analyte and ligand interaction is utilized for the separation” (Ettre, 1993) and it is also known by the names biospecific interaction chromatography (BIC) and bioselective adsorption chromatography (BAC). It is used primary with biomolecules (antigens, enzymes, proteins, viruses and hormones) for two reasons: (i) establishment of strong and stable complexes between biomolecules and ligands; and (ii) highly complex media in case biomolecules are present (Miller, 2005). It provides an elegant method for the high yield purification in a single step under mild conditions of pH and ionic strength (Braithwaite and Smith, 1996).

For purposes of affinity chromatography, a ligand with a specific binding affinity is covalently bound to the support, usually a column. Components with a specific affinity for the ligand are bound and non-bound material goes straight through the support (Braithwaite and Smith, 1996).

Ligands can be classified into two types: (i) monospecific, which recognize only one species (*e.g.* monoclonal antibodies); and (ii) group-specific, which would bind a group of analytes (*e.g.* protein A) (Miller, 2005). Some ligands are listed below in the Table 1.4.

Table 1.4: Some group-specific ligands and their specifies (adapted from Miller, 2005)

Ligand	Specificity
Natural ligands	
Antigen	Antibody
Antibody	Antigen
Concanavalin A, lentil lectin, wheat germ lectin	Polysaccharides, glycoproteins, glycolipids
Soybean trypsin inhibitor, methyl esters of various amino acids, D-amino acids	Various proteases
Glutathione	Glutathione-binding proteins
Protein A and protein G	Many immunoglobulin classes and subclasses
DNA, RNA, nucleosides, nucleotides	Nucleases, polymerases, nucleic acids
Synthetic ligands	
Phenylboronic acid	Glycosylated haemoglobins, sugars, nucleic acids, and other *cis*-diol containing substances
Cibacron Blue F3G-A dye, derivatives of AMP, NADH, and NADPH	Certain dehydrogenases via binding at the nucleotide binding site
Amino acids: lysine, arginine	Proteases
Ni(II) (IMAC)	Histidine containing proteins / peptides
Fe(III), Ga(III) (IMAC)	Phosphorylated peptides
Molecular imprinted polymers	Non-biological analytes

The majority of affinity based separations are run in a batch elution or step-gradient mode, where a change in eluent composition causes the release of the bound compounds, which are washed off the column as a band and separated from the others.

Cell affinity chromatography relies on the interaction of cell surface-bound molecules and their complementary ligands (usually monoclonal antibodies). If a ligand is directly or indirectly covalently (Figure 1.2) bound to a chromatographic support and is accessible to the cells passing it, then cell surface molecules will bind to it and will be removed from the solution (Kumar *et al.*, 2003).

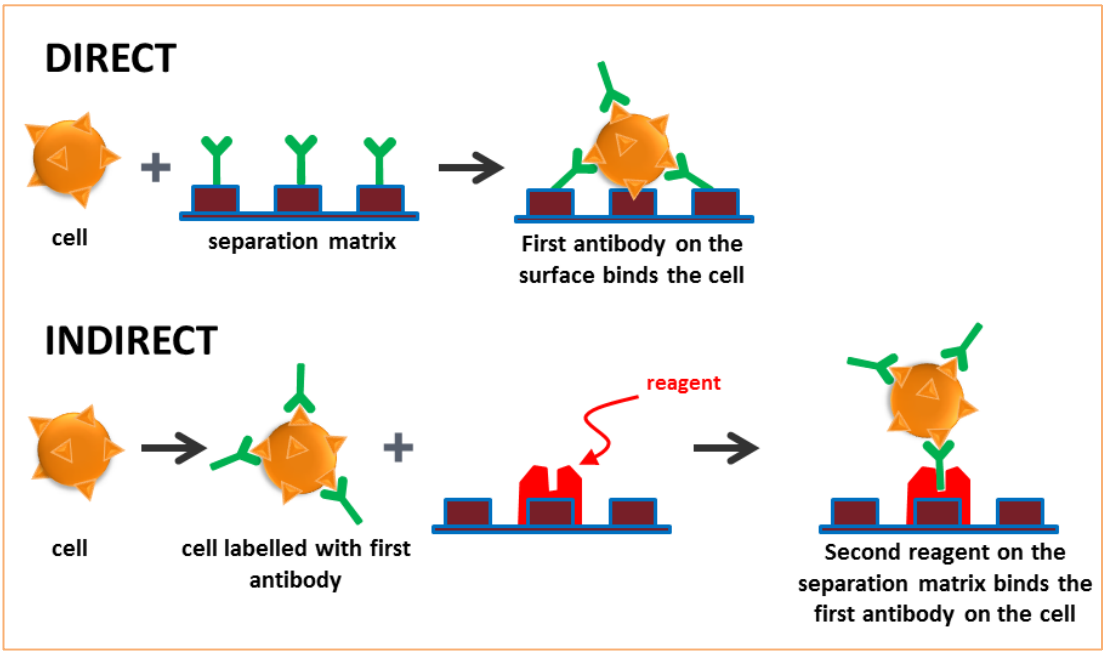
DIRECT
cell
separation matrix
First antibody on the surface binds the cell
INDIRECT
reagent
cell
cell labelled with first antibody
Second reagent on the separation matrix binds the first antibody on the cell

Figure 1.2: Direct and indirect immunoadsorption techniques (redrawn from Thomas *et al.*, 1999). With the direct technique the antibody is bound on the separation matrix, whilst in the indirect technique, the cells are labelled with antibodies which bind to a reagent on the matrix surface.

Historically, various chromatographic supports have been employed for cell separation. First attempts of packed bed chromatography for cell separation are dated back to the 1970s, when Plotz and Talal (1967) separated splenic antibody-forming cells from rats on glass bead columns. The glass beads were modified with agarose and then functionalized with polyclonal γ-globulin. Between 20 and 50 % of bound cells were eluted from the column in the viable form by buffer containing divalent cations and elution buffer enriched with EDTA.

In 1977, Kondorosi *et al.* published a comprehensive study of positive separation of rat T lymphocytes on columns packed with glass beads, polymethylmetaacrylic plastic beads and nylon wool. All materials were after surface activation functionalized with rat immunoglobulins or various proteins (bovine serum albumin, ribonuclease and lysozyme), followed by binding of rabbit anti-rat immunoglobulin and finally cells. Bound cells were then eluted in a batch by Eagle's MEM/Hepes medium supplemented with foetal bovine serum. Cells in eluted fractions were very pure (93 - 94 % purity) and with recovery between 86 and 89 %.

Besides on glass and polymethylmetaacrylic beads, packed bed chromatography of cells was demonstrated on large polyacrylamide beads (Truffa-Bachi and Wofsy, 1970) and Sephadex G-10 beads (Ly and Mishell, 1974). Although selectively of the last support can be questionable (Kanski *et al*., 1981). In the majority demonstrated methods represent positive selection of cells. Alongside gradient elution by change in mobile phase, mechanical agitation (Berenson *et al*., 1986; Thomas and Lansdorp, 1988), increased velocity (Thomas and Lansdorp, 1988), cleavage of antibody complexes (Thomas *et al*., 1989; Schlossman and Hudson, 1973) and just recently thermally mediated cell fractionation (Nagase *et al.*, 2012) were reported. Avidin coated Sephadex beads were even used for enrichment of CD34+ cells (Johnsen *et al*., 1999). In spite of this, packed bed chromatography is not widely used for cell separation due to high shear stress, long processing times, slow transport, based on diffusion, and high cost (Diogo *et al*., 2014), although there is a potential in beads as a separation matrix.

As an alternative to packed bed columns, expanded bed chromatography was proposed, since this technique is characterized by a high interparticular porosity, surface area and consequently lower shear forces. This makes it potentially an efficient and gentle affinity chromatography-based cell separation technique (Diogo *et al*., 2014). In the past this method was applied for negative and positive selection of monocytes from human peripheral blood on perfluorocarbon supports modified with avidin and functionalized with biotinylated monoclonal antibodies (Ujam *et al*., 2003).

Another alternative are monolithic connective chromatography supports, widely used for the purification of macromolecules, such as viruses, virus-like particles, plasmid DNA and cells. The transport of the target molecule through these supports is based on convection, which allows quick separation of molecules of large sizes rather than diffusion, which favours separation of small molecules. The result is high productivity and eradication of one of the basic problems connected with traditional chromatography, based on beaded porous particles, that of low diffusion rates and consequently high processing times (Jungbauer and Hahn, 2004).

Cryogels are macroporous and supermacroporous monoliths with highly interconnected pores made by polymerization in a partially frozen state where the ice crystals act as porogens (Lozinsky *et al.*, 2003). Cryogels were first reported in the late 70s, but the real breakthrough occurred in the late 90s, when their biotechnological and biological potential was recognized (Lozinsky, 2008).

For the cryogel preparation, a polymer reaction mixture, which contains gel-forming reagents, is frozen at temperatures a few degrees below the solvent crystallization point. Although the frozen system looks like a single solid block, it remains heterogeneous, because it contains so-called, unfrozen liquid microphase (UFLMP), where gel-forming reagents are concentrated. As UFLMP presents only a small portion of total initial reaction mixture, the concentration of gel precursors increases dramatically promoting the formation of gel. When crystals of frozen solvent are melted, macropores filled with solvent are left. The shape and pore diameter depends on the concentration of precursors and the regimes of cryogenic treatment (Lozinsky *et al*., 2003). Cryogels have low resistance to flow due its large interconnected pores. Another disadvantage is low binding capacity for proteins and small nanoparticles (Jungbauer and Hahn, 2004).

The primary application of supermacroporous cryogels was direct capture of proteins from crude feedstocks. Direct capture of recombinant lactate dehydrogenase expressed in *E. coli* was obtained by immobilized metal affinity chromatography (IMAC) of the His-tagged enzyme. Lactate dehydrogenase was then purified with drying at 70 °C, followed by rehydration (Jungbauer and Hahn, 2004).

Separation of cells started with bacteria and yeast separation using anion-exchange chromatography. The support allowed selective separation of yeast and *E. coli* cells using linear salt gradient (Jungbauer and Hahn, 2004).

Poly(vinyl alcohol) cryogels have been frequently used for cell immobilization, but in most cases the cryogel is the shape of beads and packed into the column housing. From the tissue engineering prospective, cryogels prepared from xanthan are used as scaffolds for fabrication of artificial organs. Xanthan cryogels are used as well in cell entrapment and food technology (Jungbauer and Hahn, 2004).

Amongst other applications, they have been employed in the separation of particular mammalian cell populations (B lymphocytes) using specific antibodies against differentially expressed cell surface targets (Dainiak *et al.*, 2007). Antibodies are immobilized through Protein A and cells have been recovered by two different approaches: treatment with a solution of secondary antibody with a higher affinity for the target cell or mechanical deformation of the cryogel matrix by compressing it to 50 % its original height. However, purification yields have been relatively low, only around 40 %, as 81 % of applied B lymphocytes were retained on the column, of which 70 % were eluted (70 % of cells in the elution fraction were B lymphocytes, 20 % were T lymphocytes and 10 % of unknown origin. Additionally, the capacity of the column was approximately $1.6*10^6$ cells which is below the desired cell number for the single therapeutic dose (Kumar and Srivastava, 2010).

As mentioned above, cryogels have been employed as well as scaffolds in tissue engineering. Cryogel scaffolds are reported to promote cellular adhesion and proliferation, which can be a downside when using cryogels as a matrix for affinity chromatography (Henderson *et al*., 2013).

Hollow fibres are another alternative to packed bed columns. They are often used when it is necessary to remove low molecular weight impurities from nanoparticles and cells. Hollow fibre modules consist of numerous semipermeable membrane tubes packed in a tailor-made housing.

Hollow fibre modules are routinely used for haemodialysis and can be a very attractive option for cell separation due to their low price, biocompatibility, production under cGMP conditions and large surface area for cell adsorption. A problem with this approach is the high level of non-specific cell attachment, which demands an additional round of enrichment (Nordon and Craig, 2007). Dissociation mechanisms for the disruption of bonds between antigen and antibody include reduction of disulphide bridges (Grimsley *et al.*, 1993), enzymatic proteolysis targeting specific peptide sequences (Nordon *et al.*, 1996; Nordon *et al.*, 1998; Civin, 1992; Sutherland *et al.*, 1992), and competitive binding using peptides (Tseng-Law *et al.*, 1995) or polyclonal antibodies (Rasmussen *et al.*, 1992).

The idea of using fibres for affinity fractionation of cells is not new. In the past cell fraction on nylon fibres was reported (Edelman *et al.*, 1971; Rutishauser and Edelman, 1972).

Aqueous two phased affinity systems is an alternative affinity separation method with possible scale-up under cGMP conditions. It is a liquid-liquid fractionation method used primary for the purification of biological products (Diogo *et al.*, 2014).

The affinity partitioning is usually performed by incubation of cell suspension with affinity ligand, usually monoclonal antibody. Afterwards it is mixed with polyethylene glycol (PEG) or its derivate and dextran. This solution can be additionally supplemented with salts to balance the electrostatic differences between phases and making the environment cell friendly. Cells of interest are partitioned in the top PEG phase, which can be easily collected and cells recovered by centrifugation and further analysed with flow cytometry (Sousa *et al.*, 2011).

Successful isolation of CD34+ cells from whole umbilical cord blood has been reported. Erythrocytes are partitioned in bottom phase, which consist of hydrophilic dextran. The purity and recovery of cells of interest in the top phase is dependent on initial antibody concentration. In total it is possible to achieve 42 % purity with more than 95 % yield (Sousa *et al.*, 2011).

1.2.1.3 Label-free methods

To reduce the cost of downstream processing of cells, tag-less methods have been introduced, where the separation is based on biophysical properties of cells.

Field flow fractionation can be used for gentle cell isolation on a laboratory scale. Separation is done in a capillary and it is based on laminar flow and field that it is applied to it. Based on physical characteristics, cells are distributed within the flow profile and therefore different fractions can be collected separately (González-González *et al.*, 2011).

The simplest variant of field flow fractionation is use of gravity field. Roda *et al.* (2009a; 2009b) have demonstrated isolation of mesenchymal stem cells from various sources and haematopoietic stem and progenitor cells from peripheral blood. Undifferentiated stem and progenitor cells have “more primitively” structure than differentiated cells and therefore separation can be done based on shape and cytoplasm-to-nucleus ratio (Diogo *et al.*, 2012).

Dielectrophoresis devices can be employed for the purposes of cell separation. Microchannels of the device are filled with buffer solution into which cell suspension is injected. When an electric field is generated, cells can be separated, moved or trapped. The cellular response is based on polarization between the suspending medium and intrinsic dielectrical properties of the cells, which depend on the cell density, size, physiology and differentiation state. Several cell enrichments have been reported so far, including enrichment of CD34+ cells and neural stem cells from various sources (Diogo *et al*., 2014).

1.2.1.4 Combined methods

Cell-rolling columns represent a novel system for continuous separation of stem cells with different surface marker expression levels by using the dynamic interaction of the cell surface and a solid surface. Cells are weakly adhering to a solid surface via multiple specific interactions between the cell surface maker molecules and the corresponding immobilized antibody. Separation depends on the hydrodynamic force and cells are slowly rolled on the solid surface of column (Yamaoka and Mahara, 2011).

Because the rolling speed is determined by the number of interactions between the cells and the ligands, the system works as a continuous-type cell separation column (Yamaoka and Mahara, 2011), and the rolling velocity is controlled by the ligand or cell surface receptor density (Eniolla *et al.*, 2003; Greenberg and Hammer, 2001; Greenberg *et al.*, 2000; Hammer and Apte, 1992; Hammer and Lauffenburger, 1987).

In nature, cell rolling is mainly observed in blood vessels as an inflammatory response of leukocytes (von Andrian *et al.*, 1991), and its mechanism is derived from the temporary interaction between the cell surface and the ligands. This principle would enable a labelling-free separation (Yamaoka and Mahara, 2011). Recently microfluidic device for cell sorting by deterministic cell rolling was presented, where the separation is based on the cell rolling and the expression of the surface markers. The separation was demonstrated with P-selectin as a specific ligand and two leukemic cell lines – one positive and another negative for the selected ligand (Choi *et al*., 2012).

Lab-on-chip methods operate on microfluidic scale using disposable closed devices and utilise a multitude of cellular characteristics for isolation of cells, predominantly are label-free. These techniques are mostly still in the experimental stage, but offer a great potential to improve cell separation not only for purposes of research, as well as for clinical applications, although at the moment, the biggest challenge is to improve sensibility – *i.e*. physicochemical and biophysical differences between cell types can often be minimal (Tomlinson *et al*., 2012). It was reported that integration with existing devices can improve the sensitivity (Weil and Veraitch, 2014), another options are affinity ligands (Diogo *et al*., 2014).

Lab-on-chip methods have several features important for smooth and stress-free separations of delicate cells, such as laminar flow and possible integration with existing systems (Diogo *et al*., 2014).

This approach for cell separation is relatively novel, but there have been already several studies of cell separation published, for example isolation of human embryonic stem cells (Diogo *et al*., 2014).

Panning is an immunoadsorption technique that utilises covalently bound affinity ligands to polystyrene cell culture flasks. Cells positive for the ligand are bound to the surface, while other cells can be easily removed by gentle washing. This technique has limited scale-up and usually purity and yield achieved are low, although it has been applied for isolation of CD34+ cells from bone marrow (Diogo *et al*., 2014).

PluriBeads have been recently put on the market as a separation technique based on size and affinity. At first, beads (standard diameter 100 µm) with immobilized antibodies are added to the cells. After completed incubation, suspension is sieved through a mesh. To increase purity, sieves are gently rinsed with buffer. After washing, sieve is transferred to a new centrifuge tube and flow is stopped with a Luer-lock adapter. Cells are then shortly incubated in detachment buffer. After an adapter is removed, cells are collected in the tube and beads maintain on the sieve. It is possible to isolate two or more cell types at the same time using a cascade of beads and complementary sieves (Heinrich and Heinrich, 2012; Pierzchalski *et al*., 2013).

This technique is still on the experimental scale and has been so far used for the isolation of CD4+ and CD8+ cells from human blood and offers yields and purities similar to MACS® (Pierzchalski *et al*., 2013).

1.2.1.5 Cell separation methods – current status and future trends

At the moment, apheresis is still the gold standard for blood derived therapies, but separation of stem, progenitor and tissue specific cells is in the majority based on the expression of membrane antigens (Weil and Veraitch, 2014).

Currently the two technologies routinely used for cell separation and purification are FACS and MACS®. As mentioned above, both are based on expression of one or two cell surface antigens, but there is a number of potential disadvantages associated with their scale-up: (i) they require multiple separation steps, (ii) they involve combined positive and negative cell separation, (iii) cells may be sensitive to components used, and (iv) cells may suffer from undesirable biological effects from the cross-linking of the selection marker. Besides FACS and MACS® there are few cell separation alternatives, the most promising being methods based on chromatography, such as hollow fibre membranes and cryogels.

Chromatography is still the unit operation of choice for the majority of high value biotherapeutics, because it can achieve high purity, combined with flexibility of operation. Therefore it offers a huge potential in cell purification and separation. Preparative chromatographic cell separation can provide a highly purified population of a specific cell type suitable for diagnostic, biotechnological and biomedical applications (Kumar and Srivastava, 2010).

The current methods used for applied cell separation are summarized in Table 1.5.

Table 1.4: Cell separation techniques

	Cell separation technique	Principle	Example	Advantages	Limitations
Physicochemical-based methods	**Apheresis** 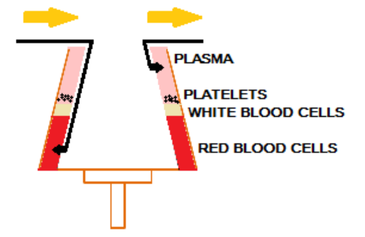 	Size, density	Continuous isolation of buffy coat (white blood cells, platelets) from whole blood (Schwartz *et al*., 2013)	Labelling not required Easy and technically feasible Continuous process Short process time Cheap Closed system	Low resolution and purity Crude separation
	Density gradient centrifugation 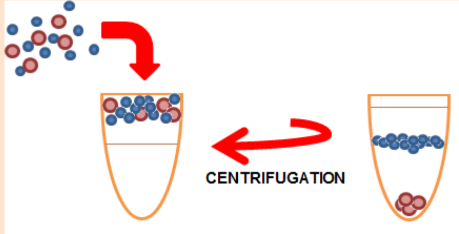 	Density	Enrichment of mononuclear cells from human cord blood with Ficoll-Paque solution (Jaatinen and Laine, 2007)	Labelling not required Easy and technically feasible Short process time	Low resolution and purity Limited scale-up
	Membrane filtration 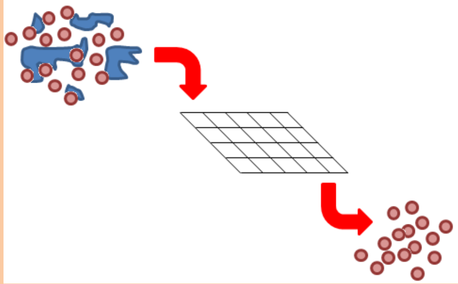	Size	Single cell isolation from dissociated primary tissue (Tomlinson *et al*., 2012)	Fast and simple Labelling not required Continuous process Closed, disposable systems Possible scale-up	Low selectivity Clumping

	Cell adhesion 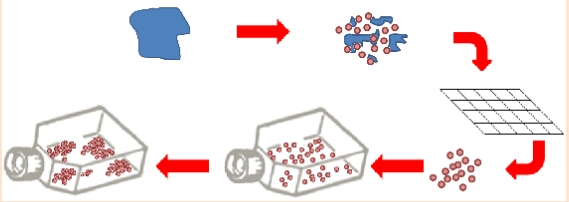	Adhesion properties	Isolation of human mesenchymal stem cells from bone marrow (Lennon and Caplan, 2006)	Simple and relatively cheap Labelling not required Possible scale-up	Low resolution and purity Limited scale-up Time consuming
Immunoaffinity-based methods	**Fluorescence activated cell sorting (FACS)** 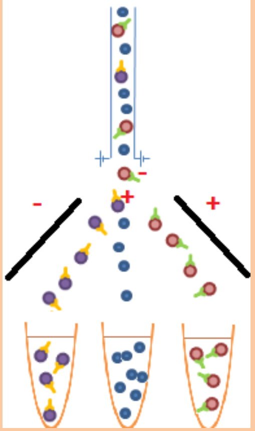 	Expression of surface markers, size	Isolation of CD34+ cells from cord blood (Brown and Wittwer, 2000)	High resolution High purity Fast Multiparametric	Cost Limited scale-up Requires trained personnel Labelling required, antibody stays on cell after sorting Low yields Shear stress
	Magnetic activated cell sorting (MACS$^{®}$) 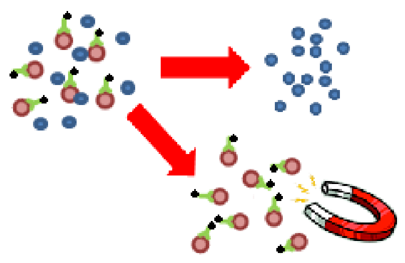	Expression of surface markers	Isolation and transplantation of CD34+ peripheral autologous progenitor cells (Handgretinger *et al.*, 2002)	Fast High purity when separation step repeated / combined with other methods Automated Closed system	Cost Labelling required, antibody stays on cell after sorting Lower selectivity than FACS Shear stress Low yields

	Affinity chromatography 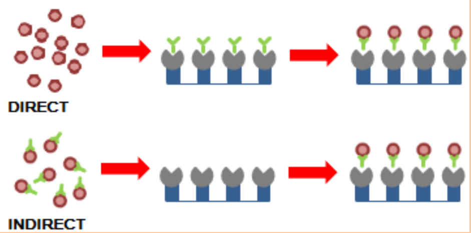	Expression of surface markers	Isolation of CD34+ cells from cord blood using cryogels (Kumar and Srivastava, 2010)	Fast Scale-up Highly selective	Cost Labelling required, antibody can stay on cell after sorting Shear stress
	Aqueous two-phase systems 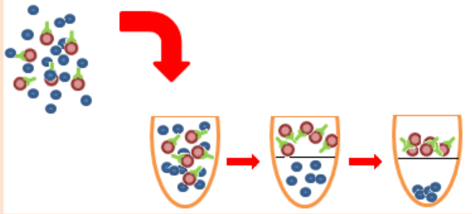	Expression of surface markers	Isolation of CD34+ cells from umbilical cord blood (Sousa *et al.*, 2011)	Scale-up	Low selectivity Labelling required, antibody can stay on cell after sorting
Label-free methods	**Field flow fractionation** 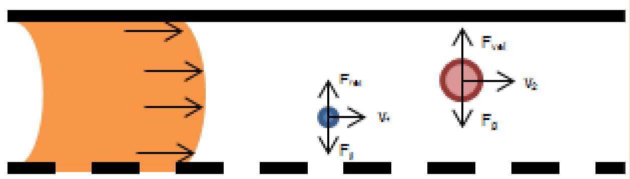	Cellular biophysical properties	Isolation of haematopoietic stem and progenitor cells from peripheral blood (Roda *et al.*, 2009b)	Label-free Cost	Low throughput Low selectivity
	Dielectrophoresis 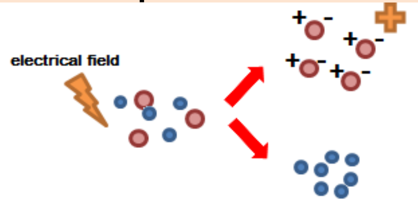	Cellular biophysical properties	Isolation of CD34+ cells from peripheral blood and bone marrow (Talary *et al.*, 1995)	Label-free Cost	Low throughput Low selectivity

Combined methods	**Cell-rolling columns** 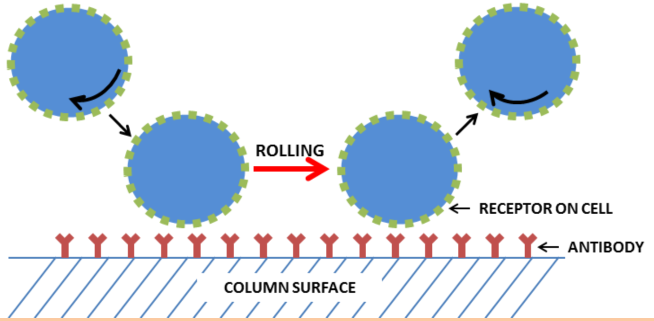 	Cell rolling, hydrophoresis	Isolation of CD34+ cells from bone marrow (Yamaoka and Mahara, 2011)	Fast Scale-up Highly selective	Labelling required, antibody can stay on cell after sorting
	Lab-on-chip devices 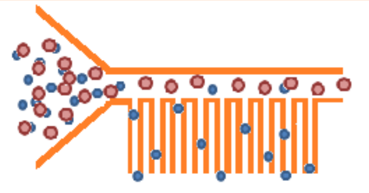	Various	Isolation of circulating tumour cells from whole blood (Nagrath *et al*., 2007)	Laminar flow Automation and integration in existing systems	Low throughput Scale-up
	Panning 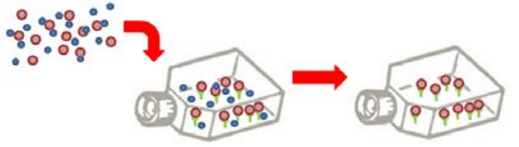	Adhesion properties, expression of surface markers	Isolation of CD34+ cells from bone marrow (Cardoso *et al*., 1995)	Simple	Time consuming Scale-up Low resolution and purity
	pluriBeads 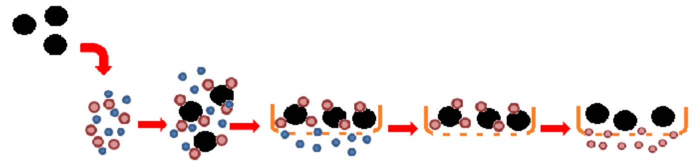	Size, expression of surface markers	Isolation of CD4+ and CD8+ cells from human blood (Pierzchalski *et al*., 2013)	Simple Fast High resolution and purity Cells do not maintain labelled	Scale-up Labelling required

Despite very few problems encountered during lab scale cell isolation, substantial barriers still exist to the efficient commercial scale preparation of large amounts of highly purified target cell populations. Commercially available cell separation devices at the moment are not generic – usually are dependent on the method of separation and cell type isolated (Weil and Veraitch, 2014). Table 1.5 summarizes the characteristics of separation devices currently being applied for purposes of cell therapies.

Table 1.5: Commercially available devices for separation of human therapeutic cells (adapted from Weil and Veraitch, 2014).

Device	Manufacturer	Method of separation	Targeted cell type	Processing time	Purity (%)	Viability (%)	Process yield (%)
Isolex® 300(i)	Baxter	Magnetic activated cell sorting	CD34+ cells	2-3 hours	90	At least 92	25-51
CliniMACS®	Miltenyi Biotec	Magnetic activated cell sorting	Haematopoietic progenitors; mesenchymal stromal cells; T-cells; dendritic cells	2.5-3 hours	78-99	78-99	15.7-43.4
CEPRATE® SC	CellPro	Continuous flow immunoadsorption	Autologous CD34+ cells	Less than 1 hour	72	36.6	41.4
Sepax®	Biosafe	Density gradient base separation	Mononuclear cells from bone marrow	35 minutes	N/D	80.5	83
CELLector™ flask	Applied Immune Science	Antibody panning selection	Various cell types	2-3 hours	32.5	15.1	17
SmartPReP 2 BMAC™	Harvest Technologies Corporation	Centrifugation	Autologous stem cells from bone marrow	Less than 15 minutes	N/D	N/D	74.6
COBE® 2991 Cell processor	CaridianBTC	Centrifugation	Autologous stem cells from bone marrow	14-28 minutes	85-90	98	47
Elutra® Cell separation system	CaridianBTC	Counter-flow elutriation	Monocyte enrichment of apheresis products	1 hour	13.6-79.5	93.8	79-100
Celution® 800/CRS	Cytori	Real-time cell processing	Adipose-derived cells	1-3 hours	60	89.2	N/D
FACSCalibur™ flow cytometer	Becton Dickinson Biosciences	Fluorescence activated cell sorting	Various cell types	2-4 hours	73.6	15.5	39.2

1.3 CELL SEPARATION PROCESS DESIGN CONSIDERATIONS

Cell separation involves the physical removal or selective killing of target cells from a mixed cell population and it is a multistep procedure. For example, gradient density centrifugation is often employed as a pre-enrichment step followed by an antibody-mediated technique (Thomas *et al.*, 1999).

Several criteria should be taken into account during set-up of separation process. The most important are the final application of the cellular product, the cellular properties, the resolution capabilities required and the scalability of the process (Diogo *et al.*, 2012).

No matter which approach is used for cell separation there is a need to evaluate efficiency by calculating cell purity, recovery and viability. **Purity** relates to the enrichment of population of interest based on known factors, such as cell surface phenotype, which are associated with target cell population. Cells are complex and therefore it is usually necessary to assess the expression of more than one marker to confirm their purity. **Recovery** is the percentage of cells, target and/or total cell population, obtained post enrichment and compared to the number of cells in origin population. In conjunction with purity, gives the information on the efficiency of the cell separation. **Viability** is one of the indicators of cell quality after separation. This parameter determinates if the depleted cell population of interest is fit for the further use (Tomlinson *et al*., 2012).

Initial planning and design is the most important step in process set-up with detailed understanding of cells of interest, their origin and function. Due to the complexity of the separation process, current methods generally offer a balance between purity and recovery (Tomlinson *et al*., 2012).

Challenges associated with the cell purification can be divided into three parts, namely (i) biological challenges; (ii) processing challenges; and (iii) engineering challenges (Weil and Veraitch, 2014) and are summarized in a schematic below (Figure 1.3).

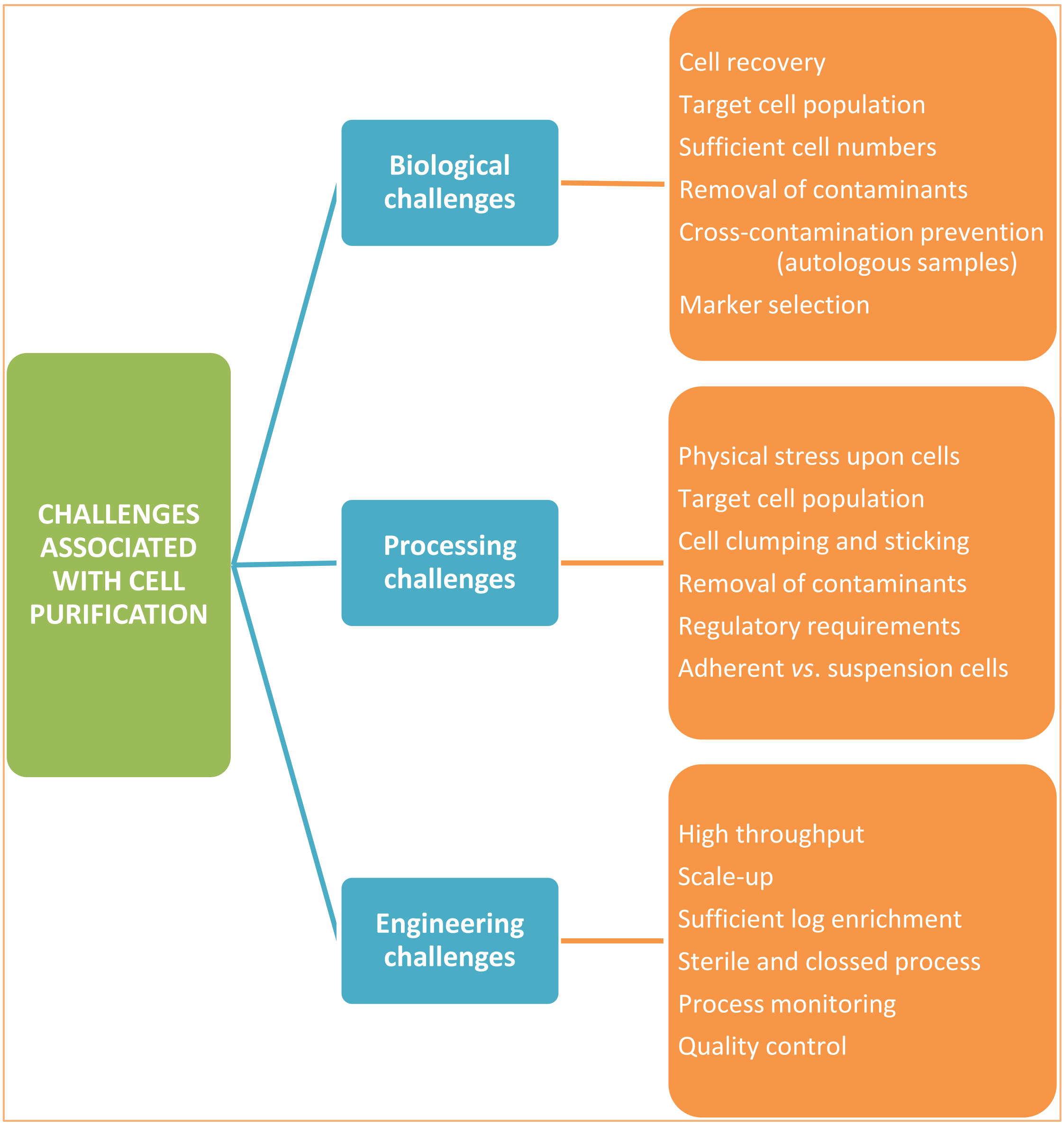
CHALLENGES ASSOCIATED WITH CELL PURIFICATION
Biological challenges
Processing challenges
Engineering challenges
Cell recovery
Target cell population
Sufficient cell numbers
Removal of contaminants
Cross-contamination prevention (autologous samples)
Marker selection
Physical stress upon cells
Target cell population
Cell clumping and sticking
Removal of contaminants
Regulatory requirements
Adherent vs. suspension cells
High throughput
Scale-up
Sufficient log enrichment
Sterile and clossed process
Process monitoring
Quality control

Figure 1.3: Challenges associated with cell separation of cellular therapies (adapted from Weil and Veraitch, 2014).

Cells are living material which requires separation process to be handled in a sterile and closed environment to maintain sterility and prevent contamination, while operating in a cell-friendly environment to maintain their viability and function (Tomlinson *et al*., 2012). When cells are exposed to a new material they undergo common conformational changes, *e.g*. changes in membrane structure, and clustering. Interactions between cell and surface can lead to changes in carbon-based molecules, so those molecules are chemically and morphologically altered and the result is conformational changes of membrane proteins. At the same time biological systems are extremely complex and usually can only function normally in aqueous media, and many important biological processes occur at relatively deeply buried interfaces, between different layers (Castner and Ratner, 2002).

“Cell-friendly” materials are so called biomaterials. They may be defined as materials which are designed to be in contact and interact with tissue, blood, cells, proteins and any other living component (Xue-Jun, 2005). Whilst in contact with cells, biomaterials should be chemically and mechanically stable, biocompatible and not induce non-specific cell attachment. The latter is currently considered as one of the biggest problems in cell separation using chromatography approach (Kumar and Srivastava, 2010). Non-specific cell surface interactions may be avoided or decreased with the use of soft materials and studies have shown that softness and elasticity of the surface are important parameters for cell-surface interactions (Dainiak *et al.*, 2006). Alternatively, decreasing the temperature has been proven to decrease non-specific binding.

Purity and process efficiency are vital due to usually low cell target numbers and cost. Cell clumping and sticking is often caused by incomplete dissociation of tissue, coagulation when blood is used and/or dead cells present in the population (Tomlinson *et al*., 2012).

Successful results obtained in clinical trials requiring stem cells have opened a niche for methods with possible scale-up to overcome the bottleneck in demand for purified stem cells (Gonzáles-Gonzáles *et al.*, 2011). Scale-up is not always possible; therefore it is important to initially choose the design which will allow high throughput separations not only on laboratory scale, but as well on the preparative scale.

One of the major biological challenges represents contaminants removal. Besides removal of unwanted cell population and cell debris, processing contaminants (growth factors, cryopreservatives, enzymes and serum) and external risks (endotoxins, bacterial, viral, fungal or parasitic infection) must be removed and assessed (Weil and Veraitch, 2014).

When separation is affinity-based, ligand selection is important step in method set-up. Monoclonal antibodies or antibody fragments are the most appropriate and commonly used ligands for effective affinity fractionation of cells.

Each antibody consists of four protein subunits, two light chains and two heavy chains, arranged in Y-shape. Disulphide bridges between cysteine amino acid residues hold the chains together. Each of the light and heavy chain consists of a constant and a variable region, which binds to the target molecule, the antigen. Breaking an antibody at the ‘hinge’ yields three segments, two identical Fab fragments and one Fc fragment. Each Fab fragment consists of one light chain and half of a heavy chain. The Fc fragment contains the lower halves of both heavy chains (Figure 1.4; Clark and Pazdernik, 2010).

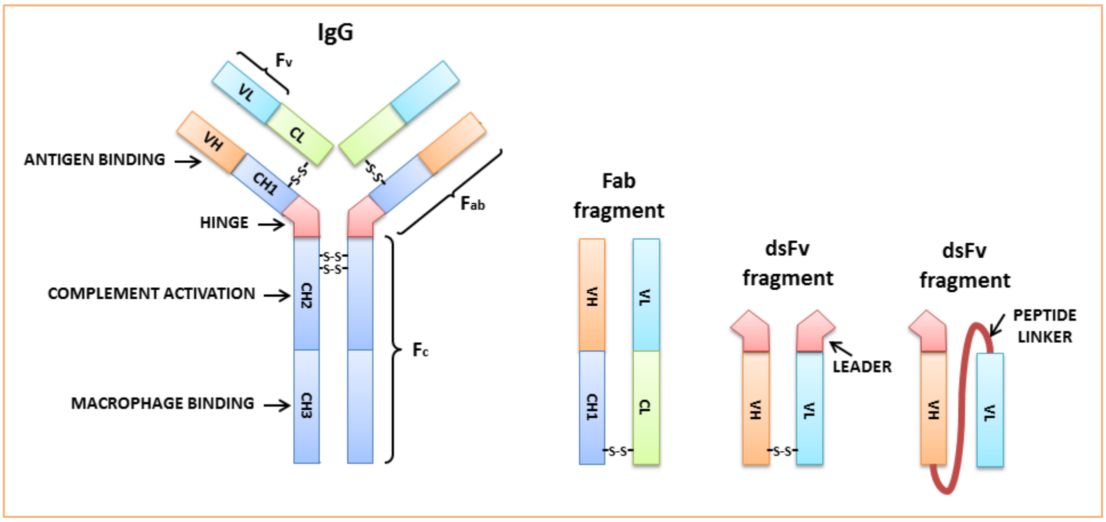

Figure 1.4: Antibody structure and antibody fragments made by antibody engineering (redrawn from Clark and Pazdernik, 2010). Antibody consist of four protein subunits, two light chains (constant light (CL) and variable light (VL)) and two heavy chains (constant heavy (CH) and variable heavy (VH)). Fab fragments are produced by protease digestion of the 'hinge' region. A disulphide bond holds the heavy and the light chains together. To make an antibody fragment without any constant region, the genes for VH and variable light VL domain are expressed on a bacterial plasmid. Because of the lack of disulphide bonds, the structure is unstable. Therefore, disulphide bonds are engineered into the two halves (dsFv fragment), or a linker is added to hold the VH and VL domains together (scFv fragment).

For efficient and specific separation it is not necessary to use the whole antibody. With antibody engineering it is possible to manipulate the antigen binding regions of the antibodies and then attach them to other molecular fragments (see Figure 1.4). The antibody fragments used include Fab, Fv, and a single chain Fv (scFv) regions. For further stabilization of the single chain Fv, a linker is added which holds both domains together. A variety of engineered antibody constructs are being investigated, such as a diabody, which consists of two scFv fragments assembled together (Clark and Pazdernik, 2010).

Antibodies used for cell separation do not need to be absolutely specific to the target cell, as long as other cells in cell suspension are not expressing the same antigen. A surprising finding has been that cell separation can also be achieved by high expression of the target antigen. In a breast cancer model system, it was demonstrated that cells expressing high levels of a target antigen were not efficiently removed by antibodies labelled on magnetic beads (Gee, 1997a). Reducing the antigen-antibody interactions by restricting the amount of monoclonal antibodies coupled to the beads, resulted in improved separation efficiency. The most likely explanation for the negative effect of high antigen density is that overcrowding of the monoclonal antibody molecules on the cell surface can cause steric hindrance and reduce binding to the secondary antibody. The criteria taken into account for the selection of the target antigen should not be focussed only on the distribution and density of the antigen, but also on its biological function. For example, highly mobile antigens that undergo rapid internalization upon cross-linking or binding are generally unsuitable (Gee, 1997b).

Affinity-based separations are very expensive mainly due to the monoclonal antibody cost. To reduce cost on large-scale production, novel immunoaffinity ligands have been proposed – aptamers (Diogo *et al*., 2014). Aptamers are synthetic peptides or highly-specific single strain nucleic acids generated by combinatorial chemistry *in vitro*. They can be developed in automated processes and then easily modified with fluorochromes, biotin or any other nanoparticle (Nery *et al.*, 2009). Aptamers are already used for stem cell isolation, *e.g*. isolation of human adult mesenchymal stem cells from bone marrow, was reported (Guo *et al*., 2006).

Aptamers can be used as an alternative when surface markers are not known or monoclonal antibodies are not commercially available. They can be employed as well when the cell type of interest does not have unique markers, which makes the isolation of a homogeneous population difficult (Tomlinson *et al*., 2012).

In the final product should be present only individual cell types in a viable form and with intact cellular function. It is important to know that product can contain more than one cell type and be still classified as pure (Halme and Kessler, 2006). To confirm retained biological cellular function, *in vitro* testing and animal models can be used (Halme and Kessler, 2006).

1.4 RESEARCH AIMS AND SCOPE

The aims for the work presented here were to advance new single-use cell affinity selection format.

The project had the following four main objectives:

I. Define an appropriate biocompatible coating for glass material;

II. Identify suitable ligands for effective attachment and detachment of cells from the support material in viable form;

III. Following preparation and characterisation of functionalised affinity glass beads, to carry out a comprehensive study using human therapeutic cells (red blood cells) and B and T lymphocytes from various cell lines to evaluate the efficiency, productivity and selectivity of cell adsorption and desorption from the supports, and the impact of the developed method on the cell viability and the expression of cell surface markers;

IV. Evaluate developed separation process and compare its performance and cost with MACS®, the gold standard in cell separation, using various cell line mixtures.

1.5 STRUCTURE OF THESIS

Thesis has been structured in the following way:

Chapter 1: Introduction: In this chapter the aims and objectives of the research are presented and the thesis structure is introduced. This chapter covers as well the literature review of downstream processing of cells in order to provide background and context to the research.

In next three chapters results of experimental work are presented. Each chapter consist of short abstract, introduction, materials and methods, results and conclusions section.

Chapter 2: Tailored surfaces for affinity selection of human therapeutic cells: In this chapter various approaches undertaken for surface modification and functionalization of glass coverslips and hollow capillary tubes are explained in order to establish "cell-friendly" environment for cell attachment and detachment.

Chapter 3: Preparation, characterization and application of non-porous glass beads for the positive selection of human red blood cells: Preparation and characterization of glass beads is presented in this chapter, as well as the development of the separation method for red blood cells.

Chapter 4: Application of glass bead chromatography for the positive selection of human white blood cells: The development of an affinity chromatography method for the positive selection of human white blood cells is explained in this chapter.

Chapter 5: Glass bead chromatography versus MACS® Microbeads: A first principle comparison: In this chapter a comparative study between developed affinity chromatography method and MACS® affinity based magnetic beads separation using various human cell suspensions is presented, together with economic comparison.

Chapter 6: Conclusions and future work: This chapter presents all the main conclusions arising from all the work presented within the thesis. It also outlines proposals for future work.

1.6 REFERENCES

von Andrian U.H., Chambers J.D., McEvoy L.M., Bargatze R.F., Arfors K.E. and Butcher E.C. 1991. Two-step model of leukocyte-endothelial cell interaction in inflammation: distinct roles for LECAM-1 and the leukocyte beta 2 integrins in vivo. *Proceedings of the National Academy of Sciences*, vol. 88, no. 17, pp. 7538-7542.

Bain B.J. 1996. *A beginner’s guide to blood cells*. Oxford: Blackwell Science.

Battula V.L., Treml S., Bareiss P.M., Gieseke F., Roelofs H., de Zwart P., Müller I., Schewe B., Skutella T., Fibbe W.E., Kanz L. and Bühring H.J. 2009. Isolation of functionally distinct mesenchymal stem cell subsets using antibodies against CD56, CD271, and mesenchymal stem cell antigen-1. *Haematologica*, vol. 94, no. 2, pp. 173-184.

Berenson R.J., Bensinger W.I. and Kalamasz D. 1986. Positive selection of viable cell populations using avidin-biotin immunoadsorption. *Journal of immunological methods*, vol. 91, no. 1, pp. 11-19.

Bjornson C.R., Rietze R.L., Reynolds B.A., Magli M.C. and Vescovi A.L. 1999. Turning brain into blood: a hematopoietic fate adopted by adult neural stem cells in vivo. *Science*, vol. 283, no. 5401, pp. 534-537.

Böyum A. 1968. Isolation of mononuclear cells and granulocytes from human blood. *Scandinavian journal of clinical and laboratory investigation. Supplementum*, vol. 21 (suppl. 97), pp. 77-89.

Bongso A. and Richards M. 2004. History and perspective of stem cell research. *Best practice and research clinical obstetrics and gynaecology*, vol. 18, no. 6, pp. 827-842.

Braithwaite A. and Smith F.J. 1996. *Chromatographic methods*. 5th ed. London, Glasgow, Weinheim, New York, Tokyo, Melbourne and Madras: Blackie Academic & Professional, pp. 1-16.

Brown M. and Wittwer C. 2000. Flow cytometry: Principles and clinical applications in hematology. *Clinical chemistry*, vol. 46, no. 8(B), pp. 1221-1229.

Cao F., van der Bogt K.E., Sadrzadeh A., Xie X., Sheikh A.Y., Wang H., Connolly A.J., Robbins R.C., Wu J.C. 2007. Spatial and temporal kinetics of teratoma formation from murine embryonic stem cell transplantation. *Stem cells and development*, vol. 16, no. 6, pp. 883-891.

Cardoso A.A., Watt S.M., Batard P., Li M.L., Hatzfeld A., Genevier H. and Hatzfeld J. 1995. An improved panning technique for the selection of CD34+ human bone marrow hematopoietic cells with high recovery of early progenitors. E*xperimental hematology*, vol. 23, no. 5, pp. 407-412.

Castner D.G. and Ratner B.D. 2002. Biomedical surface science: Foundations to frontiers. *Surface science*, vol. 500, no. 1-3, pp. 28-60.

Choi S., Karp J.M. and Karnik R. 2012. Cell sorting by deterministic cell rolling. *Lab on a chip*, vol. 12, no. 8, pp. 1427-1430.

Civin C.I. 1992. *Release of cells from affinity matrices*. US Patent 5081030.

Clark D.P. and Pazdernik N.J. 2010. Biotechnology. *Academic cell update*. London: Academic Press, pp. 174-191.

Dainiak K., Galaev I.Y. and Mattiasson B. 2007. Macroporous monolithic hydrogels in a 96-minicolumn plate format for cell surface-analysis and integrated binding/quantification of cells. *Enzyme and Microbial Technology*, vol. 40, no. 4, pp. 688-695.

Dainiak M.B., Kumar A, Galaev I.Y. and Mattiasson B. 2006. Detachment of affinity-captured bioparticles by elastic deformation of a macroporous hydrogel. Proceedings of the National Academy of Sciences, vol. 103, no. 4, pp. 849-854Daley G.Q. 2010. Stem cells: roadmap to the clinic. *The journal of clinical investigation*, vol. 120, no. 1, pp. 8-10.

Demirbag B., Huri P.Y., Kose G.T., Buyuksungur A. and Hasirci V. 2011. Advanced cell therapies with and without scaffolds. *Biotechnology journal*, vol. 6, no. 12, pp. 1437-1453.

Diogo M.M., da Silva C.L and Cabral J.M.S. 2012. Separation technologies for stem cell bioprocessing. *Biotechnology and bioengineering*, vol. 109, no. 11, pp. 2699-2709.

Diogo M.M., da Silva C.L and Cabral J.M.S. 2014. Separation technologies for stem cell bioprocessing. In: Al-Rubeai M. and Naciri M., eds. *Stem cells and cell therapy*: Dordrecht, Nederlands: Springer, pp. 157-181.

Donovan P.J. and Gearhart J. 2001. The end of the beginning for pluripotent stem cells. *Nature*, vol. 414, no. 6859, pp. 92-97.

Edelman G.M., Rutishauser U. and Millette C.F. 1971. Cell fractionation and arrangement on fibers, beads, and surfaces. *Proceedings of the National Academy of Sciences*, vol. 68, no. 9, pp. 2153-2157.

Eniolla A.O., Willcox P.J. and Hammer D.A. 2003. Interplay between rolling and film adhesion elucidated with a cell-free system engineered with two distinct receptor-ligand pairs. *Biophysical journal*, vol. 85, no. 4, pp. 2720-2731.

Evans M.J. and Kaufman M.H. 1981. Establishment in culture of pluripotential cells from mouse embryos. *Nature*, vol. 292, no. 5819, pp. 154-156.

Esser C. 1998. Historical and useful methods of preselection and preparative scale sorting. In: Recktenwald D. and Radbruch A., eds. *Cell separation methods and applications*: New York, New York, United States of America: Marcel Dekker, INC., pp. 1-14.

Ettre L. S. 1993. Nomenclature for chromatography (IUPAC recommendations 1993). *Pure and applied chemistry*, vol. 65, no. 4, pp. 819-872.

Fink D.W. Jr. 2009. FDA regulation of stem cell-based products. *Science*, vol. 324, no. 5935, pp. 1662-1663.

Gage F.H. 1998. Cell therapy. *Nature*, vol. 392, no. 6679 Suppl., pp. 18-24.

Gallico G.G.3rd., O'Connor N.E., Compton C.C., Kehinde O. and Green H. 1984. Permanent coverage of large burn wounds with autologous cultured human epithelium. *The New England journal of medicine*, vol. 311, no. 7, pp. 448-451.

Gasol B. 2005. Flow cytometric cell sorting. [online]. MarBEF. [viewed 30/06/2011]. Available from: http://www.marbef.org/training/FlowCytometry/Lectures/GASOLBASICS_CS-protocols.pdf

Gee A.P. 1997a. Antibody- and complement-mediated cell separation. In: Recktenwald D. and Radbruch A. *Cell separation methods and application*. 10th ed. New York: Marcel Dekker, INC., pp. 133-151.

Gee A.P. 1997b. Immunomagnetic cell separation using antibodies and superparamagnetic microspheres. In: Recktenwald D. and Radbruch A. *Cell separation methods and application*. 10th ed. New York: Marcel Dekker, INC., pp. 175-208.

Gonzáles-Gonzáles M., Vázquez-Villegas P., García-Salinas C. and Rito-Palomares M. 2011. Current strategies and challenges for the purification of stem cells. *Journal of chemical technology and biotechnology*, vol. 87, no. 1, pp. 2-10.

Greenberg A.W., Brunk D.K. and Hammer D.A. 2000. Cell-free rolling mediated by L-selectin and sialyl Lewis(x) reveals the shear threshold effect. *Biophysical journal*, vol. 79, no. 5, pp. 2391-2402.

Greenberg A.W., Hammer D.A. 2001. Cell separation mediated by differential rolling adhesion. *Biotechnology and bioengineering*, vol. 73, no. 2, pp. 111-124.

Grützkau A. and Radbruch A. 2010. Small but mighty: how the MACS®-technology based on nanosized superparamagnetic particles has helped to analyze the immune system within the last 20 years. *Cytometry A*, vol. 77, no. 7, pp. 643-647.

Guo K.-T., Schäfer R., Paul A., Gerber A, Ziemer G. and Wendel H.P. 2006. A new technique for the isolation and surface immobilization of mesenchymal stem cells from whole bone marrow using high-specific DNA aptamers. *Stem cells*, vol. 24, no. 10, pp. 2220-2231.

Gutierrez-Aranda I., Ramos-Mejia V., Bueno C., Munoz-Lopez M., Real P.J., Mácia A., Sanchez L., Ligero G., Garcia-Parez J.L., Menendez P. 2010. Human induced pluripotent stem cells develop teratoma more efficiently and faster than human embryonic stem cells regardless the site of injection. *Stem cells*, vol. 28, no. 9, pp. 1568-1570.

Halme D.G. and Kessler D.A. 2006. FDA regulation of stem-cell-based therapies. *The New England journal of medicine*, vol. 355, no. 16, pp. 1730-1735.

Hammer D.A. and Lauffenburger D.A. 1987. A dynamical model for receptor-mediated cell adhesion to surfaces. *Biophysical journal*, vol. 52, no. 3, pp. 475-487.

Hammer D.A. and Apte S.M. 1992. Stimulation of cell rolling and adhesion on surfaces in shear flow: general results and analysis of selectin-mediated neutrophil adhesion. *Biophysical journal*, vol. 63, no. 1, pp. 35-57.

Handgretinger R., Lang P., Ihm K., Schumm M., Geiselhart A., Koscielniak E., Hero B., Klingebiel T. and Niethammer D. 2002. Isolation and transplantation of highly purified autologous peripheral CD34(+) progenitor cells: purging efficacy, hematopoietic reconstitution and long-term outcome in children with high-risk neuroblastoma. *Bone marrow transplantation*, vol. 29, no. 9, pp. 731-736.

Heinrich H.-W. and Heinrich J.-M. 2012. *Method for separating particles and/or cells having 2 and more surface specificities*. US Patent 2012/0164634 A1

Henderson T.M.A., Ladewig K., Haylock D.N., McLean K.M. and O’Connor A.J. 2013. Cryogels for biomedical applications. *Journal of materials chemistry B*, vol. 1, pp. 2682-2695.

Herzenberg L.A., Parks D., Sahaf B., Perez O., Roederer M. and Herzenberg L.A. 2002. The history and future of the fluorescence activated cell sorter and flow cytometry: A view from Stanford. *Clinical chemistry*, vol. 48, no. 10, pp. 1819-1827.

Higuchi A., Iizuka A., Gomei Y., Miyazaki T., Sakurai M., Matsuoka Y. and Natori S.H. 2006. Separation of CD34+ cells from human peripheral blood through polyurethane foaming membranes. *Journal of biomedical materials research. Part A*, vol. 78, no. 3, pp. 491-499.

Higuchi A., Sekiya M., Gomei Y., Sakurai M., Chen W.Y., Egashira S. and Matsuoka Y. 2008. Separation of hematopoietic stem cells from human peripheral blood through modified polyurethane foaming membranes. *Journal of biomedical materials research. Part A*, vol. 85, no. 4, pp. 853-861.

Hipp J. and Atala A. 2008. Sources of stem cells for regenerative medicine. *Stem cell reviews and reports*, vol. 3, no. 1, pp. 3-11.

Jaatinen T. and Laine J. 2007. Isolation of mononuclear cells from human cord blood by Ficoll-Paque density gradient. *Current protocols in stem cell biology*, vol. 1, 1:2A.1.1.-2A.1.4.

Jiang L., Abati A.D., Wilson W., Stetler-Stevenson M. and Yuan C. 2010. Persistent non-neoplastic γδ-T cells in cerebrospinal fluid of a patient with hepatosplenic (γδ) T cell lymphoma: a case report with 6 years of flow cytometry follow-up. *International journal of clinical and experimental pathology*, vol. 3, no. 1, pp. 110-116.

Johnsen H.E., Hutchings M., Taaning E., Rasmussen T., Knudsen L.M., Hansen S.W., Andersen H., Gaarsdal E., Jensen L., Nikolajsen K., Kjaesgârd E. and Hansen N.E. 1999. Selective loss of progenitor subsets following clinical CD34+ cell enrichment by magnetic field, magnetic beads or chromatography separation. *Bone marrow transplantation*, vol. 24, no. 12, pp. 1329-1336.

Jungbauer A. and Hahn R. 2004. Monoliths for fast bioseparation and bioconversion and their applications in biotechnology. *Journal of separation science*, vol. 27, no. 10-11, pp. 767-778.

Kanski A., Spencer J. and Eremin O. 1981. Sephadex G-10 columns do not retain selectively T or B lymphocyte subpopulations. *Journal of immunological methods*, vol. 42, no. 2, pp. 147-156.

Kantor A.B., Gibbons I., Miltenyi S. and Schmitz J. 1998. Magnetic sorting with colloidal supermagnetic particles. In: Recktenwald D. and Radbruch A., eds. *Cell separation methods and applications*. 10th ed. New York: Marcel Dekker, INC., pp. 153-173.

Kastrinaki M.C., Andreakou I., Charbord P. and Papadaki H.A. 2008. Isolation of human bone marrow mesenchymal stem cells using different membrane markers: Comparison of colony/cloning efficiency, differentiation potential, and molecular profile. *Tissue engineering. Part C. Methods*, vol. 14, no. 4, pp. 333-339.

Kern S., Eichler H., Stoeve J., Klüter H. and Bieback K. 2006. Comparative analysis of mesenchymal stem cells from bone marrow, umbilical cord blood, or adipose tissue. *Stem cells*, vol. 24, no. 5, pp. 1294-1301.

Kondorosi É., Nagy J. and Dénes G. 1977. Optimal conditions for the separation of rat T lymphocytes on anti-immunoglobulin-immunoglobulin affinity columns. *Journal of immunological methods*, vol. 16, no. 1, pp. 1-13.

Kumar A., Plieva F.M., Galeav I.Y. and Mattiasson B. 2003. Affinity fractionation of lymphocytes using a monolithic cryogel. *Journal of Immunological methods*, vol. 283, no. 1-2, pp. 185-194.

Kumar A. and Srivastava A. 2010. Cell separation using cryogel-based affinity chromatography. *Nature protocols*, vol. 5, no. 11, pp. 1737-1747.

Lee A.S., Tang .C, Cao F., Xie X., van der Bogt K., Hwang A., Connolly A.J., Robbins R.C. and Wu J.C. 2009. Effects of cell number on teratoma formation by human embryonic stem cells. *Cell cycle*, vol. 8, no. 16, pp. 2608-2612.

Lemarie C., Calmels B., Malenfant C., Arneodo V., Blaise D., Viret F., Bouabdallah R., Ladaique P., Viens P. and Chabannon C. 2005. Clinical experience with the delivery of thawed and washed autologous blood cells, with automated closed fluid management device: CytoMate. *Transfusion*, vol. 45, no. 5, pp. 737-742.

Lennon D.P. and Caplan A.I. 2006. Isolation of human marrow-derived mesenchymal stem cells. *Experimental hematology*, vol. 34, no. 11, pp. 1604-1065.

Lo B. and Parham L. 2009. Ethical issues in stem cell research. *Endocrine reviews*, vol. 30, no. 3, pp. 204-213.

Lozinsky V.I., Galaev I.Y., Plieva F.M., Savina I.N., Jungvid H and Mattiasson B. 2003. Polymeric cryogels as promising materials of biotechnological interest. *Trends in biotechnology*, vol. 21, no. 10, pp. 445-451.

Lozinsky V.I. 2008. Polymeric cryogels as a new family of macroporous and supermacroporous materials for biotechnological purposes. *Russian chemical bulletin*, vol. 57, no. 5, pp. 1015-132.

Ly I.A. and Mishell R.I. 1974. Separation of mouse spleen cells by passage through columns of sephadex G-10. *Journal of immunological methods*, vol. 5, no. 3, pp. 239-247.

Malcovati L. 2009. Red blood cell transfusion therapy and iron chelation in patients with myelodysplastic syndromes. *Clinical lymphoma & myeloma*, vol. 9, suppl. 3, pp. S305-S311.

Marshak D.R., Gottlieb D. and Gardner R.L. 2001. Introduction: Stem cell biology. In: Marshak D.R., Gottlieb D. and Gardner R.L., eds. *Stem cell biology*: Cold Spring Harbour, New York, United States of America: Cold Spring Harbour Laboratory Press, pp. 1-16.

Martin G.R. 1981. Isolation of pluripotent cell line from early mouse embryos cultured in medium conditioned by teratocarcinoma stem cells. *Proceedings of the National Academy of Sciences*, vol. 78, no. 12, pp. 7634-7638.McClelland B. 2001. Blood products. In: Emmanuel J.C., McClelland B. and Page R, eds. *The clinical use of blood in medicine, obstetrics, paediatrics, surgery and anaesthesia, trauma and burns*. [online]. World Health Organisation, Department of Blood Safety and Clinical Technology, Geneva. [viewed 25/06/2011]. Available from: http://whqlibdoc.who.int/hq/2001/a72894.pdf

McLaren A. 2001. Ethical and social considerations of stem cell research. *Nature*, vol. 414, no. 6859, pp. 129-131.

Melton D.A. and Cowan C. 2004. “Stemness”: Definitions, criteria, and standards. In: Lanza R., Blau H., Gearhart J., Hogan B., Melton D., Moore M., Pedersen R., Thomas E.D., Thomson J.A., Verfaillie C., Weissman I. and West M.D., eds. *Handbook of Stem Cells: Volume 1 - Embryonic Stem Cells*: Boston, Massachusetts, United States of America: Elsevier Academic, pp. xxv.-xxxi.

Miller J.M. 2005. *Chromatography: Concepts and contrasts*. 2nd ed. New Jersey: John Wiley & Sons. pp. 423-461.

Miltenyi S., Müller W., Weichel W. and Radbruch A. 1990. High gradient magnetic cell separation with MACS. *Cytometry*, vol. 11, no. 2, pp. 231-238.

Miltenyi S. and Schmitz J. 2000. High gradient magnetic sorting. In: Radbruch A., ed. *Flow cytometry and cell sorting*. 2nd ed. Berlin, Heidelberg: Springer – Verlag, pp. 218-247.

Nagase K., Mukae N., Kikuchi A. and Okano T. 2012. Thermally modulated retention of lymphocytes on polymer-brush-grafted glass beads. *Macromolecular bioscience*, vol. 12, no. 3, pp. 333-340.

Nagrath S., Sequist L.V., Maheswaran S., Bell D.W., Irimia D., Ulkus L., Smith M.R., Kwak E.L., Digumarthy S., Muzikansky A., Ryan P., Balis U.J., Tompkins R.G., Haber D.A. and Toner M. 2007. Isolation of rare circulating tumour cells in cancer patients by microchip technology. *Nature*, vol. 450, no. 7173, pp. 1235-1239.

Nery A.A., Wrenger C. and Ulrich H. 2009. Recognition of biomarkers and cell-specific molecular signatures: Aptamers as capture agents. *Journal of separation science*, vol. 32, no. 10, pp. 1523-1530.

Nordon R.E., Havlock D.N., Gaudry L. and Schindhelm K. 1996. Hollow-fibre affinity cell separation system for $CD34^+$ cell enrichment. *Cytometry*, vol. 24, no. 4, pp. 340-347.

Nordon R.E., Milthorpe B.K., Slowiacek P.R. and Schindhelm K. 1998. *Cell separation device*. US Patent 5763194.

Nordon R.E. and Craig S. 2007. Hollow-fibre affinity cell separation. *Advances in biochemical engineering/biotechnology*, vol. 106, pp. 129-150.

Orkin S.H. 2001. Hematopoietic stem cells: Molecular diversification and developmental interrelationships. In: Marshak D.R., Gardner R.L. and Gottlieb D., eds. *Stem cell biology*. Vol. 40. New York: Cold Spring Harbor Laboratory Press, pp. 289-348.

Perin E.C., Geng Y.J. and Willerson J.T. 2003. Adult stem cell therapy in perspective. *Circulation*, vol. 107, no. 7, pp. 935-938.

Pierzchalski A., Mittag A., Bosci J. and Tarnok A. 2013. An innovative cascade system for simultaneous separation of multiple cell types. *Plos one*, vol. 8, no. 9, e74745.

Plotz P.H. and Talal N. 1967. Fractionation of splenic antibody-forming cells on glass bead columns. *The journal of immunology*, vol. 99, no. 6, pp. 1236-1242.

Presnell S.C., Petersen B. and Heidaran M. 2002. Stem cells in adult tissues. *Seminars in cell and developmental biology*, vol. 13, no. 5, pp. 369-376.

Rasmussen A.M., Smeland E.B., Erikstein B.K., Caignault L. and Funderud S. 1992. A new method for detachment of dynabeads from positively selected B lymphocytes. *Journal of immunological methods*, vol. 146, no. 2, pp. 195-202.

Reya T., Morrison S.J., Clarke M.F. and Weissman I.L. 2001. Stem cells, cancer, and cancer stem cells. *Nature*, vol. 414, no. 6859, pp. 105-111.

Roda B., Lanzoni G., Alviano F., Zattoni A., Costa R., Di Carlo A., Marchionni C., Franchina M., Ricci F., Tazzari P.L., Pagliaro P., Scalinci S.Z., Bonsi L., Reschiglian P. and Bagnara G.P. 2009a. A novel stem cell tag-less sorting method. *Stem cell reviews and reports*, vol. 5, no. 4, pp. 420-427.

Roda B., Reschiglian P., Alviano F., Lanzoni G., Baqnara G.P., Ricci F., Buzzi M, Tazzari P.L., Pagliaro P., Michelini E. and Roda A. 2009b. Gravitational field-flow fractionation of human hemopoietic stem cells. *Journal of chromatography A*, vol. 1216, no. 52, pp. 9081-9087.

Rutishauser U. and Edelman G.M. 1972. Binding of thymus- and bone marrow-derived lymphoid cells to antigen-derivated fibers. *Proceedings of the National Academy of Sciences*, vol. 69, no. 12, pp. 3774-3778.

Schlossman S.F. and Hudson L. 1973. Specific purification of lymphocyte populations on a digestible immunoabsorbent. *The journal of immunology*, vol. 110, no. 1, pp. 313-315.

Schriebl K., Lim S., Choo A., Tscheliessnig A. and Jungbauer A. 2010. Stem cell separation: a bottleneck in stem cell therapy. *Biotechnology journal*, vol. 5, no. 1, pp. 50-61.

Schwartz J., Winters J.L., Padmanabhan A., Balogun R., Delaney M., Linenberger M.L., Szczepiorkowski Z.A., Williams M.E., Wu Y. and Shaz B.H. 2013. Guidelines on the use of therapeutic apheresis in clinical practice-evidence-based approach from the writing committee of the American society for apheresis: The sixth special issue. *Journal of clinical apheresis*, vol. 28, no. 3, pp. 145-284.

Short B., Brouard N., Occhiodoro-Scott T., Ramakrishnan A. and Simmon P.J. 2003. Mesenchymal stem cells. *Archives of medical research*, vol. 34, no. 6, pp. 565-571.

Smith A.G. 2001. Embryo-derived stem cells of mice and men. *Annual review of cell biology*, vol. 17, pp. 435-462.

Sousa A.F., Andrade P.Z., Pirzgalska R.M., Galhoz T.M., Azevedo A.M., da Silva C.L., Aires-Barros M.R. and Cabral J.M. 2011. A novel method for human hematopoietic stem/progenitor cell isolation from umbilical cord blood based on immunoaffinity aqueous two-phase partitioning. *Biotechnology letters*, vol. 33, no. 12, pp. 2373-2377.

Spradling A., Drummond-Barbosa D. and Kai T. 2001. Stem cells find their niche. *Nature*, vol. 414, no. 6859, pp. 98-104.

Stem cell basics. In: Stem cell information. [online]. 2009. Bethesda, MD: National Institutes of Health, U.S. Department of Health and Human Services. [viewed 07/07/2011]. Available from: http://stemcells.nih.gov/staticresources/info/basics/SCprimer2009.pdf

Sutherland D.R., Marsh J.C., Davidson J., Baker M.A., Keating A. and Mellors A. 1992. Differential sensitivity of CD34 epitopes to cleavage by *Pasteurella haemolytica* glycoprotease: implications for purification of CD34-positive progenitor cells. *Experimental Haematology*, vol. 20, no. 5, pp. 590-599.

Talary M.S., Mills K.I., Hoy T., Bumett A.K. and Pethig R. 1995. Dielectrophoretic separation and enrichment of CD34+ cell subpopulation from bone marrow and peripheral blood stem cells. *Medical and biological engineering and computing*, vol. 33, no. 2, pp. 235-237.

Thomas E.D., Lochte H.L., Lu W.C. and Ferrebee J.W. 1957. Intravenous infusion of bone marrow in patients receiving radiation and chemotherapy. *New England journal of medicine*, vol. 257, no. 11, pp. 491-496.

Thomas T.E. and Lansdorp P.M. 1988. Immunoadsorption of T cells onto glass beads using tetramolecular complexes of monoclonal antibodies. *Journal of immunological methods*, vol. 112, no. 2, pp. 219-226.

Thomas T.E., Sutherland H.J. and Lansdorp P.M. 1989. Specific binding and release of cells from beads using cleavable tetrameric antibody complexes. *Journal of immunological methods*, vol. 120, no. 2, pp. 221-231.

Thomas T.E., Miller C.L. and Eaves C.J. 1999. Purification of hematopoietic stem cells for further biological study. *Methods*, vol. 17, no. 3, pp. 202-218.

Tomlinson M.J., Tomlinson S., Yang X.B. and Kirkham J. 2012. Cell separation: Terminology and practical considerations. *Journal of tissue engineering*, vol. 4, pp.1-14, doi: 10.1177/2041731412472690.

Trounson A., Thakar R.G., Lomax G. and Gibbons D. 2011. Clinical trials for stem cell therapies. *BMC Medicine*, vol. 9, no. 52, pp. 1-7.

Truffa-Bachi P. and Wofsy L. 1970. Specific separation of cells on affinity columns. *Proceedings of the National academy of sciences*, vol. 66, no. 3, pp. 685-692.

Tseng-Law J., Kobori J.A. and Al-Abdaly F. 1995. *Positive and positive-negative cell selection mediated by peptide release*. US Patent 5968753.

Ujam L.B., Clemmitt R.H., Clarke S.A., Brooks R.A., Rushton N. and Chase H.A. 2003. Isolation of monocytes from human peripheral blood using immune-affinity expanded-bed adsorption. Biotechnology and bioengineering, vol. 83, no. 5, pp. 554-566.

Weil B.D. and Veraitch F.S. 2014. *Bioprocessing challenges associated with the purification of cellular therapies*. In: Al-Rubeai M. and Naciri M., eds. Stem cells and cell therapy: Dordrecht, Nederlands: Springer, pp. 129-156.

Weissman I.L. 2000. Translating stem and progenitor cell biology to the clinic: barriers and opportunities. *Science*, vol. 287, no. 5457, pp. 1442-1446.

Weissman I.L., Anderson D.J. and Gage F. 2001. Stem and progenitor cells: origins, phenotypes, lineage commitments, and transdifferentiation. *Annual review of cell and developmental biology*, vol. 17, pp. 387-403.

Wognum A.W., Eaves A.C. and Thomas T.E. 2003. Identification and isolation of hematopoietic stem cells. *Archives of medical research*, vol. 34, no. 6, pp. 461-475.

Wu C.H., Lee F.K., Kumar S.S., Ling Q.D., Chang Y., Chang Y., Wang H.C., Chen H., Chen D.C., Hsu S.T. and Higuchi A. 2012. The isolation and differentiation of human adipose-derived stem cells using membrane filtration. *Biomaterials*, vol. 33, no. 33, pp. 8228-8239.

Xue-Jun W. 2005. Polymeric biomaterials for biological and pharmaceutical applications. [online]. East China University of Science and Technology, Sanghai. [viewed 17/07/2011]. Available from: www.paper.edu.cn/en_releasepaper/.../200512-85

Yamaoka T. and Mahara A. 2011. Cell rolling column in purification and differentiation analysis of stem cells. *Reactive and functional polymers*, vol. 71, no. 3, pp. 362-366.

Yin F., Battiwalla M., Ito S., Feng X., Chinian F., Melenhorst J.J., Koklanaris E., Sabatino M., Stroncek D., Samsel L., Klotz J., Hensel N.F., Robey P.G. and Barrett A.J. 2014. Bone marrow mesenchymal stromal cells to treat tissue damage in allogeneic stem cell transplant recipients: correlation of biological markers with clinical responses. *Stem cells*, vol. 32, no. 5, pp. 1278-1288.

2. TAILORED SURFACES FOR AFFINITY SELECTION OF HUMAN THERAPEUTIC CELLS

Abstract

Chromatography offers huge potential in cell purification and separation; however in most studies performed so far the adsorbent materials are unsuitable for the selection of human therapeutic cells. In this chapter are presented approaches used in the development of generic, scalable and transferrable selection system for human therapeutic cells, with an emphasis on the engineering of clinically approved materials for the highly selective affinity-based adsorption and gentle efficient detachment of human cells in a viable form are detailed. A reliable system was developed on glass coverslips and successfully transferred to small case studies, where tailored surfaces were tested under flow-conditions using glass hollow capillary tubes. The affinity separation system developed in this work can be easily applied to any chromatographic support already present on the market.

2.1 INTRODUCTION

At present there are no truly affordable, scalable, cell enrichment devices on the market capable of selecting therapeutic cells. The clinical benchmark remains magnetic affinity cell sorting (commercially known as MACS®), a method developed more than 30 years ago for the purification of human red blood cells (Molday *et al*., 1977). Alternatively, fluorescence-activated cell sorting (FACS) may be used. Both methods are deemed too expensive and inappropriate for large scale separation (Kumar and Srivastava, 2010).

To many bioprocessors, who see chromatography as the solution to all high-resolution separation problems, trust in magnetic-based methods is misplaced. However, most chromatographic studies to date have employed unsuitable adsorbent materials, such as porous Sephadex beads, and have therefore yielded very poor results in comparison to magnetic bead separation (Johnsen *et al*., 1999; Diogo *et al*., 2012).

The critical design goal for a chromatographic support for affinity selection of human therapeutic cells would be a biocompatible surface with minimal adsorption of biological fluid-borne proteins. Furthermore, to achieve high selectivity and yields, non-specific cell binding should be impeded to prevent inflammatory responses. With this in mind, specific cell interactions could be achieved by chemically grafting the appropriate density and types of cell affinity ligands on the biocompatible surface (Massia *et al*., 2000).

Various potential cell-compatible materials have been investigated in the past, with many materials and coatings being successfully applied for purposes of regenerative medicine. The most popular materials are polyethylene glycol (PEG), PEG-based hydrogels, polyacrylamide, polyvinyl alcohol and compositions of polyacrylate and PEG. Another routinely used material is cross-linked dextran, which is used not only as a cell culture microcarrier, a drug delivery vehicle, a macroporous scaffold, but it is also popular as a low protein-binding support for chromatography separations (Massia *et al*., 2000; Massia *et al*., 2003; Lévesque and Shoichet, 2006) due to the nature of dextran, as it has more peptide-grafting sites than PEG (Massia *et al*., 2000). Additionally Österberg *et al.* (1993; 1995) simultaneously reported on the capability of cross-linked dextran to further reduce non-specific protein adsorption in comparison to PEG; consequently, the level of non-specific cell attachment is reduced (Lévesque and Shoichet, 2006). As a coating, oxidized dextran forms a uniform ultrathin film on grafted surfaces (Kühner and Sackmann, 1996).

The most popular affinity chromatographic techniques are based on interactions between antibodies and antigens, lectins and sugar, and avidin and biotin (Sproβ and Sinz, 2012). Specific binding of biotin to the egg white protein avidin or the bacterial analogue streptavidin is one of the most useful interactions in immunochemistry due to its high affinity, with a dissociation constant of approximately 10^{-15} M (Green and Toms, 1973). Bound avidin is stable at extreme conditions including high and low pH's, high buffer salt concentration and even when exposed to chaotropic agents (Wilchek and Bayer, 1988).

Biotin, also known as vitamin H, vitamin B7 and coenzyme R, is a small water-soluble molecule with a molecular weight of 244.3 Da. It is present in all living cells and serves as a coenzyme in the citric acid cycle and takes a part in cell growth, affecting chromatin structure and mediating gene regulation (Zempleni, 2005). Mammals cannot synthesize biotin, so they depend on the dietary intake from microbial, plant or animal sources (Zempleni *et al.*, 2009). In the most cases, biotin does not have any negative impact on the biological systems and their activity (Zempleni, 2005). It can be used as a cell surface label and it allows highly sensitive detection of labelled molecules using streptavidin-peroxidase conjugates (Cole *et al*., 1987), even *in vivo* (Cronan and Reed, 2000). Additionally, using biotin as a derivatization reagent does not have impact on the activity of the biotinylated molecule (Diamandis and Christopoulos, 1991), therefore it is not a surprise that it is targeting of immobilized avidin or streptavidin with biotinylated molecules a powerful tool not only for separation and purification, but also for immunoassays, receptor studies, and immunocytochemical staining (Hermanson *et al*., 1997).

When applying avidin-biotin approach for the purpose of affinity chromatography, the biggest disadvantage is the severe conditions necessary to release the bound biotin or biotinylated molecule, such as reduced pH to 2.8 (Hermanson *et al*., 1997) or mechanical disruption of the bond (Kuo and Lauffenburger, 1993). To reduce the dissociation constant between avidin and biotin, several strategies have been developed, such as monomerization of tetrameric avidin, chemical modification of biotin binding site on the avidin, site-directed mutagenesis of avidin, and development of biotin analogues (Sproβ and Sinz, 2012).

Table 2.1: Dissociation constants for the interactions between various forms of avidin and biotin

System	Dissociation constant	Reference
tetrameric (strept)avidin – biotin	$K_D=10^{-15}$ M	Livnah *et al.*, 1993
	$K_D=4*10^{-14}$ M	Green, 1990
monomeric avidin (activated with cyanogen bromide) – biotin	Three classes of subunits: 1/4 subunits $K_D=5*10^{-8}$ M 1/3 subunits $K_D=1*10^{-10}$ M the remaining subunits $K_D=1*10^{-15}$ M	Green and Toms, 1973
monomeric avidin (activated with sodium borohydride) - biotin	more than 90 % of subunits $K_D=10^{-7}$ M	Green, 1970; Sproβ and Sinz, 2012
(strept)avidin - desthiobiotin	$K_D=2*10^{-9}$ M	Green, 1970
	pH dependant	Hirsch *et al.*, 2002

Table 2.1 summarizes the dissociation constants for the most common avidin-biotin interactions. It shows that the dissociation constant of biotin and avidin is significantly lower when native, tetrameric avidin is monomerized. To prevent spontaneous re-association, tetrameric avidin is at first immobilized and then its subunits are dissociated under denaturing conditions (Hermanson *et al.*, 1997). When avidin is activated with sodium borohydride, more than 90 % of subunits are in the monomeric form with a dissociation constant for biotin of 10^{-7} M (Green and Toms, 1973). Thus, it is possible to elute bound biotin and biotinylated molecules by competitive displacement using excess free biotin (Hermanson *et al.*, 1997).

In this work, approaches undertaken for the modification and functionalization of glass coverslips and glass hollow capillary tubes in order to establish environment for gentle positive cell selection are detailed.

2.2 MATERIALS AND METHODS

2.2.1 MATERIALS

Borosilicate glass coverslips (10 mm in diameter; 0.13-0.16 mm thick) were supplied by Fischer Scientific UK Ltd. (Loughborough, UK) and rectangular borosilicate glass hollow capillary tubes (inner dimensions: 3.0 mm x 0.3 mm x 100 mm) for the flow-based assay were purchased from CM Scientific Ltd. (Silsden, UK).

Liquinox® detergent, (3-aminopropyl)triethoxysilane (3-APTES; ≥98 % purity), biotin *p*-nitrophenyl ester (98 % purity), dextran from Leuconostoc spp. (Mr ≈ 70000), sodium borohydride ($NaBH_4$, 98 % purity), sodium tetraborate ($Na_2B_4O_7$, Borax; anhydrous, ≥98.0 %), picrylsulfonic acid (2,4,6-trinitrobenzenesulfonic acid, TNBS; 1 M water solution) and picric acid ($(O_2N)_3C_6H_2OH$; ≥98 % pure, moistened with water) were obtained from Sigma-Aldrich Company Ltd. (Gillingham, UK). PD-10 desalting column and HiTrap Protein G HP 1 mL column were purchased from GE Healthcare Life Sciences (Little Chalfont, UK). Quant*Tag™ Biotin kit was supplied by Vector Laboratories Ltd. (Peterborough, UK). Desiccated avidin, egg white (Molecular Probes®, Invitrogen; Mr ≈ 66000; biotin binding of 13.6 units/mg of protein), D(+)-biotin (Acros Organics; 98 % purity), 7-aminoactinomycin D (Molecular Probes®, Invitrogen; 7-AAD), streptavidin R-Phycoerythrin conjugate (Molecular Probes®, Invitrogen; SAPE; 1 mg/mL solution), Trypan blue (Molecular Probes®, Invitrogen; 0.4 % solution), RPMI-1640 liquid medium with 2.05 mM L-glutamine (Thermo Scientific HyClone; RPMI), foetal bovine serum (Thermo Scientific HyClone; FBS; standard filtered through three sequential 100 nm (0.1 μm) pore size rated filter), DSB-X biotin (Molecular Probes®, Invitrogen), Ficoll-Paque™ Plus (GE Healthcare Life Sciences) and BCA Protein assay kit (Thermo Scientific Pierce) were purchased through Fischer Scientific UK Ltd. (Loughborough, UK). All other materials and reagents were supplied by Fischer Scientific UK Ltd. (Loughborough, UK). Acetone, toluene and ethanol were HPLC grade (Fisher

Chemical brand). Sodium azide (NaN_3) was supplied as 99 % pure and suitable for cell culture. Guanidine hydrochloride (Gdm HCl) was purchased as an 8 M water solution. Ammonium bicarbonate (NH_4HCO_3), Ethylenediaminetetraacetic acid (EDTA; disodium salt dehydrate suitable for electrophoresis), glycine ($C_2H_5NO_2$; Gly), hydrogen chloride (HCl), potassium chloride (KCl), sodium acetate ($C_2H_3NaO_2$), sodium chloride (NaCl) sodium hydrogen carbonate ($NaHCO_3$), sodium hydroxide (NaOH), sodium metaperiodate ($NaIO_4$), sodium phosphate (Na_3PO_4) and tris(hydroxymethyl)aminomethane hydrochloride (Tris-HCl), salts used for preparation of buffer solutions, were analytical grade (99+ % purity) and suitable for use in cell culture. Phosphate buffered saline (PBS buffer) was supplied in a form of tablets. Each tablet prepares 100 mL of PBS buffer. Dimethyl sulfoxide (DMSO) was 99 % pure and molecular biology grade.

All solutions were prepared using water purified by a Millipore Elix Gulfstream Clinical 100 (Merck Millipore UK Ltd, Watford, UK) water purification system. Buffer solutions were prepared by dissolving a known mass of buffering species into *ca*. 80 % of the desired final volume of deionized water, titrating with 1 M solution of HCl or NaOH and adding water to yield the final volume.

Sterilization of solutions and suitable materials was performed either by autoclaving at 121 °C and 1.03 bar for 30 min using an ASB 300T autoclave (Astell Scientific, Sidcup, UK) or by sterile filtration through a 0.22 µm filter (Merck Millipore UK Ltd, Watford, UK).

Rituximab (anti-CD20 monoclonal antibody) was purchased from Roche (Basel, Switzerland), BB7.2 (anti-HLA-A2 monoclonal antibody) and anti-glycophorin A (Gly A) monoclonal antibody in cell culture supernatant were kindly provided by Dr Oliver Goodyear (School of Immunity and Infection, College of Medicine, University of Birmingham, UK).

Continuous human cell lines Jurkat E6.1, Bristol-8 and CCRF-HSB-2 were purchased from the Health Protection Agency, Culture Collection (Salisbury, UK), Toledo continuous human cell line was purchased from LGC Standards (Teddington, UK).

Red blood cells were isolated from umbilical cord blood, which was obtained from anonymous donors through NHS Blood and Transplant (NHSBT). Table 2.2 below summarizes the cells and antibodies used in this study.

Table 2.2: Cells and antibodies used in experiments

Cells	Targeted antigen	Monoclonal antibody
Red blood cells	CD235a (glycophorin A)	Anti-CD235a (anti-glycophorin A; Gly A)
Toledo cell line (B lymphocytes)	CD20	Anti-CD20 (Rituximab)
CCRF-HSB-2 cell line (T lymphoblasts)	HLA-A2	Anti-HLA-A2 (BB7.2)
Bristol-8 cell line (B lymphocytes)		

2.2.2 METHODS

2.2.2.1 Surface modification

Preparation of aminated glass material

Glass coverslips and hollow capillary tubes were cleaned by a method developed by Rowland *et al*. (1995). In short, the material was immersed in acetone in an ultrasonic bath (Fisherbrand S15, Fisher Scientific Ltd, Loughborough, UK) for 2 min, rinsed with 95 % ethanol, immersed in 95 % ethanol in ultrasonic bath for 20 min, rinsed with water, immersed in 2 % Liquinox® brand detergent in ultrasonic bath for 20 min, followed by an extensive rinsing with water. The glass surfaces were finally dried overnight at 40 ˚C in a drying cabinet (Belling, Unfield, UK).

Amination of glass surfaces was carried out as described by Massia and Stark (2001). Briefly, the cleaned surfaces were immersed in 7 % solution (v/v) of 3-APTES in toluene for 1 h, rinsed with toluene, followed by 10 min alternating cleaning in toluene and water in ultrasonic bath until there was no visible evidence of silane multilayer build on the surface. This procedure was completed by drying at room temperature overnight in a fume cupboard.

Application of aldehyde groups on the animated glass surfaces

The immobilisation of aldehyde groups on the glass surfaces is a three step procedure (see Figure 2.1) and was performed according to the protocol described by Massia and Stark (2001).

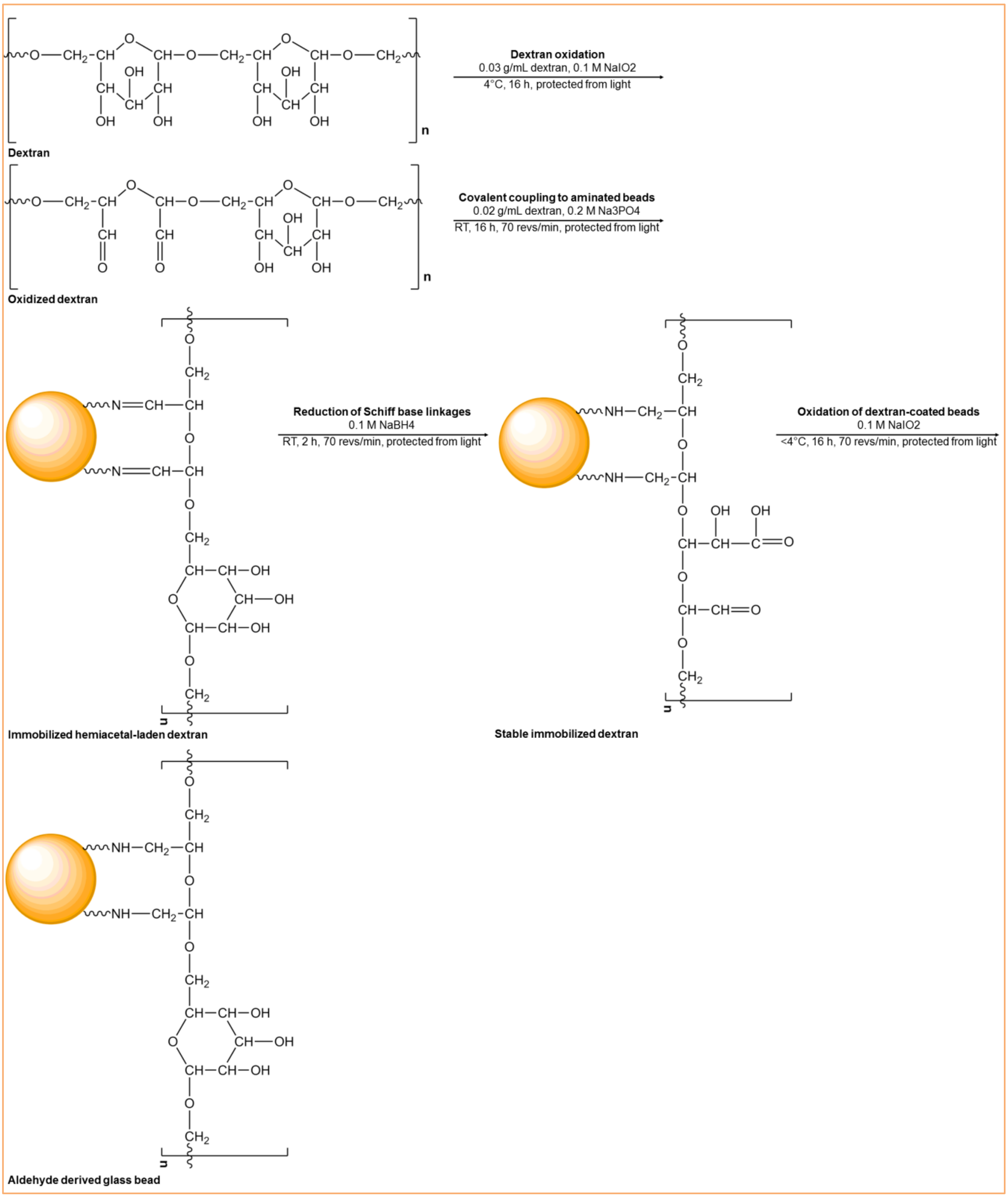
Dextran
Dextran oxidation
0.03 g/mL dextran, 0.1 M NaIO2
4°C, 16 h, protected from light
Oxidized dextran
Covalent coupling to aminated beads
0.02 g/mL dextran, 0.2 M Na3PO4
RT, 16 h, 70 revs/min, protected from light
Immobilized hemiacetal-laden dextran
Reduction of Schiff base linkages
0.1 M NaBH4
RT, 2 h, 70 revs/min, protected from light
Stable immobilized dextran
Oxidation of dextran-coated beads
0.1 M NaIO2
<4°C, 16 h, 70 revs/min, protected from light
Aldehyde derived glass bead

Figure 2.1: Reaction scheme for the surface modification of aminosilane derived glass surfaces. Dextran was oxidized by sodium metaperiodate ($NaIO_4$), and then covalently coupled to the aminosilane derived glass surface. Sodium borohydride ($NaBH_4$) was used to reduce unstable Schiff's bases. Reactivation of the surfaces was done by $NaIO_4$ oxidation.

The first step in the glass surface modification with aldehyde groups was the oxidation of dextran using $NaIO_4$. Freshly prepared 0.1 M $NaIO_4$ solution was added to dextran solution (1 g of dextran dissolved in 30 mL of water) to make 50 % molar ratio. Because of the photosensitivity of the oxidized dextran, all following steps were performed in containers wrapped in aluminium foil to protect the material from the light. The solution was stirred at 4 °C overnight, purified by dialysis in water and subsequently freeze dried using a Pirani 10 freeze dryer (Edwards, Crawley, UK). The lyophilized dextran was dissolved in 0.2 M $NaHCO_3$ buffer, pH 10, (final dextran concentration of 0.02 g/mL) and 2 mL of the above solution was added to the aminated glass surfaces. The materials were left to incubate on a 3-D rocking platform STR 9 (Stuart Scientific, Stone, UK) with shaking at 70 revs/min for 30 min at room temperature. The dextran solution was subsequently decanted and replaced by 0.1 M $NaBH_4$ in water to reduce the free Schiff's bases and to quench any free unreacted aldehyde groups. After 2 h of incubation at room temperature on a 3-D rocking platform at 70 revs/min, the $NaBH_4$ was decanted, the surfaces were rinsed three times with water, and left to dry at 40 °C overnight in a drying cabinet. The dextran derived surfaces were oxidized by adding 2 mL of fresh 0.1 M $NaIO_4$ solution and left to incubate overnight in an OLS200 linear shaking water bath (Grant Instruments, Cambridge, UK) at 4 °C. The $NaIO_4$ solution was then decanted and the modified coverslips and hollow capillary tubes were rinsed three times with water to remove any residual chemicals. The surface modification was completed by air-drying at room temperature inside a fume cupboard.

Immobilization of monomeric avidin

The aldehyde derived glass coverslips and hollow capillary tubes were functionalized with monomeric avidin, following the modified procedure, described by Sproβ and Sinz (2012). The materials were first incubated overnight at room temperature in the presence of tetrameric avidin solution (2 mL with final concentration of avidin 2.5 mg/mL in 100 mM Na_3PO_4, pH 7.0). The materials were incubated for a further 6 h in 2 mL of 80 mM $NaBH_4$ solution at room temperature, to reduce Schiff's bases and unreacted aldehyde groups. The tetrameric avidin was then cleaved to its individual subunits by the addition of 2 mL 6 M Gdm HCl in 0.2 M KCl buffer, pH 1.5. Following incubation for 66 h at room temperature, non-bound and weakly bound avidin was eluted with 0.1 M NH_4HCO_3 buffer and any irreversible biotin binding sites on the immobilized avidin were blocked with 2 mL of 0.4 mM D-biotin solution in 50 mM Tris-HCl buffer, pH 7.5. In order to release the reversible or low affinity monomeric biotin binding sites, the glass surfaces were rinsed three times with 0.1 M Gly, 0.15 M NaCl buffer, pH 2.8, and then re-equilibrated with PBS buffer, pH 7.2, as described by Hermanson *et al*. (1997).

2.2.2.2 Purification of anti-glycophorin A monoclonal antibody from cell culture supernatant

Gly A antibody, produced by HB-8162™ hybridoma cells, was purified from frozen cell culture supernatant using a 5 mL HiTrap Protein G HP column (GE Healthcare, Uppsala, Sweden) connected to an ÄKTA Explorer 100 Air chromatographic system (GE Healthcare, Uppsala, Sweden).

Following equilibration with 20 mM Na_3PO_4, pH 7, for 10 column volumes (CVs), the column was loaded with the 1 mL of defrosted supernatant containing the Gly A antibody at a flow rate of 1 mL/min (75 cm/h). The column was then washed with 5 CVs of the equilibration buffer, and the bound antibody was eluted with a linear gradient (0-100 %) of 0.1 M Gly-HCl buffer, pH 2.7 for 10 CVs. Drop by drop neutralization of the eluted antibody fraction was done by adding 1 M Tris-HCl buffer, pH 8, until a pH of 7 was achieved. The final antibody concentration was determined by absorbance reading at 280 nm using UV-VIS spectrophotometer (UV mini 1240, Shimadzu, Milton Keynes, UK). The antibody concentration was calculated using equation 2.1:

$$c_{Ab} = \frac{A_{280}}{x} \tag{2.1}$$

were: c_{Ab} represents the concentration of antibody in the solution (mg/mL); and, x is the expected absorbance of 1 mg/mL antibody solution in a 1 cm light path cuvette (mg/mL; usually 1.36 mg/mL (Pace *et al*., 1995)).

NaN_3 up to a final concentration of 0.1 % (v/v) was added to the antibody and the solution was stored at 4 °C until further use.

2.2.2.3 Biotinylation of antibodies

The biotinylation of the monoclonal antibodies used in this study was performed using a modified protocol, first devised by Kantor and Roederer in 1997. First, a buffer exchange of the antibody solution to PBS buffer was performed using a disposable PD-10 desalting column. Subsequently, D-biotin was covalently coupled to the primary amines to the constant region of the heavy chain of the antibody using the procedure described below. A fresh solution of 10 mg of D-biotin dissolved in 1 mL of anhydrous DMSO was prepared and added to the antibody solution under manual mixing (6.06 mL of D-biotin solution for each mg of antibody in the buffered solution). The mixture was then placed in a laboratory shaker (IKA-VIBRAX-VXR, JK electronic, Staufen, Germany) at a motor speed 600 for 1 h at room temperature. The reaction was stopped by adding 10 % (v/v) of 1 M Tris-HCl buffer, pH 8, any remaining D-biotin was removed and the buffer was exchanged to PBS using a PD-10 column. The amount of biotinylated antibody was determined by absorbance reading at 280 nm, using a UV-VIS spectrophotometer as described in Section 2.2.2.2. The biotinylated antibodies were subsequently stored at 4 ºC until further use.

2.2.2.4 Surface functionalization

The avidin modified glass coverslips and hollow capillary tubes were functionalized with the biotinylated antibodies as follows. The light sensitive material was first rinsed with PBS buffer, pH 7.2, and then incubated in 10 µg/mL antibody solution in PBS buffer for 1 h at room temperature on a 3-D rocking platform at 70 revs/min. The remaining antibody solution was then removed and the surfaces were rinsed once with PBS buffer. The glass surface functionalization is presented in the Figure 2.2.

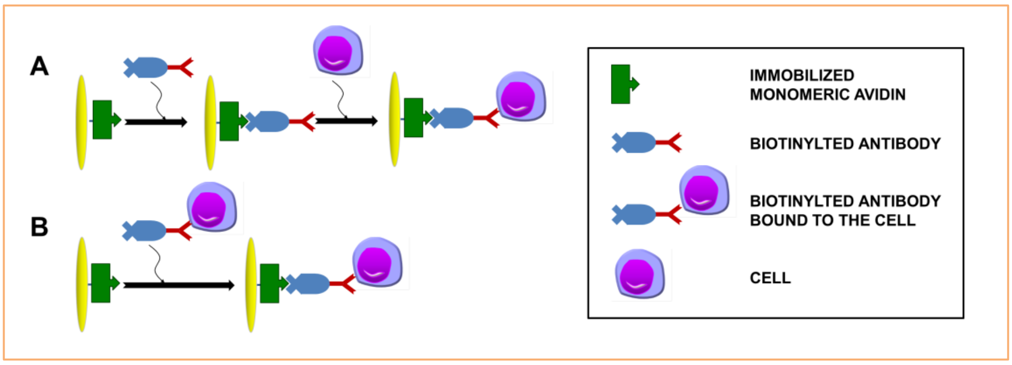
A
B
IMMOBILIZED MONOMERIC AVIDIN
BIOTINYLTED ANTIBODY
BIOTINYLTED ANTIBODY BOUND TO THE CELL
CELL

Figure 2.2: Two schematic representations of antibody coupling to glass surfaces. (A) Coupling of biotinylated antibody to mono-avidin modified supports, followed by cell binding. (B) Binding of biotinylated antibody labelled cells to mono-avidin modified supports.

The mass of bound antibody was determined using equation 2.2:

$$m_{Ab} = \left(c_{Ab,stock} - \frac{A_{280,after}}{x}\right) * V_{stock} - \left(\frac{A_{280,rinsing}}{x} * V_{rinsing}\right) \quad (2.2)$$

were: m_{Ab} is the mass of the bound antibody (mg); $c_{Ab,stock}$ and V_{stock} are the concentration (mg/mL; usually 0.05 mg/mL) and volume (mL) of the starting antibody solution respectively; $A_{280,after}$ is the absorbance at 280 nm of the antibody solution at the end of the incubation time; x is the expected absorbance of 1 mg/mL antibody solution in a 1 cm light path cuvette (mg/mL; usually 1.36 mg/mL); $A_{280,rinsing}$ and $V_{rinsing}$ are the absorbance at 280 nm and the volume (mL) of the rinsing fraction respectively.

2.2.2.5 Cell culture

All cell lines were cultured in static cell culture using RPMI medium, supplemented with 10 % (v/v) FBS. The complete growth medium was stored at 4 °C and used within one month.

Cryovials containing frozen cells were rapidly thawed in a 37 °C water bath and then transferred to a biological safety cabinet (Advanced Bio Safety Cabinet Class II, Astec Microflow, Andover, UK). The contents of each cryovial were then promptly transferred into a 15 mL centrifuge tube containing 10 mL of pre-warmed growth medium. Cell suspension was centrifuged in a Heraeus Labofuge 400R centrifuge (Thermo Scientific, Fisher Scientific, Loughborough, UK) at 200 g_{av} for 5 min at room temperature. The supernatant was decanted and the cell pellet was gently resuspended in 5 mL of growth medium. Cell viability was checked with Trypan blue exclusion assay and cells were counted using a Neubauer Improved Bright-Line haemocytometer (Sigma Aldrich, Gillingham, UK). Cells were subsequently seeded at a density of $3*10^5$ cells/mL in cell culture flasks and incubated in a Heracell 150i CO_2 incubator (Thermo Scientific, Fisher Scientific, Loughborough, UK) in controlled environment (5 % CO_2; 37 ºC). A complete growth medium exchange was performed every 48 h, with an aim not to exceed cell density of $1*10^6$ cells/mL. Viable cells were counted and $1*10^5$ cells/mL were seeded into fresh tissue culture flasks, filled with pre-warmed growth medium. If necessary were cell suspensions split between two or more flasks.

2.2.2.6 Isolation of red blood cells from umbilical cord blood

Red blood cells were isolated from umbilical cord blood by density gradient centrifugation. Routinely, fresh umbilical cord blood was diluted four times in PBS buffer supplemented with 2mM EDTA, The blood/buffer suspension (35 mL) was carefully layered over 15 mL of Ficoll-Paque Premium™ in a 50 mL centrifuge tube and centrifuged at 400 g_{av} for 30 min at room temperature in a swinging-bucket rotor Heraeus Labofuge 400R centrifuge (Thermo Scientific, Fisher Scientific, Loughborough, UK). The bottom layer containing the red blood cells was then transferred to a new 50 mL centrifuge tube and topped to the 45 mL with PBS and 2 mM EDTA buffer. The suspension was gently mixed by inversion and centrifuged once again at room temperature at 300 g_{av}

for 10 min. The supernatant was discarded and the pellet was diluted with PBS. The cells were stored at 4 °C and used within 2 weeks.

2.2.2.7 Cell labelling with antibody

Following centrifugation of cell culture or red blood cell suspension at 200 g_{av} for 5 min at room temperature, the supernatant was discarded and the cell pellet was resuspended in PBS buffer to a final concentration of $1*10^6$ cells/mL. The biotinylated antibody was added to the cells at a final concentration of 10 µg/mL and the mixture was left to incubate in the CO_2 incubator for 30 min, protected from the light. The cell suspension was centrifuged once again and the pellet was resuspeneded in PBS to a final concentration of $3.5*10^6$ cells/mL. The mass of antibody bound to the cells was calculated using equation 2.2 as described in Section 2.2.2.4.

2.2.2.8 Static binding studies

All static binding studies of the photosensitive materials were performed in 24 well non-treated cell culture plates at room temperature with shaking at 70 revs/min using a 3-D rocking platform.

The impact of the D-biotin on the viability of selected cells and their identity/functionality, cells were incubated in the presence of 0 to 3 mmol/L of D-biotin in PBS buffer for 2 h at room temperature, protected from the light. In addition, the impact of DSB-X biotin, a commercially available derivate of desthiobiotin with a seven-atom spacer, was evaluated at the concentration of 3 mmol/L.

Cell suspensions were centrifuged at 200 g_{av} for 5 min and $2.5*10^6$ cells in the pellet were resuspended in D-biotin or DSB-X biotin solution for 2 h. Cells were then collected and transferred into PBS buffer. Their viability and identify were assessed by flow cytometry (Guava easyCyte 8HT Flow Cytometer, Merck Millipore UK Ltd, Watford, UK).

The amount of the biotinylated BB7.2 antibody bound to the tetrameric or monomeric avidin immobilized on glass coverslips was determined as follows. The coverslips were first rinsed with PBS buffer and subsequently 400 µL of antibody solution of various concentrations (0–2 mg/mL) was added. After 2 h incubation at room temperature, the supernatants were collected and the coverslips were washed with 400 µL of PBS buffer. The absorbance of the supernatants and the washes was measured at 280 nm and the mass of bound antibody was calculated as described in Section 2.2.2.4 .

Cell binding capacities were evaluated for bound biotinylated CD20 antibody to coverslips and labelled cells with antibodies. In the first case, coverslips were incubated overnight at 4 °C in 20 µg/mL biotinylated antibody solution and then the next morning were coverslips gently rinsed by PBS buffer. In the second case, 5 mL of cell suspension ($2.5*10^6$ cells/mL) were incubated at room temperature on a 3-D rocking platform (70 revs/min) in the 50 µg/mL antibody solution in PBS buffer. After 1 h suspension was centrifuged at 200 g_{av} for 5 min, supernatant was decanted and pellet gently resuspended in 5 mL of fresh PBS buffer. For the cell binding studies, a set of coverslips in 24-well plates was prepared and gently rinsed by PBS buffer. To each well 400 µL of cell suspension was added with the concentrations from $2.5*10^4$ to $2.25*10^6$ cells/mL. The plates were gently agitated on a 3-D rocking platform (40 revs/min) for 30 min at room temperature, protected from the light. After completed incubation, suspensions were collected and coverslips gently rinsed by 1 mL of PBS buffer. Cells in the suspensions were evaluated and counted by Trypan blue exclusion assay (see Section 2.2.2.10, Equations 2.3 and 2.4).

The kinetics of cell attachment was determined using the two approaches presented in Figure 2.2, i.e. (A) coupling of biotinylated BB7.2 antibody (10 µg/mL) to tetrameric or monomeric avidin derived glass coverslips, followed by CCRF-HSB-2 cell binding; and, (B) binding of biotinylated BB7.2 antibody labelled CCRF-HSB-2 cells to tetrameric or monomeric avidin derived glass coverslips.

In both cases, the avidin derived or the BB7.2 functionalised glass coverslips were placed in 24 well plates and rinsed with PBS buffer. Cell suspension (400 µL of $3.5*10^6$ cells/mL) was added to each well and left to incubate on a 3-D rocking platform for the in between 0 and 8 h. At the end of the incubation, the supernatants were collected and the coverslips were washed with 400 µL of PBS. The residual cells in the supernatants and the washes were counted using a haemocytometer and their viability was checked with Trypan blue exclusion assay. The bound cells were then calculated by difference.

The kinetics of cell elution was tested using a 2 mM solution of D-biotin in PBS buffer. CCRF-HSB-2 cells ($2*10^6$ cells in PBS) were incubated with the avidin derived or the BB7.2 functionalised glass coverslips for 30 min. At the end of the incubation, the supernatants were collected, the coverslips were washed with 400 µL of PBS, and D-biotin solution (500 µL) was added to each well and left to incubate for various times (0 to 180 min). At the end of the incubation, the supernatants were collected and the coverslips were washed with 500 µL of PBS. The cells in all the supernatants and washes were counted using a haemocytometer and their viability was checked with Trypan blue exclusion assay.

Experimental data from static binding studies was fitted with One Site Saturation model with SigmaPlot 12.0 software (Systat Software Inc., Chicago, Illinois, USA). Determined were maximum number of adsorbed antibodies/cells (B_{max}), needed time to reach a half of maximal binding (k_t), binding rate (k_A) and dissociation constant (k_D).

2.2.2.9 Flow-based assay

A flow based assay is a simplified technique, developed for purposes of cell growth, adhesion, and attachment observation under controlled shear flow conditions, using glass hollow capillary tubes with a well-defined rectangular cross section and good optical quality. As shown in Figure 2.3, the system consists of a hollow capillary tube, which is glued to a microscope slide and mounted on microscope stage, a Harvard syringe pump and two flasks with cell suspension and cell-free buffer. Valves on the both flasks are connected with electronic valve (Cooke *et al*., 1993).

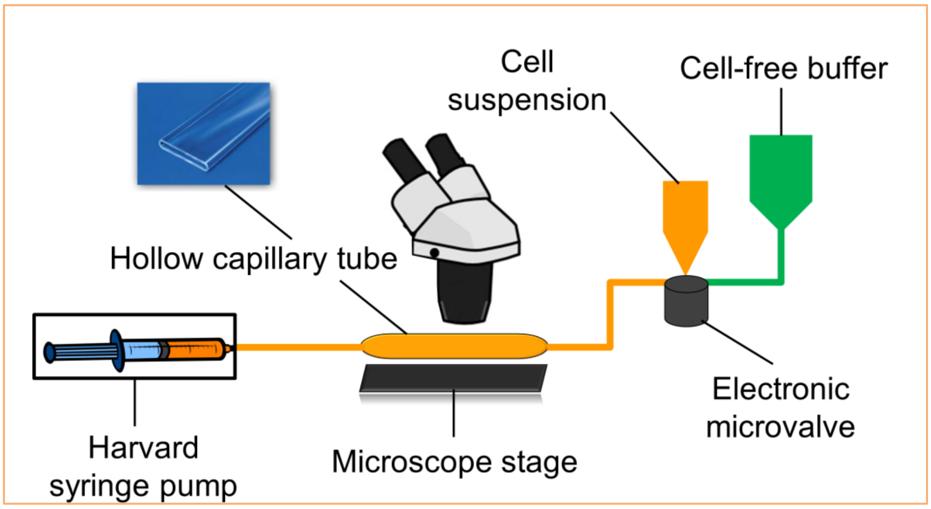

Figure 2.3: Schematic representation of the flow based assay set up. The system consists of: a hollow capillary tube mounted to a microscope stage; a Harvard syringe pump; two flasks with cell suspension and cell-free buffer; and, an electronic microvalve (redrawn from Cooke *et al.*, 1993).

The Olympus microscope (model IX70; Tokio, Japan) is connected to a video digitizer (Archimedes 310 microcomputer, Watford Electronics video digitizer; Watford Electronics, Watford, UK) thereby allowing for the on-line observation of cell attachment, rinsing of unbound cells, cell rolling and cell detachment. Consequently, the uniformity of the functionalised surface under observation as well as the ligand accessibility to the cells can be observed.

The glass hollow capillary tubes were cleaned, modified with aldehyde groups and functionalized with anti CD20 or Gly A antibody, biotinylated with D-biotin, as described in the Section 2.2.2.3. B lymphocytes or red blood cells from cord blood ($1*10^6$ cells/mL) were passed through the glass hollow capillary tubes at a flow rate of 30 cm/h (0.3 mL/min) until all cell suspension passed the capillary tube. The glass hollow capillary tubes were then rinsed with PBS buffer at 600 cm/h for 5 min and bound cells were eluted with 2 mM solution of D-biotin in PBS buffer at a flow rate of 30 cm/h until no more cells could be detected in the outlet.

2.2.2.10 Analytical methods

The surface area of the glass coverslips was measured by an ASAP 2020 accelerated surface area and porosimetry system (Micromeritics U.K. Ltd, Hexton, UK). The coverslips were degassed by means of a two-stage temperature ramping under a vacuum of <10 mmHg, followed by sample analysis at -169 °C using nitrogen gas. The surface area was determined from adsorption isotherms by the Brunauer, Emmett and Teller (BET) theory (Lowell *et al*., 2006).

The reactive amino groups on the supports were assessed with the TNBS assay. Existing amino groups would react with TNBS to form a highly coloured complex (Halling and Dunnill, 1979). The assay was performed according to Hermanson *et al.* (1997). For this an aqueous mixture of 1 M TNBS (10 µL) and 0.05 M solution of Borax (1.5 mL) was added to an aminated support and heated up to 70 °C in water bath, before being cooled to room temperature. Both coverslips and hollow capillary tubes were then consecutively washed with water, 50 % acetone in water (v/v), 100 % acetone and finally twice with water. To each sample, 5 mL of 1 M solution of NaOH was added, in order to release picric acid (2,4,6-trinitrophenol). Finally the samples were heated up to 70 °C and left to cool to room temperature. For the determination of TNBS, the absorbance of the suspensions was read at 410 nm using a UV-VIS spectrophotometer. Samples were compared with standards (Appendix A) prepared by various dilutions of picric acid in 1 M NaOH.

The presence of the amino reactive groups together with the aldehyde groups introduced by coupling the oxidized dextran to the amino-activated surfaces, was assessed using K-Alpha X-ray Photoelectron Spectrometer (XPS) System (Thermo Fisher Scientific, Waltham, Massachusetts, USA). A detailed analysis of carbon (C), nitrogen (N), sodium (Na), oxygen (O), silicon (Si), boron (B) and iodine (I) was carried out on the 0.16 mm^2 sample area at room temperature with the ion gun operated in the range of 50-1500 eV.

The mass of immobilized avidin was determined by the Pierce™ Bicinchoninic acid (BCA) Protein assay. For the assay, to the samples 50 µL of water and 950 µL of BCA reagent, prepared according to the manufacture's manual, were added. Samples were incubated for 1 h on a 3-D rocking platform (70 revs/min) at room temperature. Optical density of slurries was measured at a wavelength of 562 nm. Samples were calibrated against albumin in water (Appendix B).

Determination of the functional biotin binding sites of the immobilized avidin, which is usually lowered by active side blocking, denaturation, and steric hindrance, which was assessed calorimetrically. At first biotin *p*-nitrophenyl ester was dissolved in 100 µL of DMSO and then diluted in 0.5 M $C_2H_3NaO_2$ buffer, pH 5, to the final concentration of 0.2 mg/mL. Solution was immediately filtered and optical density was measured at 210 nm. Meanwhile supports were equilibrated in 0.5 M $C_2H_3NaO_2$ buffer, pH 5. Then 2 mL of prepared biotin *p*-nitrophenyl solution was added. In the next step, supports were rinsed several times with water. Yellow *p*-nitrophenol was eluted using 400 µL of 0.1 M NaOH solution. Optical density of eluted fractions was measured at a wavelength of 410 nm. Number of biotin binding sites calculated using equation 2.3:

$$N = A_{410nm} * V * x * M_{biotin} \qquad (2.3)$$

were: N represents number of biotin binding sites (µg biotin bound per mL of support), A_{410nm} absorbance at 410 nm, V fraction size (mL), x number of collected fractions and M_{biotin} molecular weight of biotin (244.3 g/mol).

The content of free soluble biotin in the fractions collected during the monomeric avidin immobilization were analysed by label-free Quant*Tag™ Biotin Kit. Working solution and standards were prepared according to the manufacturer. To the 20 µL of the sample or standard, 1 mL of working solution was added and incubated for 30 min at room temperature on a 3-D rocking platform. The absorbance of the slurries was measured at 535 nm and biotin was determined from the standard curve (Appendix C).

The surface of fully functionalized coverslips was visualized with 1530 VP scanning electron microscope (SEM; Carl Zeiss Microscopy Ltd, Cambridge UK). The analysis was carried out at room temperature and accelerating voltages of 1-30 kV were used. Coverslips were dried in advance at room temperature and immobilized on the aluminium stubs with double sided adhesive carbon conductive dots. Silver paint was placed on the side of the supports to act as a conductor and the samples were derived with gold in an argon atmosphere before imaging.

Cells were counted and their viability checked with Trypan blue exclusion assay using a haemocytometer. Cell suspensions were gently mixed with 0.4 % solution of Trypan blue with a 1:1 ratio (v/v). To a chamber, 10 µL of the prepared suspension was pipetted. All cells (non-viable cells were stained blue, viable cells remained opaque) were counted in at least one square under 40x magnification using Nikon Eclipse E200 microscope (Nikon Corporation, Tokyo, Japan). The total number of cells in a sample was calculated using equations 2.4 and 2.5.

$$Nr_{total} = A_{per\ square} * x * 10^4 * V_{sample} \tag{2.4}$$

Nr_{total} is the total number of cells in the suspension, $A_{per\ square}$ is the average cell count per square, x is the dilution factor and V_{sample} is the initial volume of the cell suspension. The calculation of the percentage of viable cells in the suspension was done by the following equation

$$viability = \frac{A_{viable}}{A_{total}} * 100 \tag{2.5}$$

were A_{viable} is the number of viable cells counted and A_{total} represents the total number of counted cells.

Immunophenotypic analysis of cells was determined by flow cytometry using Guava easyCyte 8HT flow cytometer (Merck Millipore UK Ltd, Watford, UK) with excitation at 488 and 640 nm. Cells for the analysis were centrifuged at 300 g for 5 min, then the supernatant was removed and the pellet resuspended in PBS buffer. Biotinylated antibodies remained on the surface of the cells were targeted with SAPE. Cells were incubated at room temperature for 30 min in the darkness. Just before the analysis 5 µL of 7-AAD viability dye was added. A minimum of 5,000 events per sample were recorded. Data was analysed with InCyte software (Merck Millipore UK Ltd, Watford, UK).

2.3 RESULTS AND DISCUSSION

2.3.1 PREPARATION AND CHARACTERIZATION OF GLASS SUPPORTS

Surface area of a single glass coverslips was determined to be 0.798392 cm^2, which is similar to the theoretical value of 0.785398 cm^2.

Preparation of glass supports for reversible cell separation can be divided into three distinct phases: (i) reductive surface amination; (ii) preparation of dextran-derived glass coverslips; and (iii) immobilization of monomeric avidin. In the first stage, reductive amination of the surface was performed with 3-APTES, followed by immobilization of oxidized dextran. Both techniques were adopted from Massia and Stark (2001). In the third phase, tetrameric egg white avidin was at first immobilized on the dextran-derived glass coverslips, and then its subunits were dissociated under denaturing conditions (Sproβ and Sinz, 2012; Hermanson *et al*., 1997).

Reactive amino groups on the glass coverslips were determined using an assay originally described by Halling and Dunnill (1979) employing TNBS. A high degree of the reproducibility between batches was achieved during the deposition of amino groups onto support. On the average (result is based on the 4 batches of aminated glass coverslips produced), 11.65 ± 0.05 mmol of picric acid was released per cm^2 of the support.

XPS analysis was performed on amino- and aldehyde-derived coverslips and results were compared to non-modified coverslips. Table 2.3 summarizes the atomic percentages (%) of the detected elements in the overall scan of the support.

Table 2.3: X-ray photoelectron spectroscopy survey of non-modified, amino- and aldehyde-derived glass coverslips. Data presented is an average based on three analyses across the coverslip.

Element	Non-modified glass coverslips	Amino-derived glass coverslips	Aldehyde-derived glass coverslips
C (atomic %)	18.82	6.00 ▼	8.18 ▲
N (atomic %)	N/D*	1.18 ▲	1.09 ▼
Na (atomic %)	3.09	0.94 ▼	1.35 ▲
O (atomic %)	47.49	58.32 ▲	56.59 ▼
Si (atomic %)	22.93	27.78 ▲	28.01 ▲
B (atomic %)	3.26	3.08 ▼	2.65 ▼
Ti (atomic %)	0.63	0.69 ▲	0.59 ▼
Zn (atomic %)	1.06	0.48 ▼	0.33 ▼
K (atomic %)	2.72	1.53 ▼	1.22 ▼

*N/D not detected, **▼decrease,** **▲increase**

The deposition of 3-APTES on the surface of glass coverslips results in the decrease of atomic percentage of carbon (C), sodium (Na), boron (B), zinc (Zn) and potassium (K), the major components of glass coverslips. An increase in nitrogen (N), oxygen (O), silicon (Si) and slightly titan (TI) was observed. This correlates with the elemental composition of 3-APTES. The increase of titan is most likely due to the surface sensitivity of the XPS and is therefore not relevant for this study. The detailed scan of Si has relieved the decrease in silicon dioxide (SiO_2), also known as silica, one of the major components in glass. An increase of silane (SiH_4) is also noted, which is part of 3-APTES. The results achieved by XPS-analyses indicates that the deposition of amino groups was successful.

In comparison to the analysis of amino-derived coverslips, covalent coupling of oxidized dextran (deposition of aldehyde groups) to the amino-derived supports leads to the increase of the atomic percentage of C, Na and slightly Si. The atomic percentage of all other elements has decreased, as expected, due to the elemental composition of oxidized dextran (Figure 2.1). High-resolution scan of C1s has shown the presence carbon connected to other elements in three different ways, namely (i) C in the ring; (ii) C-O-C or C-OH; and (iii) O-C-O. All three relations are present in the structure after completed deposition of aldehyde groups. Increase of Na is most likely due to the surface modification method, i.e. coupled oxidized dextran is furthermore oxidized by $NaIO_4$.

The biotin binding capacities of samples of immobilized tetrameric and monomeric form of avidin after completed dissociation were evaluated using a BCA-protein determination kit, following the modified procedure first described by Sorensen and Brodbeck (1986). Figure 2.4 shows that after dissociation of tetrameric avidin, the mass of bound protein is significantly reduced from tetrameric (black bar) to monomeric (light grey bar) avidin. After blocking the non-reversible biotin binding sites, the mass of accessible immobilized protein is further reduced (dark grey bar).

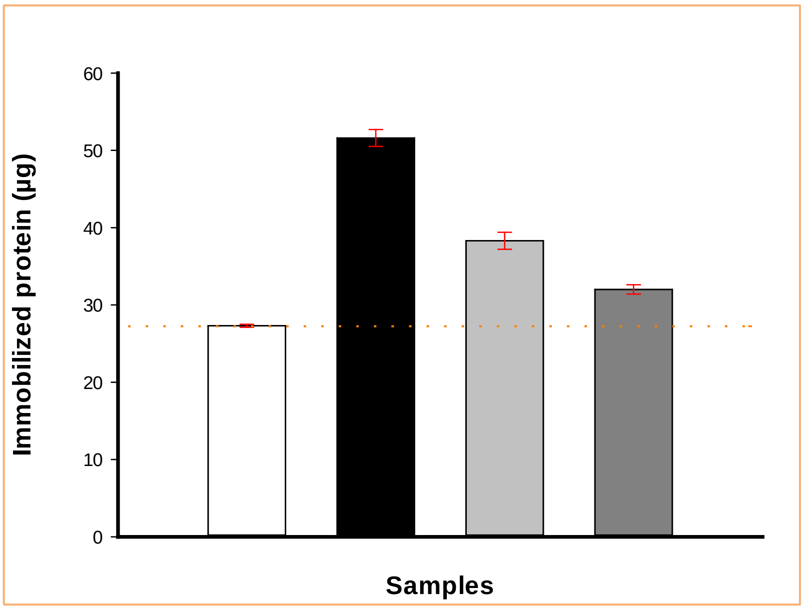

Figure 2.4: Immobilized forms of avidin on the surface of aldehyde-derived coverslips analysed by BCA assay. Mass of accessible tetrameric (black bar), monomeric avidin (light grey bar) and immobilized avidin after blocking of non-reversible biotin binding sites (dark grey bar). Immobilized aldehyde groups on glass coverslip (white bar) react with BCA assay reagent. Presented data is based on 10 analysed batches of coverslips. Bars represent an average, while error bars standard deviation.

After dissociation, native tetrameric, avidin is cleaved into four identical subunits - monomers (Figure 2.5). Each monomer has one biotin binding site, which remain intact after dissociation. The number of biotin binding sites is expressed as a mass of biotin bound per area.

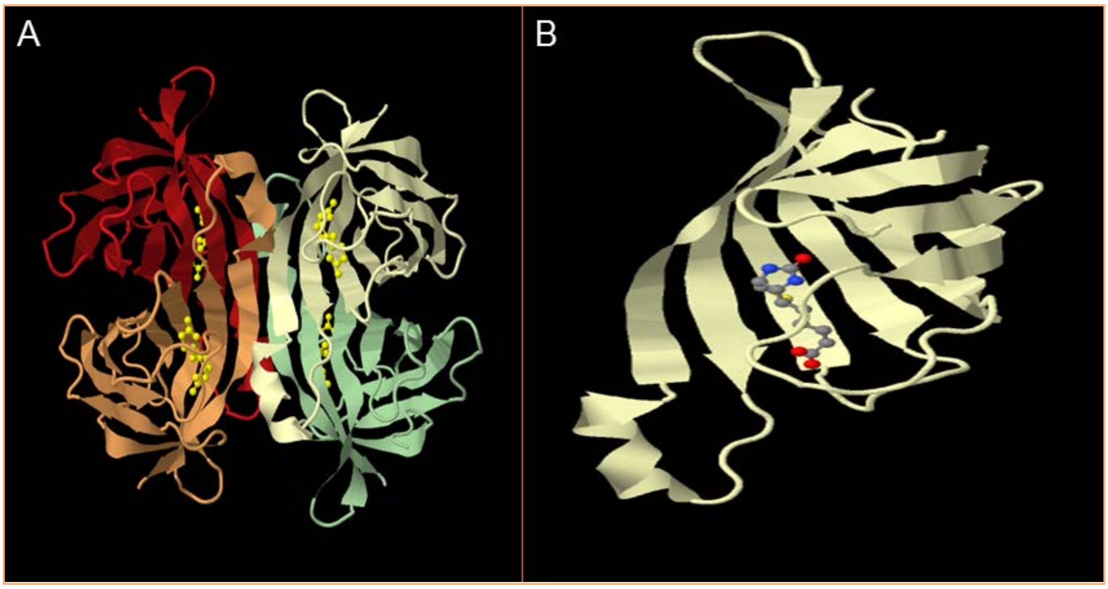

Figure 2.5: Avidin egg white structure (Livnah *et al*., 1993; structures obtained through RCSB Protein Data Bank). (A) 3D structure of avidin. Avidin is a symmetrical tetrameric glycoprotein, which consists of four identical subunits (red, white, ochre and green). Each subunit has one biotin binding site (yellow atoms). (B) Biotin molecule bound to monomeric avidin.

As bicinchoninic acid acts as a detection reagent for the formation of copper I from copper II in the presence of proteins (Hermanson *et al*., 1997), BCA assay was introduced for the evaluation of the covalently bound avidin on the surface. Based on the structure of avidin and its subunits it would be expected that the difference in the mass of the immobilized monomeric avidin would be four times lower than the mass of tetrameric avidin, but this is not the case. Additionally, it was observed that oxidized dextran immobilized on the support reacts as well with BCA assay reagents and gives a signal. Furthermore, the quantity of covalently bound protein per support is usually in the nanomolar range, but the statistical analysis has shown that the mass of the immobilized protein on the support from the same batch and even between batches produced on different occasions differs for less than 5 %. After completed dissociation of tetrameric avidin, the mass of immobilized protein assessed with BCA assay was reduced for 25.8 % and for further 16.4 % after irreversible biotin binding sites were blocked (Figure 2.4), which correlates with the data reported so far (Table 2.1; Hermanson *et al.*, 1997). Based on this, complete dissociation of the tetrameric avidin into its subunits was not expected, either achieved. On the support are left most likely immobilized all four forms of avidin – monomers, dimers, trimers and tetramers. To avoid confusion, the phrase “monomeric avidin” is from this point onwards used for the avidin after completed dissociation.

It is not necessary that only monomers have reduced dissociation constant for biotin (Green and Toms, 1973), therefore to assess the actual functional capacity of immobilized avidin on the support the determination of the number of biotin binding sites was employed.

As previously mentioned, when the protein is coupled to solid supports, the maximum binding potential is typically lowered by the blocking of the active site, denaturation and steric hindrance. Coupling of biotin *p*-nitrophenyl ester to the functionalized support with avidin allows for the measurement of the number of biotin binding sites. Cleavage of *p*-nitrophenol results in only biotin being bound to the avidin. Theoretically, avidin has a maximum activity of 14.4 units per milligram of protein (Hermanson *et al*., 1997). The mass of remaining biotin on the support after cleavage was determined to be 0.27 ± 0.1 µg/cm^2, but the distinction in the number of biotin binding sites between different conditions was less than 5 %. Due to the nature of the assay, the difference represents experimental mistake and not actual variation between accessible biotin binding sites. It is believed that the surface area of 0.798 cm^2 of each glass coverslip is too small for definitive conclusions.

Free biotin remained in the buffer after blocking of non-reversible binding sites was assessed. From 0.4 mM of biotin initially present in the blocking solution, 0.03 mM (less than 10 %) remained bound to the supports. The results correlates with reports from Green and Toms (1973) and Sproβ and Sinz (2012), who suggest that after activation of immobilized tetrameric avidin with $NaBH_4$, 90 % of the subunits remained on the surface allow reversible binding of biotin.

SEM image of non-modified and fully functionalized glass coverslip are shown in Figure 2.6.

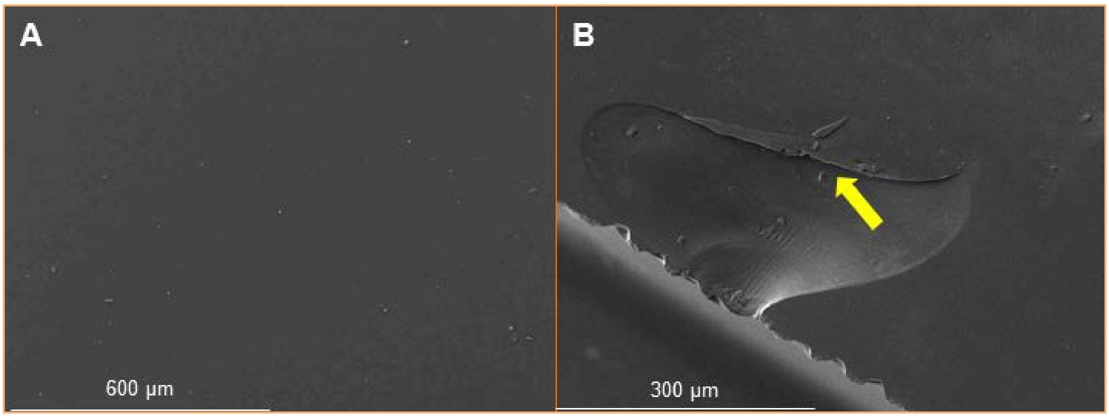

Figure 2.6: SEM analysis of non-modified and fully functionalized glass coverslip. (A) Surface of non-modified glass coverslip (600x magnification). (B) Surface of fully functionalized glass coverslips (450x magnification). The corner of the support was deliberately snapped off, so that the grafted layer (yellow arrow) can be observed. The visual appearance of all 3 analysed coverslips from various surface functionalization batches was similar.

From the SEM images a good dispersion of grafted layers is observed. The coating was so uniform that under 600x magnification it was impossible to detect the grafted film, therefore the corner of fully functionalized coverslips with biotinylated antibody was deliberately snapped off.

2.3.2 STATIC BINDING KINETIC TESTS

2.3.2.1 The impact of free biotin on cells

Prior to experiment to competitive elution of cells with biotin, the impact of various concentrations of D-biotin and DSB-X biotin on the viability of Toledo cell line and their identity/functionality was investigated. After 2 h incubation, no differences in the cell viability were detectable by Trypan blue exclusion assay. In all cases the calculated viability (Equation 2.4) was above 99 %. The starting cultures and the cells obtained after the experiment were analysed by flow cytometry to determine the expression of CD20 membrane antigen and viability was proven with 7-AAD (Table 2.4).

Table 2.4: Expression of CD20 cell surface marker and cell viability of a Toledo cell line after 2 h exposure to D-biotin and DSB-X biotin. The experiment was performed in 3 parallels using glass coverslips from different surface modification batches; the presented data is an average.

	Biotin concentration (mM)	CD20 positive and viable cells (%)	CD20 positive and dead cells (%)	CD20 negative cells (%)
D-biotin	0	98.58	0.00	1.42
	0.5	97.67	0.22	3.11
	1	97.26	0.00	2.74
	1.5	97.13	1.22	1.65
	2	97.16	0.17	2.67
	2.5	97.08	1.84	1.08
	3	96.55	1.38	2.07
DSB-X biotin	0	98.44	0.01	1.55
	2	97.25	1.64	1.10

Before and after the assay, more than 96 % of cell population was viable and positive for CD20. This suggests that neither D-biotin nor DSB-X biotin have impact on their immunophenotype and viability. In comparison to the control populations, the viability has decreased by time, but not significantly. Based on the experimental results, D-biotin solubility in PBS buffer is poor above 3 mM, additionally there was no significant difference observed between the elution efficiency with 2 mM or 3 mM D-biotin solution. Therefore it has been decided to use both biotins for further studies (see Section 2.3.2.4) at the previously recommended concentration of 2 mM (Hermanson *et al*., 1997).

Besides D-biotin and DSB-X biotin a wide selection of commercially available biotins were considered as potential biotinylation reagents and/or compounds of the elution buffer to even further reduce the dissociation constant between immobilized monomeric avidin and biotin. Due to the narrow window of cell-friendly conditions, they were all disproved. For example, 2-iminobiotin, popular guanidine analogue of D-biotin in protein separations, is not appropriate due to its poor solubility at physiological pH. Furthermore, the dissociation constant of avidin-biotin complex is pH sensitive and will bind even tightly at natural and acidic pH, with the strongest bond at pH between 9.5 and 11 (Hofmann *et al*., 1980). Other popular and commercially available biotins (*e.g.* iodoacetyl-LC-biotin) were rejected due to their insolubility in water and therefore they must be at first dissolved in dimethylformamide (DMF) or DMSO before diluting in water containing buffers (Elia, 2008). Both, DMF and DMSO, are cytotoxic, which leads to loss of cell functionality and can produce side effects in patients (Jeffers *et al*., 1995; Katkov *et al*., 2006).

2.3.2.2 Kinetics of binding of biotinylated antibody to immobilized avidin

The adsorption kinetics of the biotinylated BB7.2 antibody on glass coverslips functionalized with either monomeric or tetrameric avidin is presented in Figure 2.7. Until 60 min of incubation, there are no significant differences in the binding of biotinylated antibody to the monomeric and tetrameric avidin. After 1 h (nearly 40 % of antibody was bound to the modified support), binding of antibody to the monomeric avidin was occurring faster in comparison to the tetrameric avidin. This is most likely due to the steric hindrance present in case of tetrameric avidin, therefore the antibody bound faster to the easier accessible monomer. After 8 h of incubation more than 80 % of antibody was bound to the immobilized monomeric and tetrameric avidin.

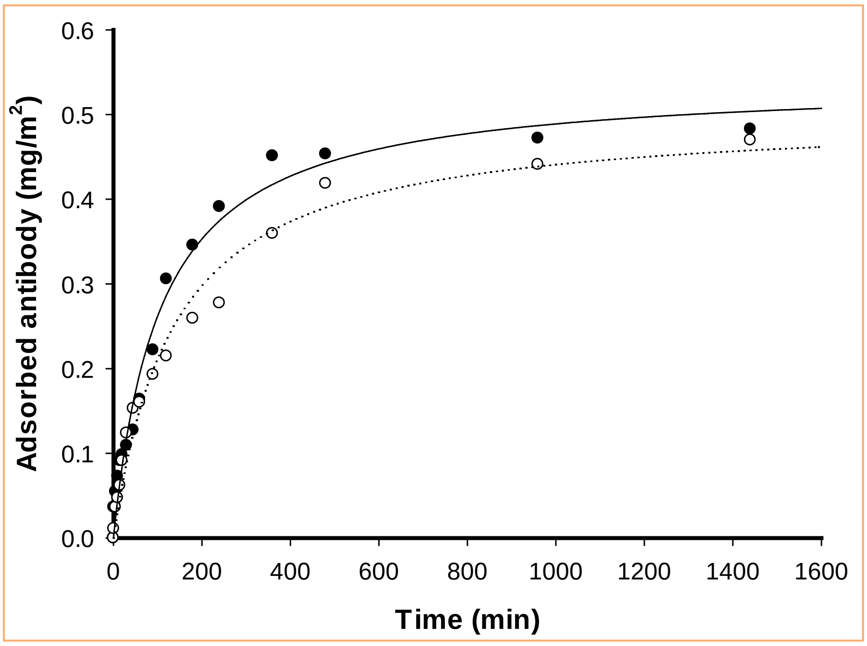

Figure 2.7: Adsorption of biotinylated BB7.2 antibody on glass coverslips, functionalized with tetrameric (white circles) and monomeric (black circles) avidin, respectively. The experiment was performed in 3 parallels, dots represent an average value. Maximum antibody adsorption is 0.5410 mg/m^2 for monomeric avidin and 0.5009 mg/m^2 for immobilized tetrameric avidin. Half of the maximum antibody adsorption is achieved within 106.5 min (monomeric avidin) and 136.3 min (tetrameric avidin). In both cases is rate of adsorbed antibody determined as 0.004 mg/m^2*min.

2.3.2.3 Binding capacities of functionalized glass surfaces

The binding capacity of prepared glass coverslips was evaluated by targeting immobilized antibody with B lymphocytes (Toledo cell line) and by application of antibody-labelled cells to the glass support (Figure 2.8).

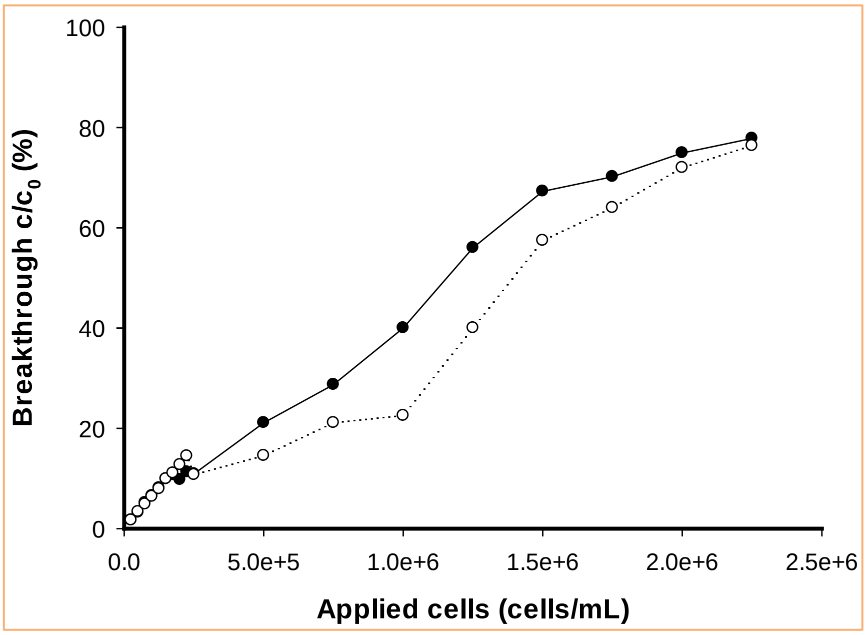

Figure 2.8: Binding capacity for the binding of B lymphocytes to the glass coverslips for the biotinylated antibody bound to the cells (black circles) and bound to the coverslips (white circles)

The comparison of specific binding of B lymphocytes to the avidin modified glass coverslips revealed slight differences in the biding of antibody labelled cells and cells binding to the immobilized biotinylated antibody. Binding up to the 2.5*10^5 cells/mL no significant differences were observed, as well as above 2.0*10^6 cells/mL. The binding efficiency between stated concentrations was improved when antibody was conjugated to cells in advance. The reason for this might be the differences in the kinetics of cell binding, as well as due to the multivalent cell attachment and consequently steric hindrance (Magdelin and Moser, 2012) – on the each cell is more than one surface antigen and each can bind to the antibody, additionally one antibody can bind to two antigens (Ginaldi *et al*., 1998). As the goal of the cell binding to the glass coverslips was to maximize the binding efficiency (with the 2.25*10^6 cells/mL nearly 80 % breakthrough was achieved) and simultaneously to use enough cells to be able to count them with haemocytometer and check their viability with Trypan blue exclusion assay, it was decided to proceed with cell concentrations above 2.0*10^6 cells/mL.

2.3.2.4 Kinetics of cell binding to functionalized glass surfaces

For a better understanding of cell attachment on immobilized monomeric and tetrameric avidin through biotinylated complementary antibodies, a set of static kinetic tests was performed on non-porous glass coverslips. For this purpose Bristol-8 cell line and biotinylated BB7.2 antibody were used. As seen in Figure 2.9, cell attachment depends on the type of immobilized avidin as well as on the location of biotinylated antibody. When cells were pre-labelled with complementary biotinylated antibodies and contacted with monomeric avidin derived glass coverslips, the kinetics of cell binding were markedly improved when cells in comparison to non-labelled cells attaching to antibody linked supports. It is believed that this is due to the fact, that when antibodies are bound to the surface antigens of cells are orientated in the most optimal way, so consequently a tail of antibody, where biotin is bound, is directly exposed to the immobilized form of avidin (Magdelin and Moser, 2012). When biotinylated antibodies are at first bound to the avidin, they might not be orientated in the optimal way. From the Figure 2.9 below can be as well seen that there are no significant differences between binding cells on the monomeric or tetrameric immobilized avidin through biotinylated antibody. The reason for this might be the avidin immobilization procedure. At first is tetrameric avidin bound to the support and then cleaved to achieve the monomeric form. According to the previous reports this results in the most optimal organization and orientation of protein with minimal steric hindrance (Massia and Stark, 2001).

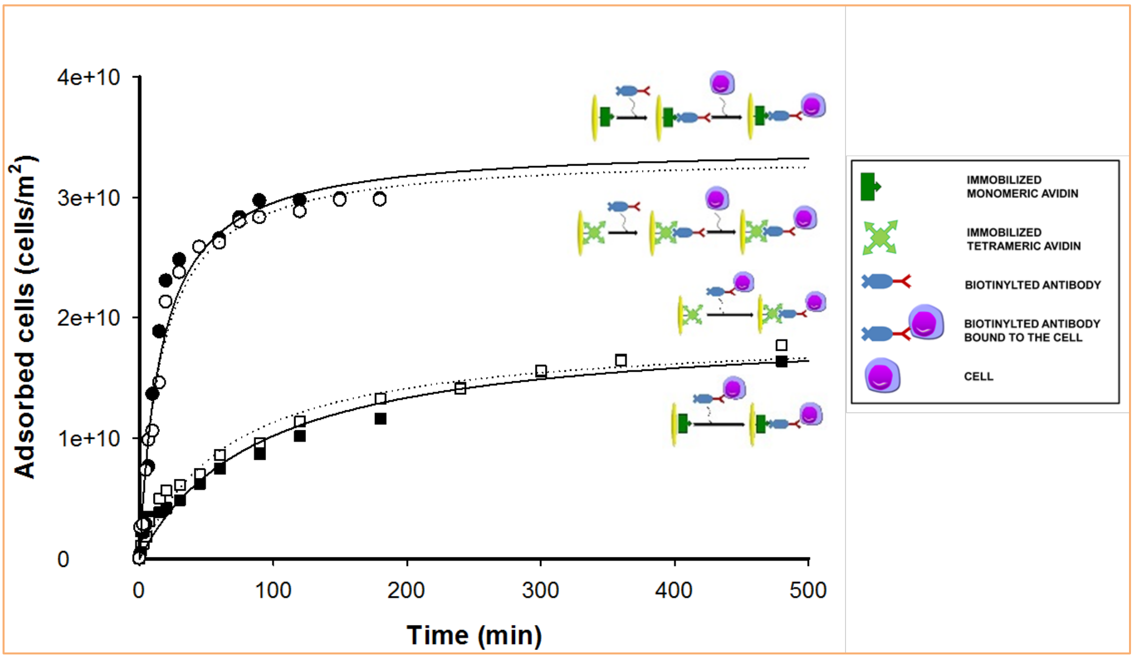

Figure 2.9: Kinetic static test of cell attachment. Comparison of binding kinetics of unlabelled target cells on biotinylated "antibody labelled" glass coverslips (monomeric avidin, white circles; native avidin, black circles) and of biotinylated "antibody labelled cells" to complementary native (white squares) and monomeric (black squares) avidin. There were no differences observed between tetrameric and monomeric avidin in terms of maximum binding capacity (3.4*10^{10} cells/m^2 when antibody is immobilized on the surface *vs*. 1.9*10^{10} cells/m^2 when cells are incubated in advance in antibody solution) as well as half of all adsorbed cells is adsorbed within 16.5 min when antibody is on the surface *vs*. 67 min when antibody in on cells.

Interestingly, the adsorption capacity of prepared supports is nearly 1.8 times greater when antibody is in advance immobilized on the avidin-derived glass support. Additionally, when comparing adsorption rates, the difference is even greater – adsorption is 20 times greater when antibody is immobilized on the surface (1.5*10^9 cells/m^2*min *vs*. 7.5*10^7 cells/m^2*min). This suggest that kinetics of binding is dependent more on the how is affinity ligand immobilized on the surface, rather than the form of immobilized avidin. By binding antibodies to the cells the impact of site hindrance is greater, therefore it takes more time to specifically bind biotinylated antibody to the avidin matrix. This might have impact on the chromatography-based separations and it might require decrease of loading flow rates in order to optimize binding efficiency.

At this stage non-specific cell binding to amino- and aldehyde-derived glass coverslips was evaluated. After completed incubation and gentle rinsing, no cells remained bound to the support, which confirms previous reports by Österberg *et al.* (1993; 1995), who state that grating oxidized dextran to the surface reduces non-specific binding.

2.3.2.5 Kinetics of cell elution from functionalized glass surfaces

As suggested by Hermanson *et al*. (1997), cell elution was performed using 2 mM solution of biotin. At first, Brisol-8 cell line was bound to the fully functionalized support through biotinylated BB7.2 antibody, followed by an elution up to a 3 hr. Bristol cell line and CCRF-HSB-2 cell line (T lymphocytes) were chosen as an alternative to Toledo cell line. The choice of the cell line was made based on the expression of the surface markers, *i.e*. number of HLA-A2 antigens on the surface of B lymphocytes is similar to the expression of CD20 surface antigens of Toledo cell line. As shown in Figure 2.9, cell elution experiments were conducted with two different antibody biotinylation reagents, D-biotin and DSB-X biotin.

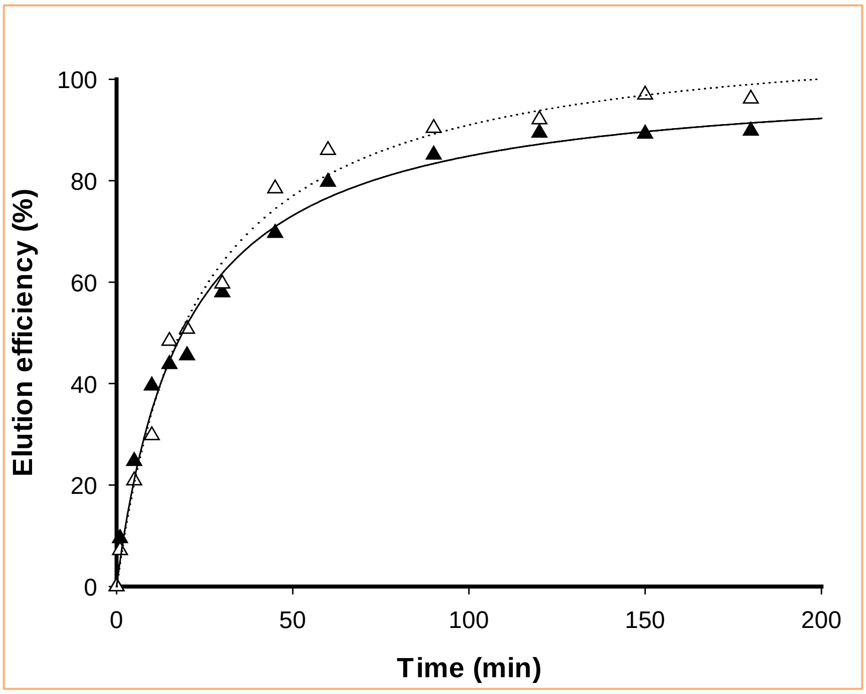

Figure 2.10: Cell detachment studies of Bristol-8 cell line (T-lymphocytes) bound to the glass coverslips through biotinylated BB7.2 antibody. In the study the elution kinetics between D-biotin (black triangles) and DSB-X biotin (white triangles) as antibody biotinylation reagent was compared. Experiment was performed in 3 parallels with triangles representing the average value. The dissociation rate, k_D, was determined to be in both cases $5*10^4$ cells/min. Half of cells were eluted within 19 min (D-biotin) and 22 min (DSB-X biotin).

DSB-X was introduced because its seven-atom spacer could potentially improve and hasten competitive elution of cells. However, this couldn’t be observed in the static test conducted on non-porous glass coverslips. Also no significant differences in comparison to D-biotin as biotinylation reagent was detectable, but it is believed that DSB-X biotin would improve cell elution in online experiments using various chromatographic supports, due to its 8 atom spacer. After 1 hr of incubation in 2 mM D-biotin or DSB-X solution in 1x PBS, approximately 80 % of cells were eluted with a viability of at least 98 % (Trypan blue exclusion assay). The immunophenotypic analysis of cells after elution has relieved the presence of HLA-A2 marker on the surface of eluted cells. In both cases more than 98 % of cell population was positive for HLA-A2 and at the same time in a viable form after 7-AAD staining. In contrast, the number of eluted cells bound on the immobilized tetrameric avidin was below the limit of detection.

The elution experiments were repeated with Toledo cell line and red blood cells. In both cases, approximately 80 % of cells were eluted within 30 min of elution on static test, as shown in Figure 2.11.

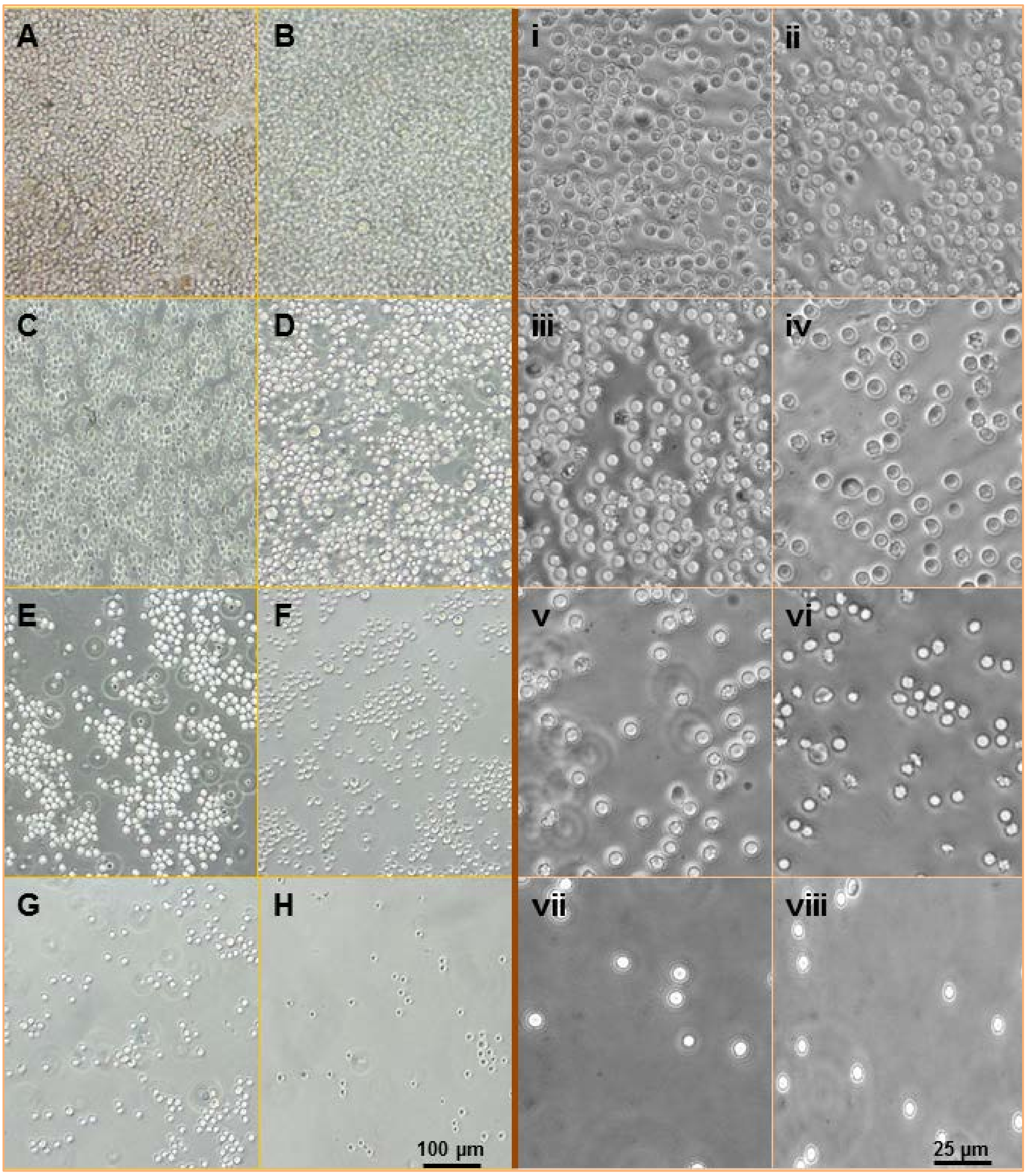

Figure 2.11: Photographs of bound B lymphocytes (Toledo cell line) and red blood cells on glass coverslips during elution under 4x magnification (Toledo cell line, A-H) and 10x magnification (red blood cells; i-viii). Photos of cells after completed incubation (A; i), after rinsing with 1x PBS (B; ii), after 1 min (C; iii), 5 min (D; iv), 10 min (E; v), 15 min (F; vi), 20 min (G; vii) and 30 min of elution (H; viii).

2.3.3 FLOW-BASED ASSAY

Following the successful elution of bound cells, the technology was tested under flow conditions in small scale using glass hollow capillary tubes. The monomeric avidin coated glass tubes were functionalized with the biotinylated antibody as described in Section 2.2.2.3. This method was adopted only for the initial qualitative analysis of functionalized surfaces; as the surface area of the single tube was too small to reliably assess modification and functionalization steps of material preparation. Additionally the number of cells used for the single experiment was below the limit of detection for Trypan blue exclusion assay and consequently cell count with haemocytometer.

Following the binding of B lymphocytes (Toledo cell line) to the support through the biotinylated anti-CD20 antibody, cell binding and elution under flow conditions were observed. Both, cell attachment and elution with 2 mM solution of D-biotin in PBS buffer were performed at a linear flow rate of 30 cm/h. In Figure 2.12 photographs of the inside of glass hollow capillary tube under 4x magnification taken during binding, rinsing of not bound and even weakly bound cells and elution are presented. After 30 min of elution significantly fewer cells remain bound in comparison to the beginning of elution.

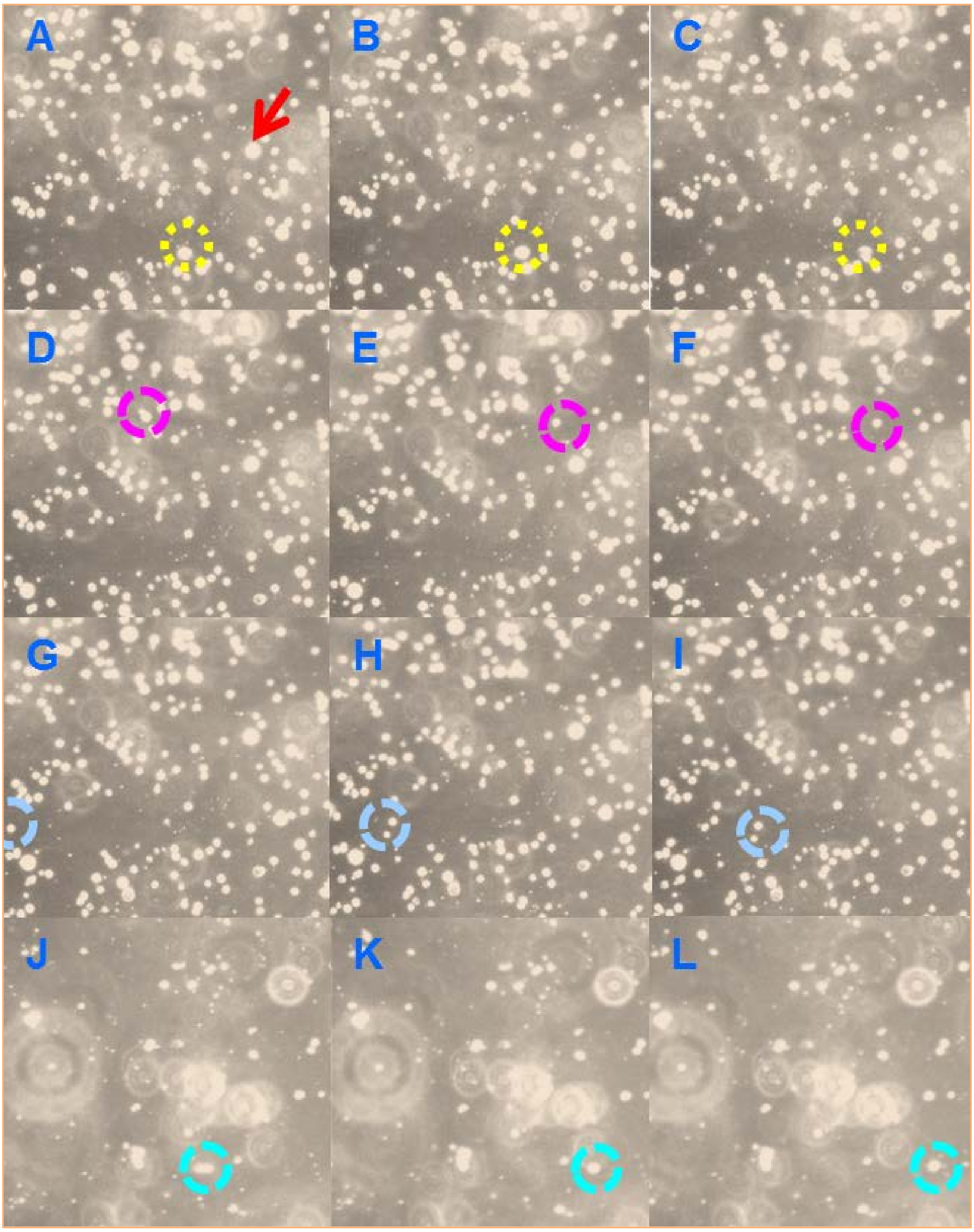

Figure 2.12: Video frame sequences of B lymphocytes (Toledo cell line) flowing through mono-avidin coated glass hollow capillary tubes functionalised with the biotinylated anti-CD20 antibody. During cell attachment (1st row) bound cells (frame A; marked with arrow) and cells passing through the hollow capillary tube (frames A-C, yellow circles) can be observed. During washing (2nd row; frames D-F), unbound and weakly-bound cells (pink circles) are passing through. Elution was performed for 30 minutes (3rd and 4th row). After 5 min cells are already eluted (frames G-I; blue circles), after 30 min significantly less cells remains bound and eluted cells are still passing through (frames J-L; turquoise circles).

Although flow-based assay was used only for the visual assessment of the developed affinity based system for the separation of human cells under flow conditions, it did confirm adequacy of the technology for the further application in the chromatography-based positive selection. As the elution took approximately 30 minutes, it was clear there is a need for the optimization of separation conditions, *e.g*. number of applied cells, flow rates and number of immobilized ligands, in order to be able to separate cells relatively fast, efficiently and in a viable form.

2.4 CONCLUDING REMARKS

In order to develop a new gentle and efficient affinity based separation technique for the purification and fractionalization of human cells a new system using, cell-friendly adsorbent materials was developed. Dextran has proven to be an appropriate choice for the base grafted layer, as it is not cytotoxic and the non-specific cell binding is minimal. In combination with monomerized avidin and biotinylated antibodies it allows an efficient binding of cells with a high affinity. At the same time it is possible to elute cells in a gentle manner with competitive binding using various biotins. It has been shown that by using affinity based separation technique; human cells can be separated under physiological conditions. This was demonstrated with B and T cells from human continuous cell lines.

Following the successful characterization and static studies on glass coverslips, the method was subsequently transferred to hollow capillary tubes for the qualitative verification. The study has demonstrated the considerable potential for application of developed technology to the affinity chromatography. Therefore, future work will concentrate on the transfer of the technology to the existing chromatography supports, *i.e*. packed bed columns.

2.5 REFERENCES

Cole S.R., Ashman L.K. and Ey P.L. 1987. Biotinylation: An alternative to radioiodination for the identification of cell surface antigens in immunoprecipitates. *Molecular immunology*, vol. 24, no. 7, pp. 699-705.

Cooke B.M., Usami S., Perry I. and Nash G.B. 1993. A simplified method for culture of endothelial cells and analysis of adhesion of blood cells under conditions of flow. *Microvascular Research*, vol. 45, no. 1, pp. 33-45.

Cronan J.E. Jr. and Reed K.E. 2000. Biotinylation of proteins *in vivo*: A useful posttranslational modification for protein analysis. *Methods in enzymology*, vol. 326, pp. 440-458.

Diamandis E.P. and Christopoulos T.K. 1991. The biotin-(strept)avidin system: Principles and applications in biotechnology. *Clinical Chemistry*, vol. 37, no. 5, pp. 625-636.

Diogo M.M., da Silva C.L and Cabral J.M.S. 2012. Separation technologies for stem cell bioprocessing. *Biotechnology and bioengineering*, vol. 109, no. 11, pp. 2699-2709.

Elia G. 2008. Biotinylation reagents for the study of cell surface proteins. *Proteomics*, vol. 8, no. 19, pp. 4012-4024.

Ginaldi L., De Martinis M., Matutes E., Farahat N., Morilla R. and Catovsky D. 1998. Levels of expression of CD19 and CD20 in chronic B cell leukaemias. *Journal of clinical pathology*, vol. 51, no. 5, pp. 364-369.

Green N.M. 1970. Spectrophotometric determination of avidin and biotin. *Methods in enzymology*, vol. 18, part A, pp. 418-424.

Green N.M. 1990. Avidin and streptavidin. *Methods in Enzymology*, vol. 184, pp. 51-67.

Green N.M. and Toms E.J. 1973. The properties of subunits of avidin coupled to Sepharose. *Biochemical Journal*, vol. 133, no. 4, pp. 687-698.

Halling P.J. and Dunnill P. 1979. Improved nonporous magnetic supports for immobilized enzymes. *Biotechnology and Bioengineering*, vol. 21, no. 3, pp. 393-416.

Hermanson G.T., Mallia A.K. and Smith P.A. 1997. Techniques of the trade. In: Hermanson G.T., Mallia A.K. and Smith P.A., eds. *Immobilized Affinity Ligand Techniques*. London: Academic Press Limited, pp.281-316.

Hirsch J.D., Eslamizar L., Filanoski B.J., Malekzadeh N., Haugland R. P., Beechem J. M. and Haugland R. P. 2002. Easily reversible desthiobiotin binding to streptavidin, avidin, and other biotin-binding proteins: uses for protein labelling, detection, and isolation. *Analytical Biochemistry*, vol. 308, no. 2, pp. 343-357.

Hofmann K., Wood S. W., Brinton C. C., Montibeller J. A. and Finn F. M. 1980. Iminobiotin affinity columns and their application to retrieval of streptavidin. *Proceedings of the National Academy of Sciences*, vol. 77, no. 8, pp. 4666-4668.

Jeffers R. J., Fend R. Q., Fowlkes J. B., Hunt J. W., Kessel D. and Cain C. A. 1995. Dimethylformamide as an enhancer of cavitation-induced cell lysis in vitro. *The Journal of the Acoustical Society of America*, vol. 97, no. 1, pp. 669-676.

Johnsen H.E., Hutchings M., Taaning E., Rasmussen T., Knudsen L.M., Hansen S.W., Andersen H., Gaarsdal E., Jensen L., Nikolajsen K., Kjaesgârd E. and Hansen N.E. 1999. Selective loss of progenitor subsets following clinical CD34+ cell enrichment by magnetic field, magnetic beads or chromatography separation. *Bone marrow transplantation*, vol. 24, no. 12, pp. 1329-1336.

Kantor A.B., Gibbons I., Miltenyi S. and Schmitz J. 1997. Magnetic sorting with colloidal supermagnetic particles. In: Recktenwald D. and Radbruch A., eds. *Cell Separation Methods and Applications*. 10th ed. New York: Marcel Dekker, INC., pp. 153-173.

Katkov I. I., Kim M. S., Bajpai R., Altman Y. S., Mercola M., Loring J. F., Terskikh A. V., Snyder E. Y. and Levine F. 2006. Cryopreservation of slow cooling with DMSO diminished production of *Oct-4* pluripotency marker in human embryonic stem cells. *Cryobiology*, vol. 53, no. 2, pp. 194-205.

Kühner M. and Sackmann E. 1996. Ultrathin hydrated dextran films grafted on glass: Preparation and Characterization of structural, viscous and elastic properties by quantitative microinterferometry. *Langmuir*, vol. 12, no. 20, pp. 4866-4876.

Kumar A. and Srivastava A. 2010. Cell separation using cryogel-based affinity chromatography. *Nature Protocols*, vol. 5, no. 11, pp. 1737-1747.

Kuo S.C. and Lauffenburger D.A. 1993. Relationship between receptor/ligand binding affinity and adhesion strength. *Biophysical journal*, vol. 65, no. 5, pp. 2191-2200.

Lévesque S.G. and Shoichet M.S. 2006. Synthesis of cell-adhesive dextran hydrogels and macroporous scaffolds. *Biomaterials*, vol. 27, no. 30, pp. 5277-5285.

Livnah O., Bayer E. A., Wilchek M. and Sussman J. L. 1993. Three-dimensional structures of avidin and the avidin-biotin complex. *Proceedings of the National Academy of Sciences*, vol. 90, no. 11, pp. 5076-5080.

Lowell S., Shields J.E., Thomas M.A. and Thommes M. 2006. *Characterization of Porous Solids and Powders: Surface Area, Pore Size and Density*. 2nd ed. Dordrecht: Springer, pp. 1-93.

Magdeldin S. and Moser A. 2012. Affinity chromatography: Principles and applications. In: Magdeldin S., eds. *Affinity chromatography*. Rijeka: InTech, pp. 3-28.

Massia S.P., Stark J. and Letbetter D.S. 2000. Surface-immobilized dextran limits cell adhesion and spreading. *Biomaterials*, vol. 21, no. 22, pp. 2253-2261.

Massia S.P. and Stark J. 2001. Immobilized RGD peptides on surface-grafted dextran promote biospecific cell attachment. *Journal of biomedical materials research*, vol. 56, no. 3, pp. 390-399.

Massia S.P., Holecko M.M. and Ehteshami G.R. 2004. In vitro assessment of bioactive coatings for neural implant applications. *Journal of biomedical materials research. Part A*, vol. 68, no. 1, pp. 177-186.

Molday R.S., Yen S.P.S. and Rembaum A. 1977. Application of magnetic microspheres in labelling and separation of cells. *Nature*, vol. 268, no. 5619, pp. 437-438.

Österberg E., Bergström K., Holmberg K., Riggs J.A., Van Alstine J.M., Schuman T.P., Burns N.L. and Harris J.M. 1993. Comparison of polysaccharide and poly(ethylene glycol) coatings for reduction of protein adsorption on polystyrene surfaces. *Colloids and Surfaces A: Physicochemical and Engineering Aspects*, vol. 77, no. 2, pp. 159-169.

Österberg E., Bergström K., Holmberg K., Schuman T.P., Riggs J.A., Burns N.L., Van Alstine J.M. and Harris J.M. 1995. Protein-rejecting ability of surface-b-ound dextran in end-on and side-on configurations: Comparison to PEG. *Journal of Biomedical Materials Research*, vol. 29, no. 6, pp. 741-747.

Pace C.N., Vajdos F., Fee L., Grimsley G. and Gray T. 1995. How to measure and predict molar absorption coefficient of a protein. *Protein science*, vol. 4, no. 11, pp. 2411-2423.

Rowland S.A., Shalaby S.W., Latour R.A. Jr. and von Recum A.F. 1995. Effectiveness of cleaning surgical implants: Quantitative analysis of contaminant removal. *Journal of applied biomaterials*, vol. 6, no. 1, pp.1-7.

Sorensen K. and Brodbeck U. 1986. Assessment of coating-efficiency in ELISA plated by direct protein determination. *Journal of Immunological Methods*, vol. 95, no. 2, pp. 291-293.

Sproβ J. and Sinz A. 2012. Monolithic columns with immobilized monomeric avidin: preparation and application for affinity chromatography. *Analytical and Bioanalytical Chemistry*, vol. 402, no. 7, pp. 2395-2405.

Wilchek M. and Bayer E. A. 1988. The avidin-biotin complex in bioanalytical applications. *Analytical Biochemistry*, vol. 171, no. 1, pp. 1-32.

Zempleni J. 2005. Uptake, localization, and noncarboxylase roles of biotin. *Annual review of nutrition*, vol. 25, pp. 175-196.

Zempleni J., Wijeratne S.S.K. and Hassan Y. 2009. Biotin. *Biofactors*, vol. 35, no. 1, pp. 36-46.

3. PREPARATION, CHARACTERIZATION AND APPLICATION OF NON-POROUS GLASS BEADS FOR THE POSITIVE SELECTION OF HUMAN RED BLOOD CELLS

Abstract

Following the successful development and application of affinity selection technology on glass coverslips and hollow capillary tubes, the development and evaluation of a human cell affinity selection system based on high grade smooth monodisperse 98 μm non-porous glass beads is presented in this chapter. The beads were converted into materials for positive, and importantly reversible, affinity selection of human therapeutic cells, in a rigorously characterized multi-step ‘layer-by-layer’ deposition procedure culminating in dextran-coated supports bearing monomeric avidin, and subsequently employed in packed bed chromatography experiments with human red blood cells isolated from cord blood. Initial chromatography experiments offer promising results for further development.

3.1 INTRODUCTION

Glass beads packed into column were the first choice when the formidable task of the isolation of individual morphologic cell types appeared in early 1970s. As the separation was based on the differences in the adherence on the glass it lacked selectivity. Various types of beads and experimental designs were tested, with a goal of achieving as purer cell type of interest as possible (Rabinowitz, 1964; Rabinowitz 1965).

Affinity chromatography has been investigated for the positive and negative separation of mammalian cells from the late 1970s with an emphasis on the selective binding of cells on various chromatographic matrices (Plotz and

Talal, 1967; Wigzell and Andersson, 1969; Truffa-Bachi and Wofsy, 1970; Venter *et al*., 1976; Yui *et al*., 1985). Some attempts for the cell recovery of adherent cells were made, but researchers have experienced difficulties.

Biotinylation and its affinity for immobilized avidin was at first exploited for the selective adsorption of thymocytes by Jasiewicz and his coworkers in 1976, but no cell retrieval was obtained. The first successful recovery of murine cells, in a viable form, using avidin-biotin technology was made by combining the affinity approach with rosetting. Unfortunately, this led target population coated with sheep erythrocytes used for rosetting and could potentially affect the function of cells (Wormmeester *et al*., 1984).

First reports of positive selection of viable cell populations using avidin-biotin immunoadsorption are date back to 1986, when Berenson and his co-workers successfully enriched Leu-4 positive cells from the human bone marrow mononuclear cells with avidin-Sepharose 6MB and Biogel P-30 column. The selectivity of the method exploited high affinity constant between tetrameric avidin and D-biotin and elution was achieved by mechanical agitation with plastic Pasteur pipette. Although yields and purities where promising, the method had negative impact on cell viability and low repeatability, as well as limited scale-up (Berenson *et al*., 1986a; Berenson *et al*., 1986b).

Although the discovery of monomeric avidin and its much lowered dissociation constant for avidin was first published in 1973 by Green and Toms, to date no reports of its use for the separation of human cells have been published.

In this section various approaches are undertaken for the modification and functionalization of glass beads, its characterization and initial affinity chromatography method development for the separation of human therapeutic cells using red blood cells are explained.

3.2 MATERIALS AND METHODS

3.2.1 MATERIALS

Medical grade nonporous borosilicate glass spheres GL-0179B5 (90-106 µm in diameter with 2.2 g/cm^3 density and 1.472 refractive index) were obtained from MO-SCI Specialty Products, L.L.C (Rolla, Missouri, USA).

Liquinox® detergent, (3-aminopropyl)triethoxysilane (3-APTES; ≥98 % purity), biotin *p*-nitrophenyl ester (98 % purity), dextran from *Leuconostoc* spp. ($M_r \approx 70000$) and sodium borohydride ($NaBH_4$, 98 % purity) were obtained from Sigma-Aldrich Company Ltd. (Gillingham, UK). PD-10 desalting column were purchased from GE Healthcare Life Sciences (Little Chalfont, UK). Quant*Tag™ Biotin kit was supplied by Vector Laboratories Ltd. (Peterborough, UK). Desiccated avidin, egg white (Molecular Probes®, Invitrogen; $M_r \approx 66000$; biotin binding of 13.6 units/mg of protein), D(+)-biotin (Acros Organics; 98% purity), Ficoll-Paque™ Plus (GE Healthcare Life Sciences), BCA Protein assay kit (Thermo Scientific Pierce) and Alexa Fluor® 488 tetrafluorophenyl (TFP) ester fluorescent dye (10 mg/mL solution in DMSO; Invitrogen) were purchased through Fischer Scientific UK Ltd. (Loughborough, UK). All other materials and reagents were supplied by Fischer Scientific UK Ltd. (Loughborough, UK).

Acetone, toluene and ethanol were HPLC grade (Fisher Chemical brand). Guanidine hydrochloride (Gdm HCl) was purchased as 8 M water solution. Sodium azide (NaN_3) and glycerol were supplied as 99 % pure and suitable for cell culture. Ammonium bicarbonate (NH_4HCO_3), ethylenediaminetetraacetic acid (EDTA; disodium salt dehydrate suitable for electrophoresis), glycine ($C_2H_5NO_2$; Gly), hydrogen chloride (HCl), potassium chloride (KCl), sodium acetate ($C_2H_3NaO_2$), sodium chloride (NaCl) sodium hydrogen carbonate ($NaHCO_3$), sodium hydroxide (NaOH), sodium metaperiodate ($NaIO_4$), sodium phosphate (Na_3PO_4) and tris(hydroxymethyl)aminomethane hydrochloride (Tris-HCl), salts used for preparation of buffer solutions, were analytical grade (99+ % purity) and suitable for use in cell culture. Phosphate buffered saline (PBS buffer) was supplied in a form of tablets. Each tablet prepares 100 mL of PBS buffer. Dimethyl sulfoxide (DMSO), trichloroacetic acid (TCA) and dithiothreitol (DTT) were 99 % pure and molecular biology grade.

All solutions were prepared using water purified by a Millipore Elix Gulfstream Clinical 100 (Merck Millipore UK Ltd, Watford, UK) water purification system and analytical grade reagents. Buffer solutions were prepared by dissolving a known mass of buffering species into *ca*. 80 % of the desired final volume of deionized water, titrating with 1 M solution of HCl or NaOH and adding water to yield the final solution volume.

Sterilization of solutions and suitable materials was performed either by autoclaving at 121 °C for 30 min using ASB 300T autoclave (Astell Scientific, Sidcup, UK) or by filtering through (Merck Millipore UK Ltd, Watford, UK).

Anti-glycophorin A (anti Gly-A) monoclonal antibody in cell culture supernatant was a generous gift from Dr Oliver Goodyear (School of Immunity and Infection, College of Medicine, University of Birmingham, UK).

Red blood cells were isolated by density gradient centrifugation from umbilical cord blood, which was obtained from anonymous donors through NHS Blood and Transplant (NHSBT).

Tricorn 5/50 column and complementary Tricorn 5 coarse filter kit were supplied by GE Healthcare (Uppsala, Sweden).

Disposable 35 mm plastic petri dishes with 10 mm glass bottom (MatTek, Ashland, Ohio, USA) for the confocal microscopy were a generous gift from Dr Nuno Reis (Chemical Engineering Department, School of Aeronautical, Automotive, Chemical and Materials Engineering, Loughborough University, UK).

3.2.2 METHODS

3.2.2.1 Surface modification

Surface modification of glass beads was performed following the protocol already described in Section 2.2.1.1, with a slight modification. Amination of surface was obtained according to Thermo Scientific Tech tip #5 (2008). Cleaned beads were immersed in 2 % solution of 3-APTES in acetone (v/v) for 1 min, followed by rinsing with acetone. Beads were dried overnight at room temperature in a laminar flow hood.

3.2.2.2 Surface functionalization

When applicable, modified glass beads were functionalized with biotinylated anti-glycophorin a monoclonal antibody as described in Section 2.2.2.4. The antibody was purified in advance following the method from the Section 2.2.2.2 and biotinylated with D-biotin as described in Section 2.2.2.3.

3.2.2.3 Isolation of red blood cells from the umbilical cord blood

Red blood cells were isolated from umbilical cord blood by density gradient centrifugation as previously described in the Section 2.2.2.6.

3.2.2.4 Labelling beads with biotinylated anti-glycopherin A antibody

Functionalized glass beads were incubated for 12 h in the solution of biotinylated antibodies. To the 5 mL of bead slurry (1:1 ratio beads:water (v/v); in the average 1 mL of bead slurry contained 0.5845 g of dry beads) antibody was added up to the final antibody concentration of 50 µg/mL and incubated at 4 °C protected from the light. After incubation, the supernatant was collected and beads gently rinsed once with 5 mL of PBS buffer. Absorbance of all supernatants at 280 nm was measured in order to calculate mass of bound antibody on the beads with equation 2.2 from the Section 2.2.2.4.

3.2.2.5 Analytical methods

The size distribution of the beads was measured by a particle size analyser, Mastersizer 2000 (Malvern Instruments, Malvern, UK), in the range 0.05 up to 880 µm. The measurement was performed with beads in the air and with the reflection index of beads (1.472) taken into consideration. The measurement zone (a distance from the face of the range lens along the analyser beam) was set to 2.40 mm. Analysis of so obtained data was polydisperse.

Surface area of non-modified and dry glass beads was measured by physical adsorption of krypton (Kr) at -169 °C using ASAP2020 Surface Area and Polarity Analyser (Micrometrics, Norcross, Georgia, USA). Data was evaluated according to the Brunauer, Emmet and Teller (BET) theory. For the analysis 11.0 ± 0.5 g beads were dried and gradually degassed under vacuum for 720 min. Before and after analysis sample tube was filled with liquid nitrogen (N_2). Kr was dosed to sample gradually at 5 mm Hg, with a relative pressure tolerance of 5 %. At each step, the sample was equilibrated for 10 s. The amount of adsorbed gas is the difference of admitted gas and the gas filling the dead volume (free space in sample tube) and the adsorption isotherm is a plot of the adsorbed gas versus the relative pressure (Lowell *et al*., 2006).

For X-ray photoelectron spectrometry (XPS analysis), dried beads were immobilized onto sample holder with double tape. The analysis was performed as described in the Section 2.2.2.10.

Naked (non-modified) and fully functionalized glass beads were visualized with scanning electron microscopy (SEM), following the method from the Section 2.2.2.10.

Surface modification of beads was further assed with atomic force microscope Explorer (Vecco, Plainview, New York, USA). 10 µm x 10 µm sections of immobilized dried beads were analysed at frequency of 330 kHz and surface tension in the range 20 and 80 N/m. Analyses were performed in non-contact mode.

Qualitative evaluation of functionalization with avidin and biotinlyated antibody was carried out with inverted confocal microscope Eclipse TE300 (Nikon, Tokyo, Japan) in the combination with LaserSharp 2000 software (Zeiss, BioRad, Hemel Hempstead, UK). To the 500 µL of beads, Alexa Fluor® 488 tetrafluorophenyl (TFP) ester fluorescent dye was added to a final concentration of 0.2 ng/mL. Beads were incubated for 1 h at room temperature on 3-D rocking platform STR 9 (Stuart Scientific, Stone, UK) with shaking at 70 revs/min. Excess dye was then removed by triple rinsing of beads with 1 mL of PBS. Before 20 µL of beads were transferred into 35 mm disposable plastic petri dishes with 10 mm glass and topped with 1 mL of glycerol in order to enhance imaging. So prepared samples were immediately scanned using an objective lens with a magnification of 20 times and emission filter HQ500. The pinhole aperture varied. Fluorescence was excited by argon/krypton laser at 488 nm wavelength. Cross sections of beads were automatically scanned at varying depths using a 2 µm step. Kalman averaging of 3 steps was introduced to further reduce noise and consequently improve images. All images were in the size 512 x 512 pixels and the pixel size was 0.41 µm. For the analysis, images were translated into fluorescence intensity profiles using ImageJ software (National Institutes of Health, Bethesda, Maryland, USA) as previously described by Ljunglöf and Hjorth (1996), Ljunglöf and Thömmes (1998) and Ljunglöf *et al*. (1999). The selected area along the particle in pixels was then plotted against the fluorescence in arbitrary units.

The Pierce™ Bicinchoninic acid (BCA) Protein assay, the number of biotin binding sites and the content of free soluble D-biotin in the fractions collected during the monomeric avidin immobilization were performed as described in Section 2.2.2.10.

Mass of immobilized avidin on the beads was further indirectly evaluated by TCA precipitation of avidin from the slurries collected during monomeric avidin immobilization. Protein precipitation solution (20 % TCA, 0.2 % DTT in iced-cold acetone) and wash solution (0.2 % DTT in iced-cold acetone) were prepared in advance and stored at – 20 °C until further use. The method was performed on ice and in a dark. To 3 parts of the slurry, 1 part of precipitation solution was added. Samples were incubated overnight in the fridge at 4 °C. The following day samples were centrifugated at 3400 g_{av} and pellet was resuspended in 1 mL of ice-cold wash solution. Samples were centrifugated again and pellets resuspended in 1 mL of ice-cold acetone. Acetone above precipitated proteins was then carefully decanted and samples were dried overnight in a bell jar. The following day were tubes with precipitated proteins collected and immediately weighted.

3.2.2.6 Affinity chromatography

Beads were packed under gravity into Tricorn™ 5/50 Empty High Performance column (internal diameter: 5.0 mm; adjustable bed height: 35 - 59 mm), equipped with coarse filters (porosity: ≥ 25 µm) and one adaptor unit (GE Healthcare, Uppsala, Sweden). The column was then connected to an Äkta Explorer 100 Air or Äkta Prime Plus lab-scale chromatography system (GE Healthcare, Uppsala, Sweden). All the experiments listed in this section were performed at room temperature.

Column efficiency testing was done with pulse test and performed on the non-modified beads packed into column (bed height: 55 mm). After the column was equilibrated with water, 0.5 mL of 1 % acetone in water (v/v) was injected onto column at flow rate 3000 cm/h. For the detection ultraviolet (UV) monitor was used at 280 nm wavelength. From the chromatogram were calculated the reduced plate height and the asymmetry of the peak.

Reduced plate height (h) was calculated from height equivalent to the theoretical plate (HETP) normalized for the diameter of particles (d_p) packed in the column and it was calculated from the equation 3.1 below:

$$h = \frac{HETP}{d_p} \tag{3.1}$$

Height equivalent to the theoretical plate (HETP) was calculated from the equation 3.2 below:

$$HETP = \frac{L}{N} \tag{3.2}$$

where: L is the total length of the column and N is number of theoretical plates. To calculate the number of theoretical plates for a packed column, equation 3.3 has been introduced:

$$N = 16\left(\frac{t_r}{W_b}\right)^2 \tag{3.3}$$

where: N is number of theoretical plates, t_r is the retention time of the probe molecule and W_b is the width of the peak at the baseline.

Asymmetry (A_s) of the peak was defined as (equation 3.4 below):

$$A_s = \frac{b}{a} \tag{3.4}$$

where: a is the distance from the leading edge to the midpoint and b is the distance from the midpoint to the tailing edge of the peak. The asymmetry factor was calculated from the peak width at 10 % of the peak height and describes the deviation of the peak from an ideal Gaussian peak shape (Hagel *et al*., 2008).

Pressure drop on the column packed with non-modified glass beads was measured using differential manometer (Relative and differential pressure transmitter type 692 (pressure range from 0.1 to 25 bar); Huba Control, Würenlos, Switzerland) at various linear flow rates between 30 and 3000 cm/h using water as a mobile phase. The column was packed under gravity with beads up to the height of 36 or 58 mm and then connected to the chromatographic system together with manometer using standard capillary tubing and tee bore PEEK fingertight union (0.020 inch thread ¼-28; Supelco, Bellefonte, Pennsylvania, USA).

Experiments with red blood cells were performed in the following way. Mobile phase A (running buffer; PBS, pH 7.4) and mobile phase B (elution buffer; 2 mM D-biotin in PBS, pH 7.4) were prepared in advance by filtering through a 0.22 µm filter unit and degassing for 10 min in ultrasonic bath (Fisherbrand S15, Fisher Scientific Ltd., Loughborough, UK). The column was then equilibrated with mobile phase A until UV signal at 215 and 280 nm was stable for 1 min (acceptable UV fluctuation: 20 mAu). If UV signal was not stable after 10 min of equilibration, the column was removed from the system, beads decanted and column was then re-packed with fresh beads. After completed equilibration, 0.5 mL cell suspension was injected through injection valve onto the column from the top or the bottom or *vice versa* at linear flow rate of 30 cm/h (0.1 mL/min). To maximize recovery, the sample loop was overfilled, i.e. into 0.5 mL loop 1 mL of cell suspension was injected. Injection valve was then emptied with 2 mL of mobile phase A at linear velocity of 30 cm/h. Washing (mobile phase A; 300 cm/h) and elution (mobile phase B; 30 cm/h) were conducted under same and reversed flow conditions. During elution flow might be stopped for in between 30 and 120 minutes. Cells in all fractions were counted using a Neubauer Improved Bright-Line haemocytometer (Sigma Aldrich, Gillingham, UK) as previously described in Section 2.2.2.10.

3.3 RESULTS AND DISCUSSION

3.3.1 PREPARATION AND CHARACTERIZATION OF GLASS BEADS

According to the manufacturer, the glass beads supplied were sieved in order to achieve size distribution between 90 and 106 µm in diameter (GL-0179 Data Sheet, Appendix D). The size distribution of beads was additionally evaluated and results support manufacturer’s data, as the beads diameter was in the range 79.12 and 118.59 µm, with an average diameter of 98.43 µm (Appendix E).

Used glass beads were relatively large in diameter and non-porous, therefore, the expected surface area was at the lower end of the detection limit of the analyser, which is 0.01 m^2/g (Micromeritics, 2004-2010). The specific surface area was measured four times; each time with the different sample from the same container. In order to aid the analysis the samples were degassed and heated for 24 h in order to remove all impurities, which might have impact on the surface area. The average measured surface area was 0.02963 ± 0.00158 m^2/g (5.33 % RSD).

Each step of surface modification (animation and deposition of aldehyde groups) of beads was evaluated by XPS. Table 3.1 below summarizes the atomic percentages (%) of detected elements in the overall scan of the supports.

Table 3.1: Elemental evaluation of surface modification of beads by XPS

Element (atomic %)	XPS analysis of glass beads	Deposition of 3-APTES (amination)		Deposition of oxidized dextran (aldehyde groups)	
C	7.49	16.16	▲	22.13	▲
N	N/D	4.15	▲	2.13	▼
Na	52.49	48.00	▼	47.98	—
O	10.01	0.95	▼	1.54	▲
Si	22.95	30.74	▲	25.78	▼
B	7.06	N/D	▼	N/D	—
I	N/D	N/D	—	0.44	▲

N/D: not detected; ▼decrease; ▲increase; — no change

XPS results were evaluated according to NIST X-ray Photoelectron Spectroscopy Database (National Institute of Standards and Technology, 2012). Amination of non-modified beads resulted in increase of C, N and O and decrease of Na and O. This was expected due to the use of 3-APTES (molecular formula: $C_9H_{23}NO_3Si$) as an amination reagent. Detailed scan of C and Si on the surface of unmodified and aminated glass beads revealed differences in the spectral line of both elements. In the case of non-modifed glass beads, detected spectral line indicates presence of only silica (glass), while in the case of aminated glass beads 67.3 % of measured Si represents spectral line distinctive for silanes, such as 3-APTES. The remaining Si is silica. For all other detected elements the differences between spectral lines were not significant.

The deposition of oxidized dextran to the aminated beads achieved a further increase of C, while the N and Si decreased, simultaneously an increase in O was observed. This was all expected due to the structure of deposited dextran (Figure 2.1). By oxidation, the ring of dextran, which does not have any N or Si present in its structure, is opened, and therefore more C and O is exposed. Detected I was most likely due to the preparation of aldehyde glass beads, *i.e*. $NaIO_4$ was used during the oxidation of dextran. This is additionally confirmed by the atomic percentage of the detected Na, which remained the same, although it was expected to drop slightly. The detailed scan of the C present on the sample revealed significant changes in the ratio between spectral lines of C. While the spectral lines characteristic for C in the ring and C-O-C or C-OH remained basically the same, the deposition of aldehyde groups resulted in increased spectral line for O-C-O formula by 18.2 %. O-C-O is present in the structural formula of immobilized oxidized dextran, which was used for the deposition of aldehyde groups on the surface (Figure 2.1).

A high degree of reproducibility was achieved during the deposition of aldehyde groups and immobilization of monomeric avidin, which was confirmed by BCA assay, determination of the number of biotin binding sites and TCA precipitation of avidin from the experimental slurries. BCA assay revealed that after completed immobilization of tetrameric avidin, 4.2 mg remained bound per m^2 (0.1244 mg/g of dried beads). Its dissociation resulted in the reduction of immobilized protein to 1.1 mg of avidin with reversible biotin binding sites per 1 m^2 (0.0326 mg/g of dried beads). To confirm this, TCA assay was introduced. Protein contents in all the slurries collected during the immobilization of monomeric avidin were precipitated with a goal to close mass balances. Results revealed that initially 5.0 mg of tetrameric avidin was immobilized and after completed preparation of monomeric beads, 1.017 mg of avidin remained bound per m^2 (0.0301 mg/g of dried support). Several methods were considered in order to determinate the state of remaining bound avidin, but no method was sensitive enough to detect differences between individual forms of bound avidin on the glass beads. Based on previous reports (Green and Toms, 1973; Sproβ and Sinz, 2012) it was concluded that, it was most likely that after the preparation of the glass beads, bound avidin is monomeric, dimeric, trimeric and tetrameric, but it has reduced dissociation constant for biotin.

According to the manufacturer (Certificate of analysis; Appendix E), the tetrameric avidin from egg white had a specific activity of 13.6 units/mg (1 unit is equal to 1 µg of D-biotin bound per mg of avidin), which means that in theory, to the 1 g of immobilized tetrameric avidin on the beads, between 13.8 (according to results obtained by TCA assay) and 15.0 µg of D-biotin (BCA assay results) could be bound, if ignoring steric hindrance. In the case that all the tetrameric avidin was dissociated to 4 subunits of which 1 remained bound on the beads and 3 were successfully removed from the surface, between 3.5 (TCA assay) and 3.75 µg of D-biotin (BCA assay) could be bound. This was evaluated experimentally by the determination of number of biotin binding sites. Before the dissociation of immobilized tetrameric avidin to its subunits, 3.6 µg of D-biotin could be bound. After the immobilization and blocking procedure were completed, the D-biotin was further reduced to 3.2 µg per 1 g of dried beads (10.8 µg of D-biotin per m^2 of the support). Reduction of the capacity of the support correlates with previous publications (Green and Toms, 1973; Sproβ and Sinz, 2012), which state that approximately 90 % of remaining avidin on the support has a dissociation constant for biotin of 10^{-7} M, which allows gentle elution by displacement of bound biotin with free D-biotin in elution buffer, *i.e*. the capacity for the D-biotin after immobilization and blocking of monomeric avidin is reduced by only 10 % (11.1 % based on research work described in this Chapter).

SEM was used to visualize unmodified and fully modified and functionalized beads with biotinlyted antibody. Figure 3.1 shows that the selected beads are relatively uniform in the size and shape.

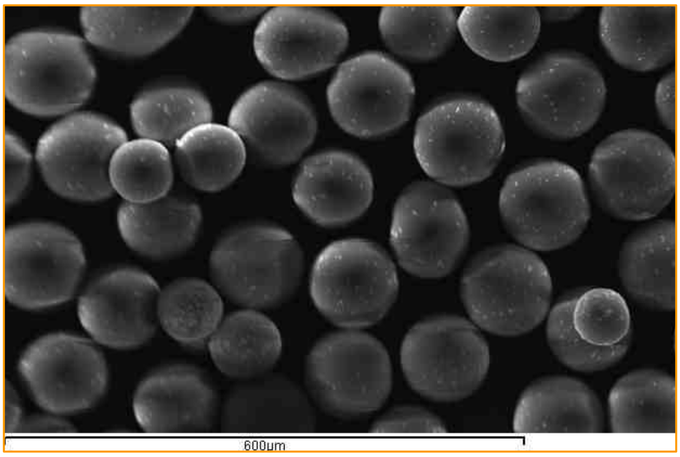

Figure 3.1: Unmodified glass beads (300x magnification)

After functionalization beads were kept as sterile bead-buffer slurry in dark at 4 °C. Because SEM is performed in the vacuum, beads were dried overnight at room temperature before the analysis (protected from the light), which resulted in the cracking of the grafted layers (Figure 3.2 below).

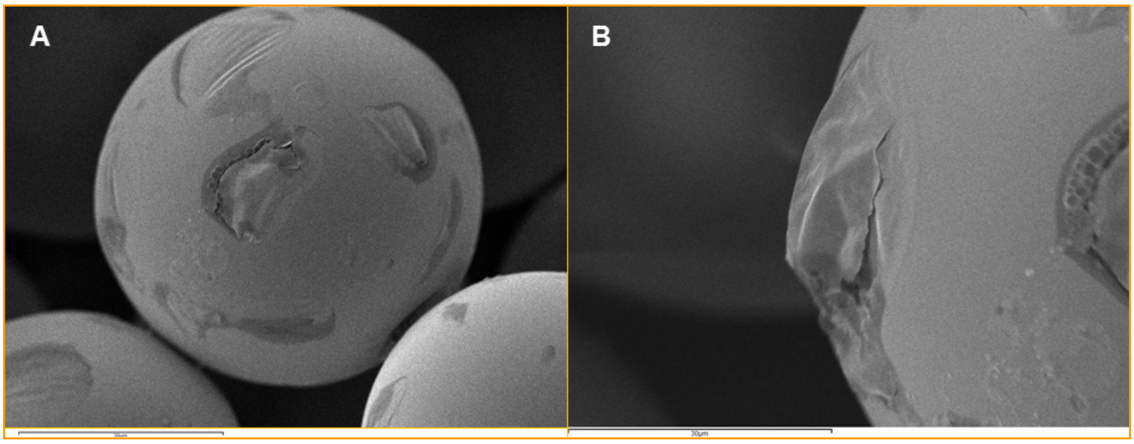

Figure 3.2: Modified and functionalized bead under SEM microscope. (A) Surface of bead (550x magnification). Cracklings in the grafted layers can be observed. (B) Under 650x magnification is clearly visible deformation of the modified bead, most likely due to the vacuum in which analysis was performed.

To confirm deformation of modified beads is due to the experimental SEM set-up, immobilized proteins and peptides on the beads were fluorescently labelled with Alexa Flour® dye (Molecular Probes by Life Technologies, 2013), and visualized with confocal microscopy in wet conditions (Figure 3.3).

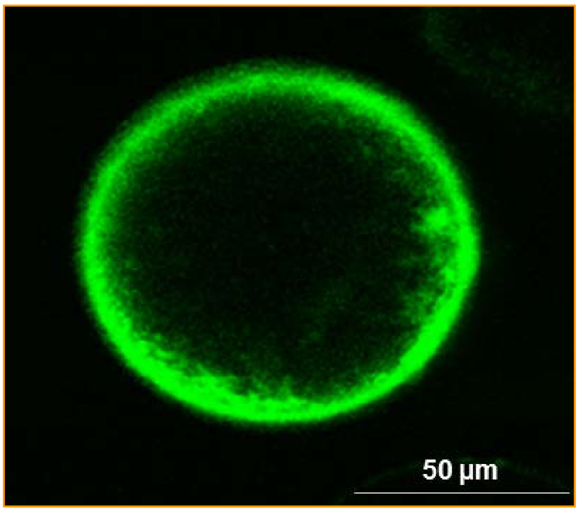

Figure 3.3: Functionalized glass bead analysed by confocal microscopy. For the qualitative evaluation of functionalization with avidin and biotinlyated antibody confocal microscopy was used. Immobilized proteins were in advance labelled with Alexa Fluor® 488 tetrafluorophenyl (TFP) ester, followed by scan of cross-section of the bead (300 x magnification).

On the outside of each modified bead a green fluorescent ring is formed, which represents labelled immobilized proteins, *i.e*. monomeric avidin and biotinlyted antibody. The thickness of the fluorescently labelled grafted area was then determined from the fluorescent intensity profile below (Figure 3.4).

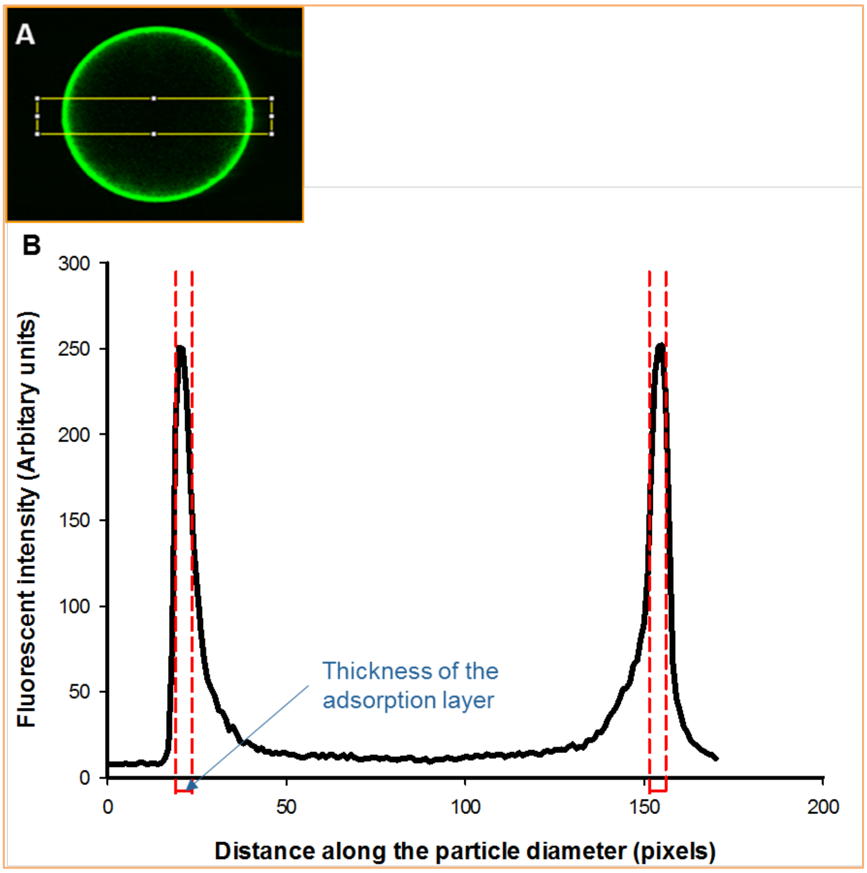

Figure 3.4: Fluorescence intensity profile of analysed glass bead. (A) Cross-section of the fluorescently labelled bead. The area used for the evaluation is shown by rectangular box. (B) Fluorescence intensity profile is plotted as distance along the particle in pixels versus fluorescent intensity (arbitrary units). Thickness of the adsorption layer is indicated by arrow.

In the presented example, the fluorescently labelled grafted layer on the left side of the bead is equivalent to 4.633 pixels (1.900 µm), while the thickness of the adsorbed layer on the right hand side is 4.637 pixels (1.901µm). This additionally confirms the uniformity of the grafting across the bead.

The surface of beads was furthermore scanned after each step of modification and functionalization by AFM. Results are presented in Figure 3.5.

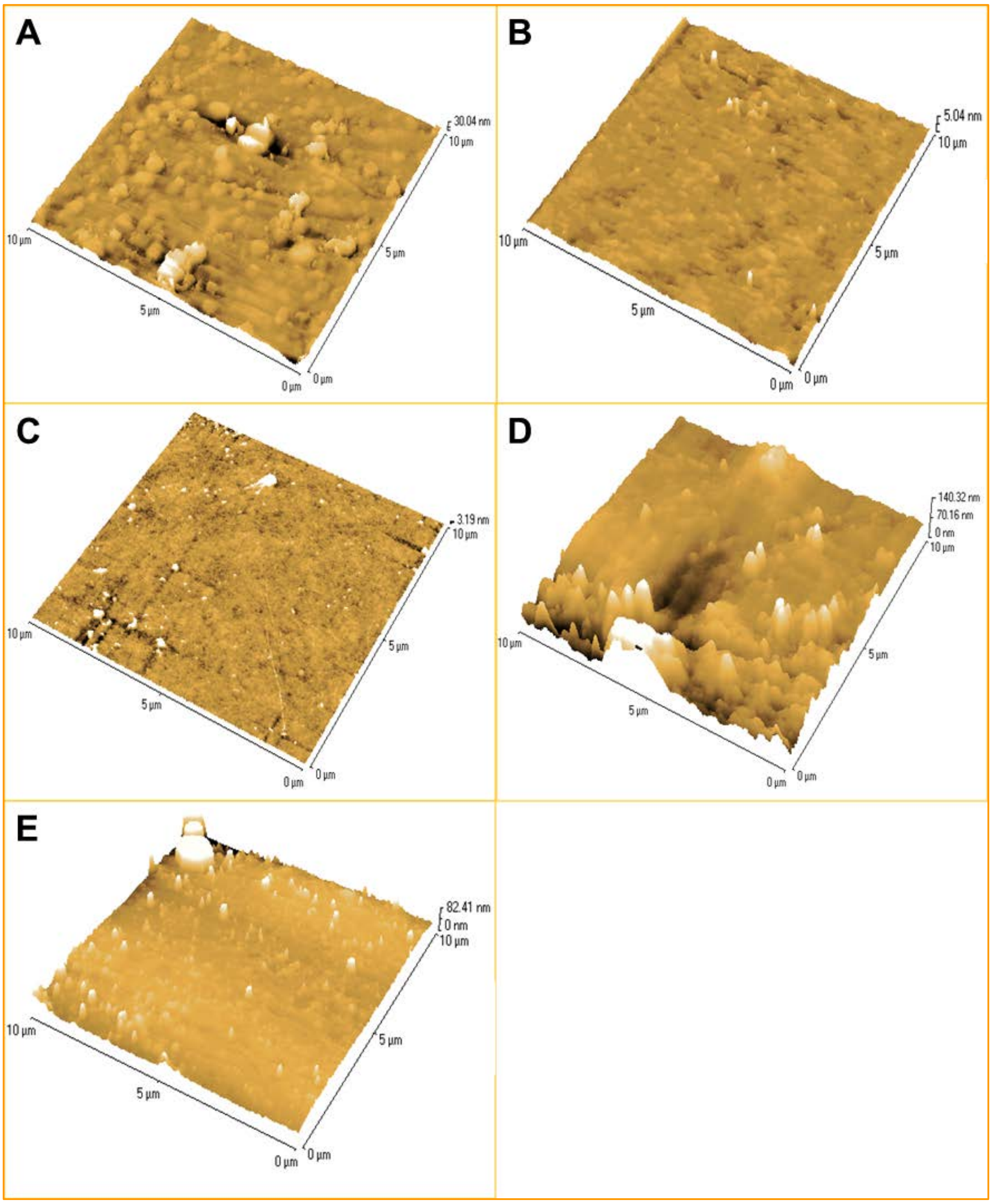
A
30.04 nm
10 µm
10 µm
5 µm
5 µm
0 µm
0 µm
B
5.04 nm
10 µm
10 µm
5 µm
5 µm
0 µm
0 µm
C
3.19 nm
10 µm
10 µm
5 µm
5 µm
0 µm
0 µm
D
140.32 nm
70.16 nm
0 nm
10 µm
10 µm
5 µm
5 µm
0 µm
0 µm
E
82.41 nm
0 nm
10 µm
10 µm
5 µm
5 µm
0 µm
0 µm

Figure 3.5: 3D AFM images of 10 µm x 10 µm sections of glass bead surfaces (A) The surface of unmodified non-porous glass bead is smooth. (B) After deposition of 3-APTES the surface is even more uniform, which suggests successful modification. (C) Deposited oxidized dextran forms thin and uniform biocompatible film. (D) Binding of native, tetrameric, egg white avidin results in the change of the morphology and its depth. (E) Cleaveage of tetrameric avidin to its monomeric form results in the reduction of the depth for more than 40%.

The AFM probe was oscillating across the surface of immobilized bead and imaging the topology of the surface. Unmodified beads are smooth and uniform. 3-APTES formed even smother monolayer on the surface. The deposition of oxidized dextran, which forms thin, uniform and biocompatible films on the surface (Kühner and Sackmann, 1996; Massia *et al*., 2000), resulting in uniform grafting, with the difference in the depth across scanned section of only 3.19 nm. Cleavage of immobilized tetrameric avidin into its form with reversible biotin binding sites caused significant change in the topology of the analysed sample, *i.e.* the height of the peaks was reduced from 140.32 to 82.41 nm.

3.3.2 APPLICATION OF PREPARED GASS BEADS IN AFFINITY CHROMATOGRAPHY

Prepared beads were packed under gravity into Tricorn column and the quality of column packing was evaluated prior the experiments with cells. Calculated reduced plate height of 0.81 suggests efficient column packing and no interaction between glass beads and acetone, as the value is below 3 (Rathore *et al*., 2003; GE Healthcare Application note). The asymmetry factor of the peak was between 0.8 and 1.8 (1.5 precisely), which indicates beads were not packed too tight or too loose, this confirms no air pockets were present and sample injection technique was appropriate (Rathore *et al*., 2003; GE Healthcare Application note; Hagel *et al*., 2008).

The next step was to messure the pressure drop on the column in order to assess if selected chromatographic support is suitable for the application. Mehta and Hawley (1969) recommend that the ratio between the column and particle diameter is 50:1 or less to be able to accurately correlate pressure drop *vs*. flow rate through packed beds. This parameter was fulfilled. Besides velocity and the ratio between the particle and column diameter, pressure drop on the column also depends on the viscosity and density of mobile phase, porosity of the bed, orientation of the packing and the size, shape and surface of the particles (Ribero *et al*., 2010). Due to the nature of human cells, the experimental design was limited and all experiments were designed with a goal to retain the viability and function of target cells intact. For example, during the selection of chromatographic support, porous glass beads were rejected – not only because the inaccessibility of the surface area inside pores to the cells due to their size, but also to the significantly increased pressure drops across the column, which was expected (Chhabra *et al*., 2001). In the study made by Gu and his co-workers back in the 2000, the sensitivity of white blood cells from donors when exposed to to the shear stress, pressure drop and various other parameters was measured using hollow capillary tubes and flat membranes. Although the characteristics of the selected devices for their study cannot be directly compared to the conditions in the column packed with nonporous glass beads, study gave a good indication of the sensitivity of cells and at the same time confirmed adequacy of selected chromatographic format. Their study suggests that even cells from unhealthy patients demonstrated pressure drops between 99 ± 4 mmHg (0.13 ± 0.01 bar) and 111 ± 9 mmHg (0.15 ± 0.01 bar). As shown in Figure 3.6, cells applied to the column at a flow rate of 305 cm/h (1 mL/min) were not exposed to the pressure drop above the suggested values (below 0.15 bar) and even when using flow rate of 3050 cm/h (10 mL/min), pressure drop on the column did not exceed 1.2 bar.

Additionally, several reports have been published in which researchers were exposing mammalian cells to the hydrostatic pressure of 200 atm (283.71 bar) and higher, these reports show that the cells did not show any long term defects as long as pressure did not exceed their threshold, which differs between cell types. Cells can adapt to the high pressure for short period of time (up to 1 h) by ‘‘rounding up’’ and when pressure is released, cells spread out again (Bourns *et al*., 1988; Crenshaw *et al*., 1996). For example, human cell line HeLa is resistant to short exposure to the hydrostatic pressure up to 200 atm (202.65 bar; Crenshaw *et al*., 1996).

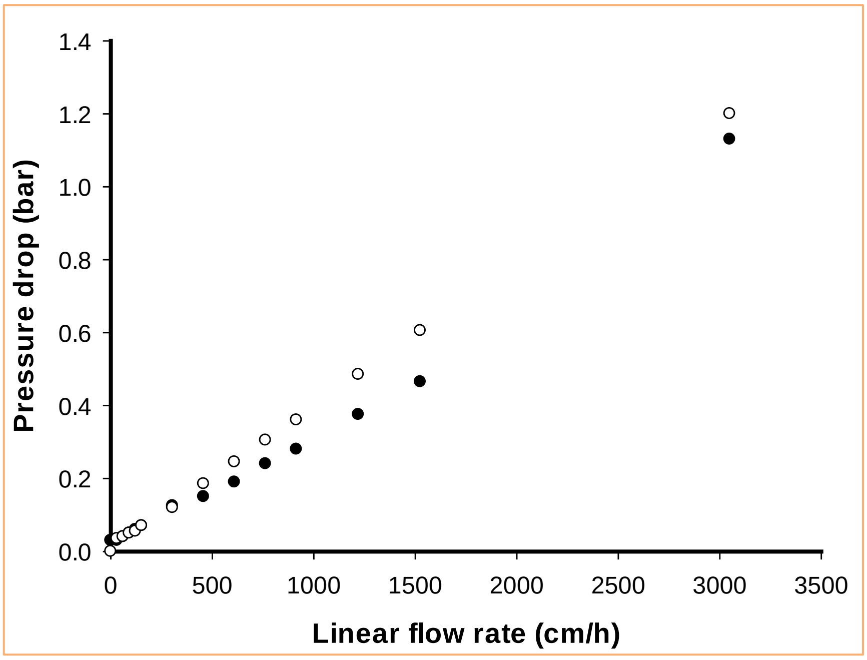

Figure 3.6: Pressure drop on the packed column at various flow rates. Tricorn 5/50 column was packed with non-modified beads up to the minimum bed height of 36 mm (black circles) and maximum bed height of 58 mm (white circles). Pressure drop at various linear flow rates was measured with differential manometer and with deionized water as mobile phase.

Following the successful characterization of modified beads and chromatographic support, initial chromatographic experiments were performed with red blood cells. Although they cannot be representative of other suspension cells due to their biconcave disk shape, size and structure, they allow visual observation of the separation process because of their colour and therefore do not require any labelling which might interfere with the experimental set-up. Not only it was possible to observe the state of the column during loading, wash (removal of non-specifically and weakly bound cells), elution and after the experiment, cells could also be observed in collected fractions during separation (Figure 3.7 below). More red blood cells were present on the column or in the fraction, red tones were observed.

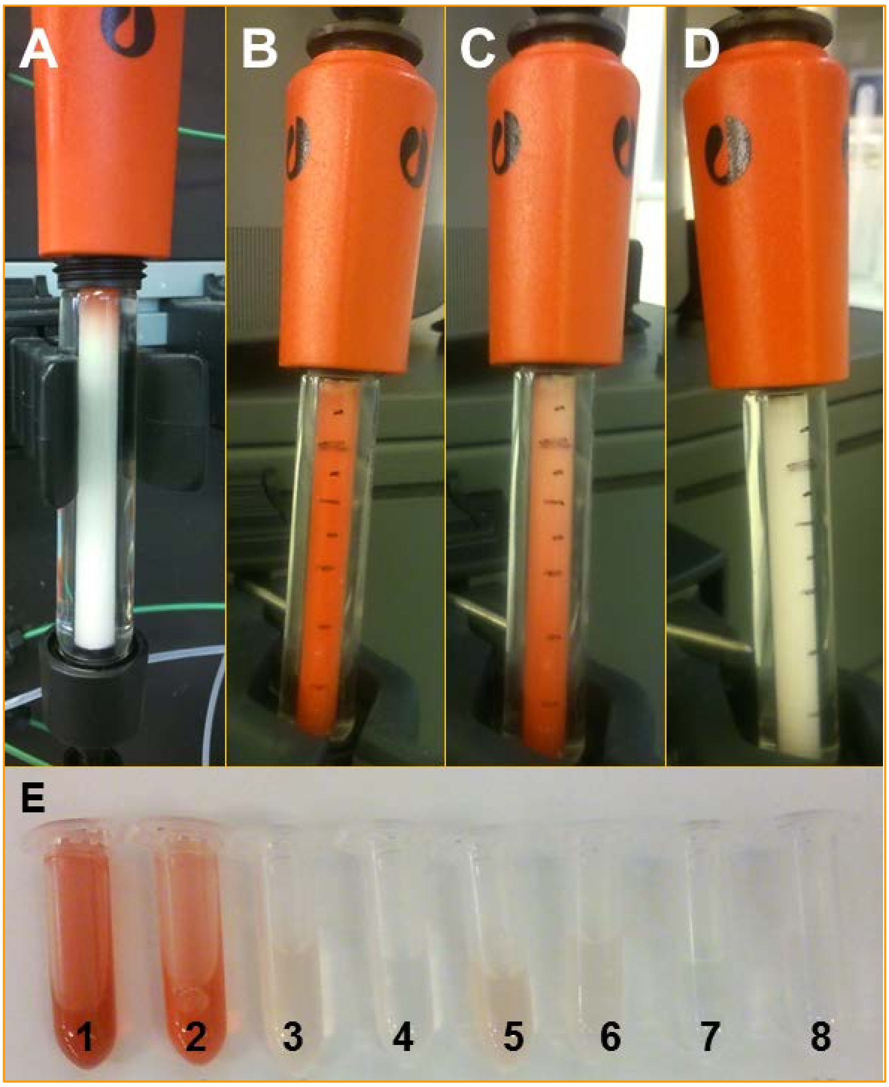

Figure 3.7: Photographs of column and collected fractions during affinity based separation of red blood cells. Column at the beginning of the loading of cells (A), after red blood cells were loaded (B), during washing step in order to remove all non-specifically bound cells (C) and after completed elution (D). Red blood cells can be observed as well in the collected fractions (E). An excess of cells applied onto the column is present in the fraction collected during loading (E-1), plenty of non-specifically bound cells is rinsed from the support during wash step (E-2, E-3, E-4). Eluted cells are dying collected fractions during elution in red tones (E-5, E-6, E-7, E-8).

Besides “proof of principle” experiments, red blood cells were also used for the initial determination of the ideal separation conditions, *i.e*. flow rates, contact and incubation times, and the length of the load, wash and elution step. Red blood cells were chosen due to their clinical relevance in a treatment of anaemia patients as well as their colour, which allowed on-line observation of the separation process without the need for an additional labelling, which might interfere with the affinity based separation. They are unique in their size and shape (Bain, 1996), therefore cannot be representative for the other human therapeutic cells, *e.g*. white blood cells and stem cells. Initial design of the chromatography separation was based on the results obtained on glass coverslips, as described in Chapter 2.

Two approaches for the loading and elution were evaluated, namely loading from the top of the column or from the bottom up to the top and then in the next step elution with the same or reversed flow path. In terms of loading, there were no significant differences between the number of specifically bound cells between approaches, therefore it was proceeded with the second option (loading from the bottom to the top of the column) to eliminate the effect of the gravity and consequently all the bound cells were concentrated at the bottom of the column, which was an advantage during the elution and wash step when reversed flow was applied (Figure 3.8 below).

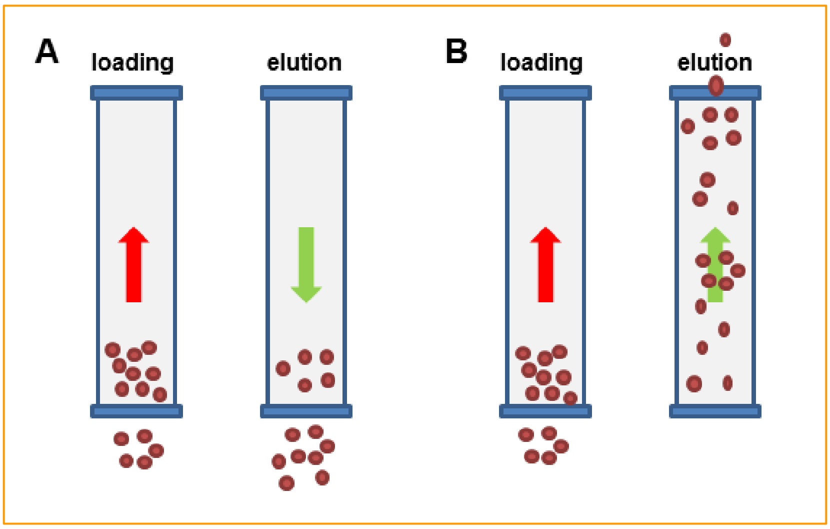

Figure 3.8: Chromatography of red blood cells elution flow path strategies. (A) When cells are loaded from the bottom to the top of the column (red arrow) and then eluted with reversed flow path (green arrow), cells are not passing the top part of the column, while when (B) cells are loaded (red arrow) and eluted (green arrow) with the same flow direction, therefore eluted cells are passing through the whole column and can re-bound to the affinity support.

By washing and eluting cells with reversed flow elution the efficiency was improved significantly (for $3.5*10^6$ injected cells from 40.92 % up to 48.75 %). The difference, nearly 8 %, is most likely due to cells passing through the remaining part of the column during the washing and elution, these cells were potentially, specifically and non-superficially re-bound to the chromatographic support, which slowed down the elution process and as well reduced yields.

Initially $3*10^6$ cells were injected onto column at a linear flow rate of 30 cm/h (0.1 mL/min). Due to the low number of cells present in the elution fractions and the low detection limit of the selected method for the evaluation of cell number in samples, it was preceded with greater cell injections rather than combining individual fractions in order to be able to evaluate number of cells after completed separation. The bed height in the column was fixed to 5.5 cm, which was equal to 1 mL of bead slurry (1 column volume). The selected approach allowed for comparison between the experiments and closer tracking of cells throughout the whole separation process. The only limitation was the fraction size, which was set to 1 column volume (1 mL; 1 CV). Initial loading and elution of red blood cells at 30 cm/h did not have any impact on their viability, it was therefore retained, but the washing of any non-specifically bound cells was performed at 300 cm/h. This increase in the flow rate was introduced with a goal to remove all non-bound cells as well as to prevent any clogging and mechanical entrapment within the column. This precaution was made due to the “sticky” nature of red blood cells (Chasis and Mohandas, 1992).

Surprisingly the desorption kinetics between cells tagged with biotinylated antibody and immobilized avidin on the surface of the beads was slow and necessitated pausing the flow during the elution to allow sufficient time for D-biotin present in the elution buffer to compete with biotinylated antibody and consequently release cells from the support. With red blood cells only partial optimization of stops during elution was made due to their characteristics (size, shape, “stickiness”), but the best elution efficiency was achieved when retained red blood cells were eluted by pausing the flow sequentially three times for 1.5 h.

After optimization of the sample size, flow direction, linear flow rate and partially the elution step, a series of experiments were performed with the aim of testing the capacity and the elution efficiency of the prepared chromatographic support. The results are present in the Table 3.2.

Table 3.2: Summary of representative data of affinity chromatography of human red blood cells on antibody labelled monoavidin/dextran coated glass beads. Red font colour is used for the experiment with the best elution efficiency (%).

Number of viable red blood cells (*10^6)	**3.5**	**4.5**	**15**	**23**	**53**	**64**	**82.5**
Cells in flow through and washout fractions (*10^6)	1.7	2.4	9.9	6.0	19.3	10.7	15.8
Retained cells on the column (*10^6)	1.8	2.1	5.1	17.0	33.7	63.9	66.7
Eluted cells (*10^6)	0.9	1.8	0.7	0.3	0.71	0.6	0.2
Elution efficiency (%)	48.8	85.0	14.3	1.9	0.02	0.01	0.003
Number of elution steps	4	3	2	3	3	3	3
Total elution time (h)	4.5	4.5	4	4.5	3.5	3.5	3.5
Lost cells (*10^6)	0.9	0.3	4.4	16.7	33.0	63.3	66.5

The beads packed in the column were challenged with 3.5*10^6 cells up to 8.25*10^7 cells. Surprisingly, the elution efficiency depends on the number of loaded cells, it dropped exceptionally when more than 4.5*10^6 cells were applied. Preliminary experiments have shown that the number of elution steps has a little impact on the elution efficiency; more significant is the duration of a single pause. After 15 min flow pause no cells were detected in the elution fractions, while pausing the flow for 1.5 h had a positive impact on the number of eluted cells. It was concluded that the D-biotin mediated displacement of cells from the affinity support is slow, therefore the decision was made to limit the elution time to 4.5 h in order to retain the separation process within a reasonable time frame.

Mechanical entrainment within the interstices was identified as the most significant problem, and the extent to which this occurred was correlated with the cell concentration in the feed. This phenomenon could be explained by the interactions between red blood cells (Figure 3.9). So called rouleau formation is a physiological condition in vertebrates, is a result of a weak cell-cell interaction which temporary overcome the negative surface charge of cells. These interactions can be relatively easily dissociated. On the other hand, the aggregation of red blood cells is an outcome when associations between red blood cells are strong and regulated usually by antibodies. This type of interactions requires much greater forces for cell dissociation (Chasis and Mohandas, 1992).

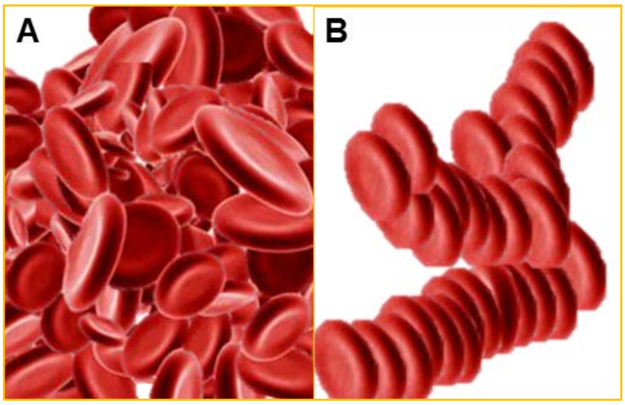

Figure 3.9: Interactions between red blood cells. (A) Rouleau formations are physiologically common weak cell-cell interactions and are readily dissociated, while (B) aggregation of red blood cells is induced by antibodies and requires greater forces for its dissociation.

Rouleau formations should not have any significant impact on the elution of cells from the column except, but it might slow down the displacement of free D-biotin in elution buffer with biotinylated antibody. However, although anti Gly-A, antibody used for the positive selection, is immobilized on the support, it might induce aggregation of red blood cells in the column, especially after the elution buffer is applied on the column and free biotinylated antibody and cells labelled with biotinylated antibody are released from the surface. These cells and antibodies can interact with each other as well as with any uneluted cells and form large aggregates. The more cells that are applied to the column, the higher their concentration is during loading, washing and elution, giving them more chance to interact, hence the elution efficiency drops drastically (Figure 3.10 below).

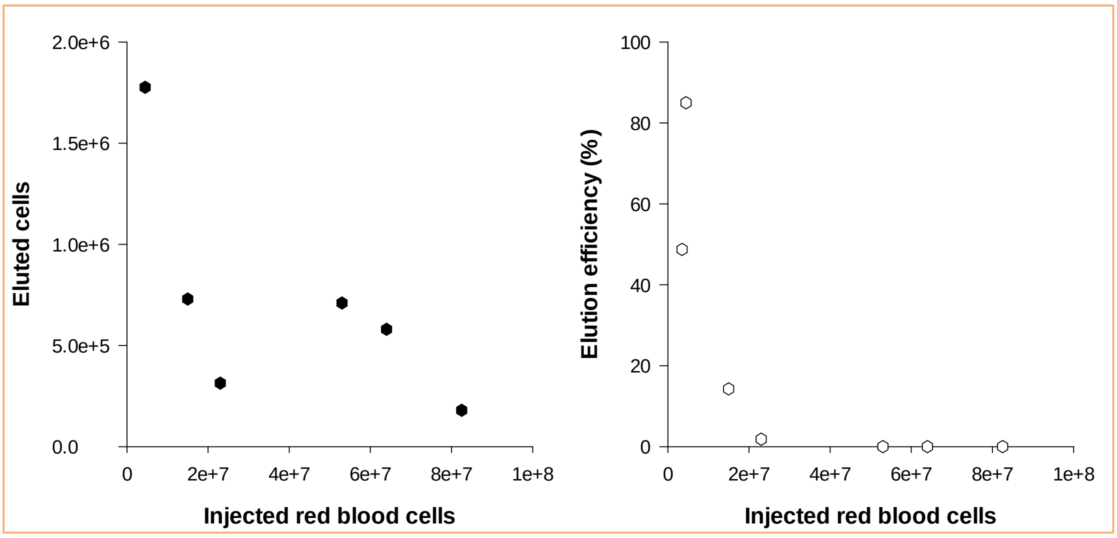

Figure 3.10: Impact of cell loading on subsequent elution. The number of red blood cells applied onto affinity chromatographic support has a major impact on the number of eluted cells (left graph; black circles) and elution efficiency (right graph; white circles). Optimum elution efficiency was noted at cell load of $4.5*10^6$ cells.

The best elution efficiency (85.0 %) was achieved when the column was challenged with $4.5*10^6$ cells. An upper limit for 1 mL of packed bead slurry was identified as less than $15*10^6$ cells, beyond which the column elution efficiency dropped below 14.3 % and therefore the column does not function as an effective affinity chromatographic matrix.

A closer look at the chromatogram of the run with $4.5*10^6$ red blood cells (Figure 3.11) revealed that during loading no significant changes in the pressure on the system were recorded, suggesting no, or very little, cell entrapment and aggregation was present. The increase during washing step was due to the increased flow rate (from 30 cm/h to 300 cm/h). Only small changes were observed during experiments with greater cell numbers, but the change was below 7 % in all cases, and could be treated as an experimental mistake. Additionally, the pressure is measured on the whole Äkta system and it is not sensitive enough to define presence of cell entrapment and/or aggregation on the column. Unfortunately the system did not allowed observation of the pressure drop on the column, which would give better indication of cell entrapment.

Measuring absorbance at 215 nm was useful especially during the elution because it allowed the identification of the onset of the competitive D-biotin elution. Conductivity values remained constant throughout the whole experiment (within the difference of 17 mS/cm), indicating that no cell lysis occurred during the time spent on the column.

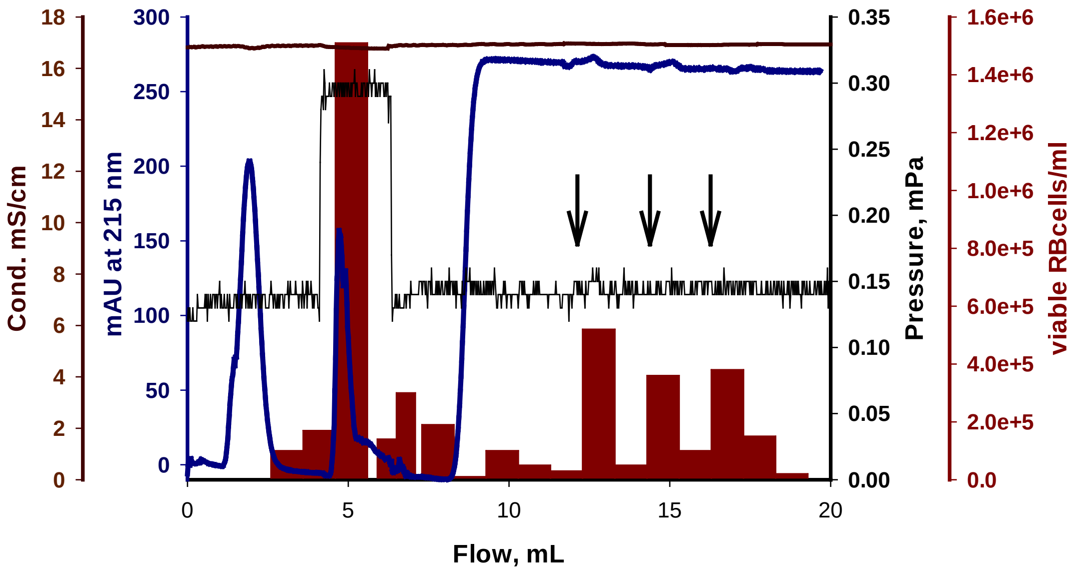

Figure 3.11: Affinity chromatography of human red blood cells (4.5*10^6 cells injected) on antibody labelled monomeric avidin coated glass beads. Black line indicates pressure (mPa) on the system during the run, dark brown conductivity (mS/cm) and blue line represents absorbance at 215 nm (mAU). Dark red bars show cell counts of fractions. With black arrows are indicated points at which flow was paused for 1.5 hours.

The desorption kinetics of tightly adsorbed cells was surprisingly slow, which is the opposite from the results obtained with batch static set-up (Chapter 2), therefore it was essential to pause the flow twice for 1.5 h and once for 1 h after 3 mL of elution buffer passed the column. This proved an effective elution as the majority of the cells were eluted immediately after flow was paused. To confirm cells were not eluted due to the mechanical force after flow was set-up, the same experimental procedure was repeated with tetrameric avidin, a form with higher dissociation constant for D-biotin, immobilized on the beads. This time red blood cells were present only in the fractions collected during the load and wash steps.

Additionally, the specificity of the cell binding to the immobilized antibody on the chromatographic matrix was assessed. An experiment was conducted with naked, amino-derived and dextran coated beads packed into column (bed height: 5.5 cm). In all three cases, $3*10^6$ cells were injected through 500 µL loop on the column and all the injected red blood cells were detected in flow through and wash fractions. When non-modified beads were challenged with red blood cells, 98.2 % of applied cells were detected in flow through fraction, remaining were present in rinsing fraction. 93.5 % of cells applied to the amino-derived beads were present in flow through fraction, additionally 5.7 % of applied cells were detected in rinsing fraction. Furthermore, dextran coated beads do not promote non-specific cell binding as 98.6 % of applied cells were present in flow through fraction, remaining 0.9 % was detected in rinsing fraction. This additionally confirmed that the selected chemistry was appropriate as it did not promote nonspecific cell binding.

3.4 CONCLUDING REMARKS

The adsorption and desorption kinetic rate are the two most important factors in the affinity separation of human cells. Especially as slow desorption kinetics have proven to be the most challenging part of process.

The findings presented in this study have shown the adequacy of the developed monomeric avidin–biotin technology for the use in packed bed chromatography for the positive selection of human therapeutic cells. The use of red blood cells in the experiments might have impacted on the yields and elution efficiency, as well as on the duration of the separation process. Therefore, it is necessary to further optimize the separation conditions, preferably using a different feedstock. Possible candidates are white blood cells (B and T lymphocytes). Additionally, there is a need to assess cell viability with another, more precise, method and to measure the cell function before and after the experiments. For example, the functionality of red blood cells can be visually assessed under microscope since the main role of red blood cells in the human body is to transport oxygen bound to hemoglobin, iron-rich protein. Cells which have lost their main functionality look smaller and paler (Cook, 2005).

3.5 REFERENCES

Bain B.J. 1996. *A beginner's guide to blood cells*. Oxford: Blackwell Science.

Berenson R.J., Bensinger W.I., Kalamasz D. and Martin P. 1986a. Elimination of Daudi lymphoblasts from human bone marrow using avidin- biotin immunoadsorption. *Blood*, vol. 67, no. 2, pp. 509-515.

Berenson R.J., Bensinger W.I. and Kalamasz D. 1986b. Positive selection of viable cell populations using avidin-biotin immunoadsorption. *Journal of immunological methods*, vol. 91, no. 1, pp. 11-19.

Bourns B., Franklin S., Cassimeris L. and Salmon E.D. 1988. High hydrostatic pressure effects in vivo: Changes in cell morphology, microtubule assembly, and actin organization. *Cell motility and the cytoskeleton*, vol. 10, no. 3, pp. 380-390.

Chasis J.A. and Mohandas N. 1992. Red blood cell glycophorins. *Blood*, vol. 80, no. 8, pp. 1869-1879.

Chhabra R.P., Comiti J. and Machač I. 2001. Flow of non-Newtonian fluids in fixed and fluidised beds. *Chemical engineering science*, vol. 56, no. 1, pp. 1-27.

Cook J.D. 2005. Diagnosis and management of iron-deficiency anaemia. *Best Practice & Research Clinical Haematology*, vol. 18, no. 2, pp. 319–332.

Crenshaw H.C., Allen J.A., Skeen V., Harris A. and Salmon E.D. 1996. Hydrostatic pressure has different effects on the assembly of tubulin, actin, myosin II, vinculin, talin, vimentin, and cytokeratin in mammalian tissue cells. *Experimental cell research*, vol. 227, no. 2, pp. 285-297.

GE Healthcare Application note 28-9372-07 AA. Column efficiency testing. [online]. [viewed 07/01/2014]. *GE Healthcare, Uppsala, Sweden*, pp. 1-6.
Available from:
https://www.gelifesciences.com/gehcls_images/GELS/Related%20Content/Files/1352880951136/litdoc28937207_20141127221416.pdf

Green N. M. and Toms E. J. 1973. The properties of subunits of avidin coupled to Sepharose. *Biochemical Journal*, vol. 133, no. 4, pp. 687-698.

Gu Y.J., Boonstra P.W., Graaff R., Rijnsburger A.A., Mungroop H. and van Oeveren W. 2000. Pressure drop, shear stress, and activation of leukocytes during cardiopulmonary bypass: A comparison between hollow fiber and flat sheet membrane oxygenators. *Artificial organs*, vol. 24, no. 1, pp. 43-48.

Hagel L., Jagschies G. and Sofer G. 2008. *Handbook of Process Chromatography: Development, Manufacturing, Validation and Economics*. 2nd ed. London: Academic Press, pp. 1-330.

Jasiewicz M.L., Schoenberg D.R. and Mueller G.C. 1976. Selective retrieval of biotin-labelled cells using immobilized avidin. *Experimental cell research*, vol. 100, no. 1, pp. 213-217.

Kühner M. and Sackmann E. 1996. Ultrathin hydrated dextran films grafted on glass: Preparation and Characterization of structural, viscous and elastic properties by quantitative microinterferometry. *Langmuir*, vol. 12, no. 20, pp. 4866-4876.

Ljunglöf A., Bergvall P., Bhikhabhai R. and Hjorth R. 1999. Direct visualisation of plasmid DNA in individual chromatography adsorbent particles by confocal scanning laser microscopy. *Journal of Chromatography A*, vol. 844, no. 1-2, pp. 129-135.

Ljunglöf A. and Hjorth R. 1996. Confocal microscopy as a tool for studying protein adsorption to chromatographic matrices. *Journal of Chromatography A*, vol. 743, no. 1, pp. 75-83.

Ljunglöf A. and Thömmes J. 1998. Visualising intraparticle protein transport in porous adsorbents by confocal microscopy. *Journal of Chromatography A*, vol. 813, no. 2, pp. 387-395.

Lowell S., Shields J.E., Thomas M.A. and Thommes M. 2006. *Characterization of Porous Solids and Powders: Surface Area, Pore Size and Density*. 2nd ed. Dordrecht: Springer, pp. 1-93.

Massia S.P., Stark J. and Letbetter D.S. 2000. Surface-immobilized dextran limits cell adhesion and spreading. *Biomaterials*, vol. 21, no. 22, pp. 2253-2261.

Mehta D. and Hawley M.C. 1969. Wall effect in packed columns. *Industrial and engineering chemistry process design and development*, vol. 8, no. 2, pp. 280-282.

Micromeritics. ASAP 2020. Accelerated surface area and porosimetry system. User’s manual V3.04. 2004-2010. *Micromeritics Instrument Corporation*. 462 pp.

Molecular Probes by Life Technologies. Amine-reactive probes. 2013. [online]. [viewed 28/05/2013]. Thermo Fisher Scientific, Carlsbad, USA, pp. 1-11. Available from: https://tools.lifetechnologies.com/content/sfs/manuals/mp00143.pdf

NIST X-ray Photoelectron Spectroscopy Database. Version 4.1. 2012. [online]. [viewed 13/07/2014]. *National Institute of Standards and Technology, Gaithersburg, USA*. Available from: http://srdata.nist.gov/xps/

Plotz P.H. and Talal N. 1967. Fractionation of splenic antibody-forming cells on glass bead columns. *The journal of immunology*, vol. 99, no. 6, pp. 1236-1242.

Rabinowitz Y. 1964. Separation of lymphocytes, polymorphonuclear leukocytes and monocytes on glass columns, including tissue culture observations. *Blood*, vol. 23, no. 6, pp. 811-828.

Rabinowitz Y. 1965. Brief report: Adherence and separation of leukemic cells on glass bead columns. *Blood*, vol. 26, no. 1, pp. 100-103.

Rathore A.S., Kennedy R.M., O’Donnell J.K., Bemberis I. and Kaltenbrunner O. 2003. Qualification of a chromatographic column. Why and how to do it. *BioPharm International*, vol. 16, no. 3, pp. 30-40.

Ribeiro A.M., Neto P. and Pinho C. 2010. Mean porosity and pressure drop measurements in packed beds of monosized spheres: Side wall effects. *International review of chemical engineering*, vol. 2, no. 1, pp. 40-46.

Sproβ J. and Sinz A. 2012. Monolithic columns with immobilized monomeric avidin: preparation and application for affinity chromatography. *Analytical and Bioanalytical Chemistry*, vol. 402, no. 7, pp. 2395-2405.

Thermo Scientific Tech tip #5. Attach an antibody onto glass, silica or quartz surface. 2008. [online]. [viewed 14/05/2012]. *Pierce Biotechnology, Rockford, USA*, pp. 1-4. Available from: https://www.piercenet.com/instructions/2160905.pdf

Truffa-Bachi P. and Wofsy L. 1970. Specific separation of cells on affinity columns. *Proceedings of the National academy of sciences*, vol. 66, no. 3, pp. 685-692.

Venter B.R., Venter J.C. and Kaplan N.O. 1976. Affinity isolation of cultured tumor cells by means of drugs and hormones covalently bound to glass and Sepharose beads. *Proceedings of the National academy of sciences*, vol. 73, no. 6, pp. 2013-2017.

Wigzell H. and Andersson B. 1969. Cell separation on antigen-coated columns. Elimination of high rate antibody-forming cells and immunological memory cells. *The journal of experimental medicine*, vol. 129, no. 1, pp. 23-36.

Wormmeester J., Stiekema F. and De Groot K. 1984. A simple method for immunoselective cell separation with the avidin-biotin system. *Journal of immunological methods*, vol. 67, no. 2, pp. 389-394.

Yui N., Sanui K., Ogata N., Kataoka K., Okano T. and Sakurai Y. 1985. Reversibility of granulocyte adhesion using polyamine-grafted nylon-6 as a new column substrate for granulocyte separation. *Biomaterials*, vol. 6, no. 6, pp. 409-415.

4. APPLICATION OF GLASS BEAD CHROMATOGRAPHY FOR THE POSITIVE SELECTION OF HUMAN WHITE BLOOD CELLS

Abstract

A developed monomeric avidin packed bed column is implemented for the positive selection of white blood cells, namely B lymphocytes, by biotin mediated displacement. Evaluated are two approaches: (i) binding of the selected biotinylated antibody to the chromatographic support; and (ii) labelling cells in advance with biotinylated antibody. The effects of cell concentration, number of applied cells, loading, wash and elution linear flow rates and flow pause on the binding efficiency, elution efficiency and yield are evaluated in order to develop an effective, highly selective and fast affinity based separation.

4.1 INTRODUCTION

The avidin/biotin system has been widely used for an affinity separation of mammalian cells (Berenson *et al*., 1986a; Berenson *et al*., 1986b). Early studies exploited the high affinity between protein avidin and vitamin biotin to achieve specific cell attachment, but, as the adhesion strength of a bond is not dependent on the affinities, it allows mechanical disruption of the bond and consequently release of a cell (Kuo and Lauffenburger, 1993). Besides mechanical release, various other approaches could be utilized, for example non-specific elution by change of pH, temperature or salt concentration, or shear forces to physically dislodge cells from the support, but the most elegant approach is the competitive displacement, although it might not work when the number of interactions is more than ten, as it is unlikely that a monovalent competitor could be used at sufficient high concentration to be an effective displacer (Cao *et al*., 2002). For example, 6 M guanidine hydrochloride at pH 1.5 is commonly used to elute biotinylated molecules, however it is a harsh condition not always suitable for biomolecules (Magdeldin and Moser, 2012), therefore it is not a surprise it has not beenwidely used in commercial separations (Lightfoot and Moscariello, 2004).

The monomeric form of avidin has a much lower affinity constant towards biotin, as each subunit consists only of one biotin binding site (Qureshi and Wong, 2002). The preparation of affinity support is a multistep procedure, which consists of the immobilization of native, tetrameric, avidin, followed by its denaturation and renaturation of the monomeric avidin support with a dissociation constant of $1.8*10^{-7}$ M (Kohanski and Lane, 1990). First report for the preparation of monomeric avidin affinity column is dated back to the 1979, used for the specific isolation of biotin-containing enzymes, namely propionyl-CoA carboxylase and methylmalonyl-CoA pyruvate transcarboxylase, both originate from bacteria (Henrikson *et al*., 1979). Just a year later, purification of a human liver propionyl-CoA carboxylase was reported (Gravel *et al*., 1980). Since then it has been used for the purification of biotinylated proteins (Qureshi and Wong, 2002), but has never been applied so far for the positive selection of human or mammalian cells.

Besides gentle elution, monomeric avidin-biotin approach allows as well site-specific attachment of antibody, which minimalize steric hindrance and consequently improves binding, since immobilized avidin has a role as a linker and therefore improves accessibility of biotinylated antibodies for surface antigens on the cells (Magdeldin and Moser, 2012).

4.2 MATERIALS AND METHODS

4.2.1 MATERIALS

Medical grade nonporous borosilicate glass spheres GL-0179B5 (90-106 µm in diameter with 2.2 g/cm^3 density and 1.472 refractive index) were obtained from MO-SCI Specialty Products, L.L.C (Rolla, Missouri, USA).

Ethylenediaminetetraacetic acid, disodium salt dehydrate for electrophoresis (EDTA; Acros Organics), bovine serum albumin (BSA; cell culture grade, pH 7.0, lyophilised powder; Thermo Scientific HyClone), D(+)-biotin (Acros Organics; 98 % purity), 7-aminoactinomycin D (Molecular Probes®, Invitrogen; 7-AAD), streptavidin R-Phycoerythrin conjugate (Molecular Probes®, Invitrogen; SAPE; 1 mg/mL solution), RPMI-1640 liquid medium with 2.05 mM L-glutamine (Thermo Scientific HyClone; RPMI), foetal bovine serum (Thermo Scientific HyClone; FBS; standard filtered through three sequential 100 nm (0.1 µm) pore size rated filter) and Trypan blue (Molecular Probes®, Invitrogen; 0.4 % solution) were purchased through Fischer Scientific UK Ltd. (Loughborough, UK), as well as phosphate buffered saline (PBS buffer) in a tablet form. Each tablet prepares 100 mL of PBS buffer.

Analytical grade (99+ % purity) hydrogen chloride (HCl) and sodium hydroxide (NaOH) supplied by Fischer Scientific UK Ltd. (Loughborough, UK) were used for preparation of buffer solutions and were and suitable for cell culture.

All solutions were prepared using water purified by a Millipore Elix Gulfstream Clinical 100 (Merck Millipore UK Ltd, Watford, UK) water purification system. Buffer solutions were prepared by dissolving a known mass of buffering species into *ca*. 80% of the desired final volume of deionized water, titrating with 1 M solution of HCl or NaOH and adding water to yield the final solution volume.

Sterilization of solutions and suitable materials was performed either by autoclaving at 121 °C for 30 min using ASB 300T autoclave (Astell Scientific, Sidcup, UK) or by filtering through through a 0.22 µm syringe filter (Merck Millipore UK Ltd, Watford, UK).

Rituximab (anti-CD20 monoclonal antibody) was purchased from Roche (Basel, Switzerland). Toledo ATCC® CRL2631™ continuous cell line (CD20 positive cell line (Gabay *et al*., 1999) was purchased from LGC Standards (Teddington, UK) and CCRF-HSB-2 cell line was purchased from the Health Protection Agency, Culture Collection (Salisbury, UK).

Tricorn 5/50 column and complementary Tricorn 5 coarse filter kit were supplied by GE Healthcare (Uppsala, Sweden).

4.2.2 METHODS

4.2.2.1 Preparation of antibodies and cells

Rituximab antibody was biotinylated in advance following the procedure from the Section 2.2.2.3.

Toledo cell line was cultured as described in the Section 2.2.2.5. Prior the use was cell suspension collected, cells counted and their viability checked by Trypan blue exclusion method. Cells were then centrifuged at room temperature at 200 g_{av} for 5 min in a Heraeus Labofuge 400R centrifuge (Thermo Scientific, Fisher Scientific, Loughborough, UK). After completed centrifugation supernatant was decanted and pellet resuspended in 1 mL of PBS buffer. Just before the use was suspension gently mixed by pipette and diluted with RPMI medium without supplements to the required concentration.

4.2.2.2 Preparation of affinity support

Beads were prepared and characterized as previously described in the section 3.2.2 and stored at 4 °C, protected from the light, until use.

On the day of experiment were beads packed into Tricorn column under gravity to the height of 5.5 cm. Column was then connected to the Äkta Pure chromatographic system (GE Healthcare, Uppsala, Sweden) and ready for the use.

4.2.2.3 Coupling of biotinylated antibody to the beads

To the 5 mL of bead slurry (1:1 ratio beads:buffer) the antibody suspension was added to a final concentration of 50 µg/mL and incubated overnight at 4 °C, protected from the light. Before the use, beads were centrifugated (200 g_{av} for 2 min, without a brake) and gently rinsed with 2.5 mL of PBS buffer. All the suspensions were collected to measure absorbance at 280 nm (UV mini 1240 UV/VIS Spectrophotometer, Shimadzu, Milton Keynes, UK) and mass of antibody in the suspension was calculated using equation 2.1.

4.2.2.4 Binding of biotinylated antibody to cells

When required, cell suspensions were incubated with biotinylated. To the 5 mL of cell suspension ($4*10^7$ cells/mL; $2*10^8$ cells in total) in PBS buffer supplemented with 2 mM EDTA and 0.5 % BSA, antibody solution was added to a final concentration of between 0.5 and 50 µg/mL. The suspension was then incubated on the 3-D rocking platform STR 9 (Stuart Scientific, Stone, UK) with shaking at 70 revs/min for 1 h at room temperature, followed by centrifugation at 200 g_{av} at room temperature for 5 min. Supernatant was decanted and pellet resuspended in 10 mL of RPMI medium without supplements.

4.2.2.5 Affinity chromatography

The development of the affinity method for the positive selection of human cells was performed in a following way. Mobile phase A (running buffer; PBS, pH 7.4) and mobile phase B (elution buffer; 2 mM D-biotin in PBS, pH 7.4) were filtered through a 0.22 µm filter unit, to sterilise, and degassed for 10 min in ultrasonic bath (Fisherbrand S15, Fisher Scientific Ltd., Loughborough, UK). The column was at first equilibrated with mobile phase A until UV signal at 280 nm remained stable for 1 min (acceptable UV fluctuation: 20 mAu). If the UV signal was not stable after 10 min of equilibration, column was removed from the system, beads decanted and column was re-packed with fresh beads. After equilibrium was achieved, 0.5, 2 or 5 mL of cell suspension was injected onto the column from the top or the bottom at linear flow rate of 30 cm/h (0.1 mL/min) or 60 cm/h (0.2 mL/min). To maximize recovery, sample loop was overfilled, *i.e*. into 0.5 mL loop, 1 mL of cell suspension was injected. The injection valve was then emptied using the mobile phase at a volume of twice that of the sample loop. Washing to remove non-specifically and weakly bound cells were conducted under the same or reversed flow conditions with 10 mL (10 column volumes, *i.e.* 10 CV) of mobile phase A at flow rate from 30 cm/h up to 600 cm/h. Elution (mobile phase B) varried from 30 cm/h to 600 cm/h and both, the same or reversed flow, were evaluated. During elution the flow was stopped for in between 15 and 120 minutes to allow competitive displacement of biotinylated antibody and cells with D-biotin. Cells in all fractions were counted using a Neubauer Improved Bright-Line haemocytometer (Sigma Aldrich, Gillingham, UK) as previously described in Section 2.2.2.10. Elution was stopped after the viability of cells, assessed by Trypan blue exclusion method, dropped below 60 %.

4.2.2.6 Immunophenotypic analysis of cells

Immunophenotypic analysis of cells was determined by flow cytometry using Guava easyCyte 8HT flow cytometer (Merck Millipore UK Ltd, Watford, UK) and the data was analysed with InCyte software (Merck Millipore UK Ltd, Watford, UK) following the procedure from the Section 2.2.2.10.

4.3 RESULTS AND DISCUSSION

Following the successful modification, functionalization and characterization of the beads with immobilized avidin with the revisable biotin binding sites and initial development of the affinity method for the positive selection of human therapeutic cells with red blood cells, the positive selection method described in Chapter 3 was further optimized with Toledo cell line, *i.e*. B lymphocytes, which were introduced together with T lymphocytes from various human cell lines, as they are more similar to the CD34+ progenitor cells, the most popular target population in the positive cell selection, which can be sourced from bone marrow and peripheral blood (Hipp and Atala, 2008).

The first part of experiments was performed with antibody immobilized on beads and injection of $3*10^6$ cells onto column.

Cells were initially loaded, eluted and non-specific and weakly bound cells removed at linear flow rate of 30 cm/h from the bottom to the top of the column. But no cells were eluted, the majority (>90 %) of cells present in fractions collected during load and wash step were not in a viable form. This indicated that cells were being starved of nutrients and were exposed for too long to shear stress, even with a relatively short loading time of 10 min and washing step of 100 min. This is in agreement with Gu *et al*. (2000) who found that human cells might be resistant to the high shear stress, but for only limited time. In the comparison, Kumar and his group (2003) were applying cells to their affinity monolithic cryogel columns at flow rate 1.5 mL/min (linear flow rate not available). Although the structure of monolithic columns cannot be directly comparable with packed bed column, and consequently the mass transfer in packed bed differs from the mass transfer in monoliths (Jungbauer and Hahn, 2004), it was agreed that this is a good indication of cell resistance and therefore it is worth to try and proceed with increased flow rates.

Initially cells were injected in PBS buffer; however, to improve their viability and to be able to indirectly track them during loading and partially wash, samples were prepared in the basic cell culture medium RPMI 1640 without supplements, which absorbs at 280 nm.

Simultaneously with the injection of cell suspension in RPMI medium and the increase of flow rates, sequential stops during elution were introduced. The increase of the loading flow rate from 30 cm/h to 60 cm/h still allowed enough of contact time between immobilized antibodies and antigens on the surface of cells in order for cells to specifically bound, and also resulted in an increased viability of cells collected in flow-through fractions (at least 75 % viability assessed by Trypan blue assay). The washing flow rate was gradually increased to 600 cm/h (2 mL/min), which was high enough to remove all non-specifically bound cells, as well as weakly bound cells and did not have any negative impact on the viability of eluted cells. Subsequently it was discovered that the washing step does not only remove non-specifically bound cells, but also dead CD20 positive cells. The elution flow rate was also increased to 600 cm/h, with a goal to reduce elution time and, potentially improve cell viability. The time intervals, during which the flow was paused in order to allow D-biotin to competitive displace immobilized biotinlyted antibody and cells were gradually decreased from 120 min to 15 min. Pausing the flow was an efficient way to elute cells, but long stops increased the duration of a single experiment and consequently the viability of the cells was poor (below 50 %, assessed with Trypan blue exclusion method) when stops lasted for 45 min or more. Stopping the flow for 30 min or less resulted not only in significantly increased viability of cells (above 80 %), but also in a greater number of eluted cells. A pause in the flow for 15 min was long enough for D-biotin to remove cells from the surface and it allowed at least 6 stops to elute more cells in a viable condition (above 70 %) in less than 2 h. Over the time, the viability of cells dropped as expected based on previous findings (Gu *et al*., 2000), for example after the first stop the average viability was 94 % but after 6th stop was only 71%.

To confirm that elution was due to the displacement of D-biotin and not to the instant increase of flow rate from 0 to 600 cm/h, the experiment was conducted with beads with immobilized tetrameric form of avidin. As no cells were eluted it was concluded that elution is based on competitive basis rather than mechanical one.

Reversed flow during the washing and elution proved an efficient way to elute more red blood cells (see Section 3.3.2), this approach was also tested with white blood cells, but without success. Not only were fewer cells eluted, all were dead and simultaneously a change in the conductivity was observed, which suggests the conditions were suboptimal and the cells underwent lysis. Therefore it was switched back to the same flow path during all three separation steps, *i.e*. from the bottom of the column to the top.

The selectivity of the developed method was tested by challenging naked (non-modified) beads, amino derived and dextran coated beads with B lymphocytes. In all three cases, the majority of injected cells (more than 95 %) were detected in flow through fractions and remaining ones in washing fractions. This confirms the adequacy of the selected chemistry. In the next step monomeric avidin beads with immobilized biotinylated anti-CD20 antibody were challenged with CD20 negative cells (CCRF-HSB-2 cell line) to evaluate the selectivity of the developed method. Once again, the majority of cells (87 %) were present in flow through fractions, while the remaining ones were washed through by mobile phase A.

After conditions were optimized, various numbers of cells were applied onto a column with a goal to determinate its capacity for B lymphocytes. Results are presented in the Table 4.1 below.

Table 4.1: Overview of results obtained by challenging the monomeric avidin immobilized in a packed bed column with various number of cells.

Number of injected B lymphocytes (Toledo cell line) (*10^6)	**3.0**	**6.6**	**23.0**	**35.0**	**40.0**	**75.2**	**100.0**	**120.0**	**270.0**
Cell concentration (*10^6 cells/mL)	6.0	13.3	46.0	70.0	20.0	15.0	20.0	48.0	108.0
Loop size (mL)	0.5	0.5	0.5	0.5	2	5	5	5	5
Cells in flow through and washout fractions (*10^6)	0.05	0.1	13.0	13.2	9.5	7.8	23.2	24.3	140.0
Retained cells on the column (*10^6)	2.95	6.53	10.2	22.0	30.5	67.4	76.8	95.7	130.0
Eluted cells (*10^6)	0.13	0.15	3.3	8.4	13.6	28.8	37.3	48.5	55.2
Elution efficiency (%)	4.3	2.3	32.10	38.72	44.64	42.78	48.52	50.71	42.39
Number of elution steps	6	6	7	9	8	8	7	7	7
Total elution time (h)	1.75	1.75	2	2.5	2.25	2.25	2	2	2
Lost cells (*10^6)	2.82	6.38	6.9	13.6	16.9	38.6	39.5	47.2	74.8

It is important to stress that all presented separations of B lymphocytes did not take more than 3 h.

Initially it was observed that the cell concentration of loaded cell suspension has the impact on the binding efficiency and the viability of eluted cells (Figure 4.1 below). The results demonstrated that the number of bound cell was inversely proportional to the initial concentration of cells, moreover, poorer cell viability was observed with a high initial concentration. The breakthrough point was determinated as 4*10^7 cells/mL.

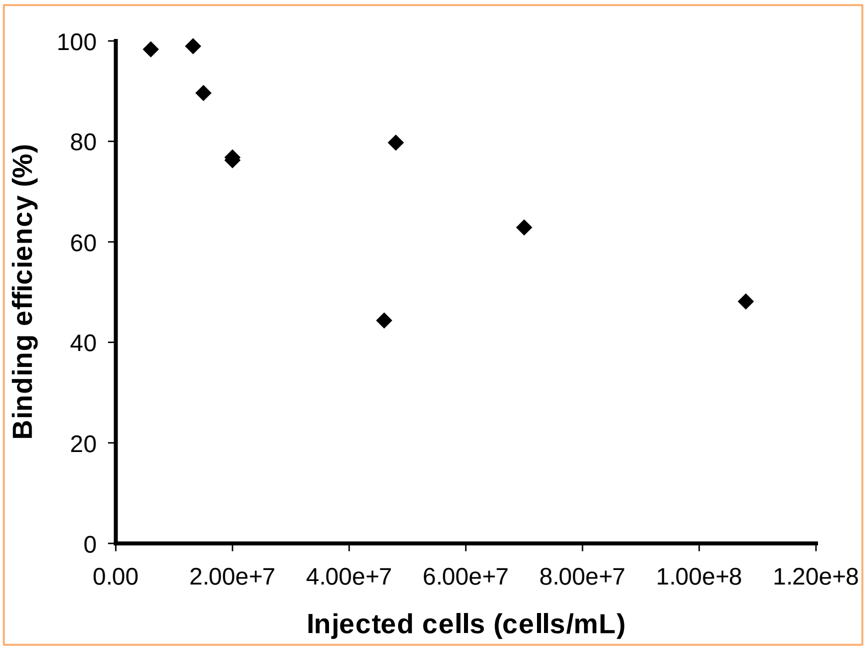

Figure 4.1: The impact of concentration of injected cell suspension on the binding efficiency (%) on the monomeric avidin packed bed column.

To reduce the impact of the concentration of cell suspension on the cell binding and viability the loop size was increased proportionately from 0.5 to 5 mL.

The number of specifically bound cells has an influence on the elution efficiency (Figure 4.2 below). The best elution efficiency (50.71 %) was achieved when $9.57*10^7$ cells were specifically bound to the support.

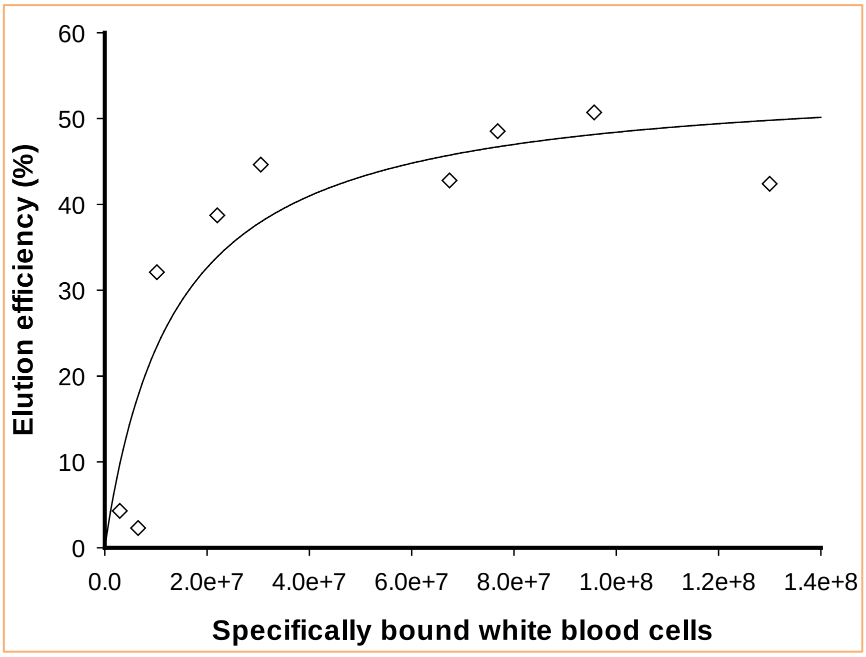

Figure 4.2: The impact of the number of specifically bound cells onto elution efficiency (%) from the monomeric avidin affinity support.

The elution efficiency decreases dramatically when less than $2.3*10^7$ cells are injected onto column. This might be due to the fact that on the column was an excess of immobilized antibodies. According to the absorbance measurements of supernatants after antibody immobilization, between 34.2 and 38.5 µg of the antibody was immobilized per mL of bead slurry (approximately 1:1 ratio between beads and buffer). In a single packed bed column there was between 36.9 and 41.5 µg immobilized antibody, which is equal to in between 0.84 and 0.94 mg of antibody per m^2. Based on the experiments with red blood cells (Section 3.3.2), D-biotin is gradually replacing biotinylated antibody. Although there might be a lot of cells released from the matrix surface after the first pause of the flow, an excess of immobilized antibody gives them a chance to re-bind. When more cells are initially bound to the surface; fewer antibodies are accessible for cells to rebound. Additionally is important not to neglect steric hindrance, as more cells are bound, steric hindrance has a greater impact on the binding. To confirm this, $3*10^6$ cells were loaded under various linear flow rates (Figure 4.3).

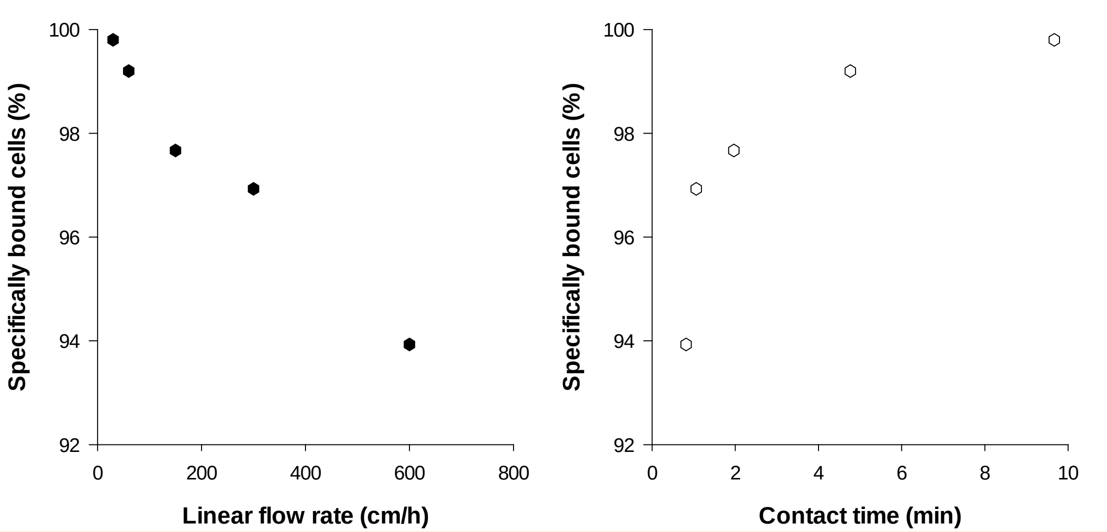

Figure 4.3: The impact of linear flow rate (cm/h; left graph; black circles) and contact time (min; right graph; white circles) on the specifically bound cells (%).

Although the number of specifically bound cells correlates with the loading flow rate, linear flow rate of 600 cm/h is still slow enough to allow specific binding of 94 % loaded cells, even though the contact time (the time a single cell is retained on the column) is only 1.25 min. Having in mind that each cell expresses at least 1.23*10^5 CD20 antigens on the surface (Ginaldi *et al.*, 1998), this is likely to happen.

In order to have more control over re-binding of cells during the elution, cells were incubated in advance with the biotinylated antibody before being separated on the affinity packed bed column, aiming to reduce the level of rebinding during the elution step. After an initial test run it was evident that the loading flow rate of 60 cm/h was no longer appropriate. It was too high and had the negative impact on the binding efficiency, which dropped below 45 %. Therefore, the loading linear flow rate was reduced to 30 cm/h (volumetric flow rate of 0.1 mL/min) before proceeding with a series of experiments which varied the concentrations of antibody in the cell suspension.

Based on the results of experiments with antibodies immobilized on beads were for the evaluation of the impact of antibody concentration in cell suspension used 2*10^7 cells/mL (1*10^8 cells in total), which were injected on the column using 5 mL loop. The concentration of the antibody was gradually decreased from 50 µg/mL down to 0.5 µg/mL.

Unfortunately the detection of free antibodies in the supernatants after completed incubation was not doable due to the presence of cell metabolites, therefore, the amount of antibody needed was calculated based on the data published by Ginaldi and his coworkers (1998). For the calculations, the assumption that 1 µg of IgG antibody (CD20, for an example) consists of $3.6*10^{12}$ molecules, was made. As each antibody has 2 antigen binding sites, in theory 1 µg of IgG can bind to $7.2*10^{12}$ antigen molecules. As a typical antigen may be present in 10^4 or 10^5 copies per cell, 1 µg should be enough for between $7.2*10^7$ and $7.2*10^8$ cells. If in the cell suspension only, for example, 20 % of cells are positive for the selected marker; this number of cells should be multiplied by a factor of 20, as the total number of antigens is 20 times lower. From the antibody concentration the number of antibody molecules needed for a single B lymphocyte from a human peripheral blood was calculated. Usually B lymphocytes from a healthy donor has $9.4*10^4$ copies of CD20 antigen per cell (Ginaldi *et al*., 1998). Calculations are summarized in the Table 4.2.

Table 4.2: Theoretical percentage of the occupancy of surface CD20 antigens on the single B lymphocyte from a peripheral blood of a healthy donor by various antibody concentrations. Red font is used for the cases when antibody is in excess.

Antibody concentration (µg/mL)	Percentage of antigens occupied per cell (%)	
	1 antibody per 1 antigen	1 antibody per 2 antigens
50.0	191.49	765.96
10.0	38.30	153.19
1.0	3.83	15.32
0.5	1.91	7.66
0.1	0.38	1.53

In theory, when the concentration of antibody is 50 µg/mL, the antibody is in abundance, while in 0.1 µg/mL might not be enough of antibody present to label each CD20 positive cell which would have negative impact on the yield; therefore experiments were carried out only with antibody concentration between 50 and 0.5 µg/mL. Results of affinity chromatography are presented in the Table 4.3.

Table 4.3: The summary of the positive selection of B lymphocytes from Toledo cell line labelled with biotinylated antibody on the immobilized monomeric avidin in the packed bed column.

Antibody concentration (µg/mL)	**50.0**	**10.0**	**1.0**	**0.5**
Number of injected B lymphocytes (*10^6)	100	100	100	100
Cells in flow-through and washout fractions (*10^6)	11.5	14.9	15.3	16.5
Retained cells on the column (*10^6)	88.5	85.1	84.7	83.5
Eluted cells (*10^6)	30.6	37.5	41.4	45.2
Elution efficiency (%)	34.58	44.12	48.80	54.21
Number of elution steps	5	7	7	7
Total elution time (h)	1.5	2	2	2
Lost cells (*10^6)	57.9	47.6	43.3	38.3

As it can be seen in the Figure 4.4 below, the antibody concentration has an impact on the binding and elution efficiency. The number of specifically bound cells and consequently the binding efficiency depends on the antibody concentration - the higher it is the more cells are bound. On the other hand the elution efficiency is increasing by titrating down the antibody.

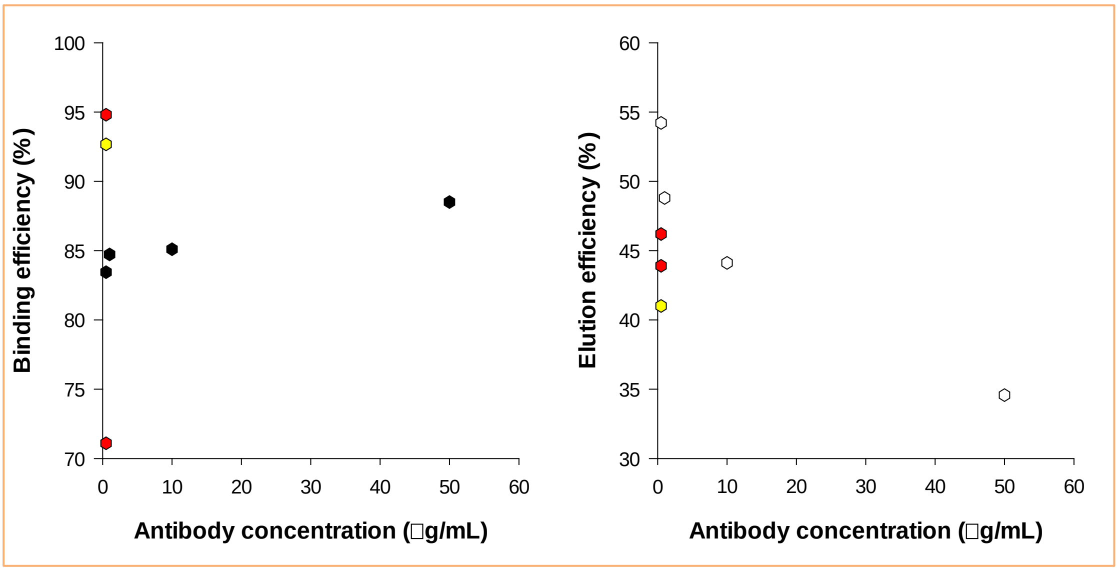

Figure 4.4: The impact of antibody concentration on the binding (left graph) and elution efficiency (right graph) of white blood cells to and from the affinity packed bed with immobilized monomeric avidin. Black and white dots represent experiments with 1*10^8 cells (2*10^7 cells/mL) injected, red dots represent loaded 1*10^7 cells (2*10^7 cells/mL) on the column and yellow dots are results from the experiments with loaded 3*10^6 cells (6*10^6 cells/ml).

Comparing the results when the same number of cells ($1*10^8$ cells) was applied to the immobilized antibody on the column, the binding efficiency is higher in all cases (76.82 % was when antibody was immobilized on the beads), most likely due to the decreased loading flow rate, as cells labelled with antibody are retained on the column for twice as long (Figure 4.3; right part of the figure). In terms of elution efficiency, results from the experiment with antibody on the beads were comparable with the ones when cells were incubated in the presence of 1 µg of antibody per mL of suspension and better in comparison with 50 and 10 µg/mL. Elution efficiency correlates with antibody concentration, as by reducing concentration of antibody and cell suspension from 50 µg/mL to 0.5 µg/mL, elution efficiency was increased from 34.6 to 54.2 %. Overall the best elution efficiency (54.21 %) was achieved after cells were incubated in 0.5 µg of antibody per mL.

Cell viability assessed by Trypan blue was reduced by an average of 4 %, but after 6 stops cell viability was still at least 65 %. The reason for this might be in the length on the separation method, as the loading took twice as long, but together with the incubation of cells in the presence of antibodies, the experiment did not take more than 3.5 h.

Following this, the number of cells labelled in 0.5 µg/mL antibody solution, was decreased from $1*10^8$ to $1*10^7$ cells, while the concentration of injected samples remained the same. It was observed that the binding efficiency remained basically the same (from 83.45 % dropped slightly to 82.95 %), while the impact on the elution efficiency was greater. By decreasing the number of specifically bound cells for the factor ≈10, elution efficiency dropped from 54.21 % to 45.05 %. But the elution efficiency for injected $1*10^7$ cells is still for nearly 12 % greater when antibody is bound on the cells in comparison to the case, when the same number of cells was applied to the column with immobilized biotinylated antibody.

Cells may be lost during the centrifugation during the preparation of sample for injection and cell counting after collected fractions, as each centrifugation step can result to the losses of 20-30 % (Lemarie *et al*., 2005).

The chromatogram from one of the runs injected with $1*10^7$ cells after incubation in 0.5 µg/mL antibody solution is presented in the Figure 4.5 below.

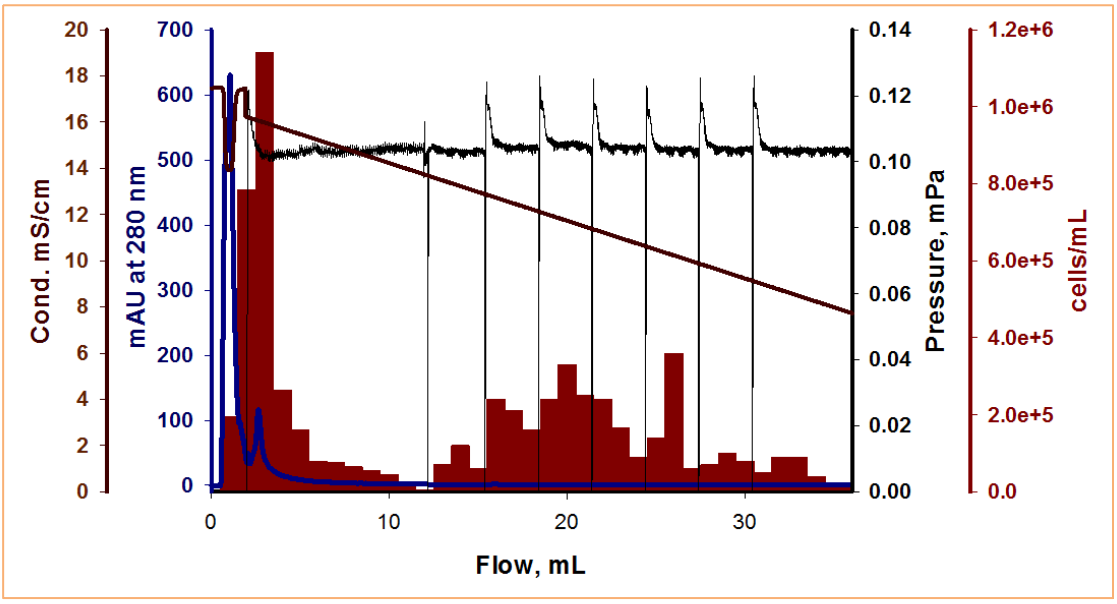

Figure 4.5: Affinity chromatography of human CD20 positive cells (challenge = $1x10^7$ cells) labelled in advance with biotinlyated monoclonal antibody. Black line indicates pressure (mPa) on the system during the run, dark brown conductivity (mS/cm) and blue line represents absorbance at 280 nm (mAU). Dark red bars show cell counts of fractions during load, wash and D-biotin mediated elution. Change in the pressure to 0 mPa indicates where flow was stopped for 15 min.

In the case of white blood cells, in contrast to red blood cells, conductivity slowly and linearly dropped during the elution. The final conductivity had dropped from 16 to 8 mS/cm. This explains gradual decrease in cell viability over time. Additionally, cells were eluted by D-biotin throughout the elution step of the separation, while in the case of red blood cells (Figure 3.11), the majority of cells were eluted in the first of three fractions after stopped flow. The reason for this might be in the differences in the cell structures and characteristics (for example, B lymphocytes are round, while red blood cells are biconcave shape), as well as in the interactions between red blood cells (see Section 3.3.2, Figure 3.9).

The pressure drop on the system changed during the run for the 0.02 mPa, which indicates that very little or no cell entrapment was present on the column during the experiment. Each time pressure dropped to zero was due to the flow being stopped.

Cell fractions collected during the same separation step were then combined and analysed by flow cytometry to compare the cellular function of cells before and after the assay and additionally assess cell viability as Trypan blue exclusion method could be ambiguities in the identification of stained, nonviable cells (Altman *et al*., 1993).

The goal of the analysis of the samples after performed affinity separation with the developed monomeric avidin-biotin technology was to confirm the presence of CD20 marker on cells from the selected cell line and to assess the impact of the separation on the viability and immunophenotype of cells. Results are summarized in the Table 4.4.

Table 4.4: The overview of the flow cytometry results of injected sample and fractions collected during positive separation of CD20 positive cells on monomeric avidin packed bed column.

Sample source	Injected cell suspension	Loading	Wash	Elution
CD20 positive and viable cells (%)	95.62	80.84	18.16	92.64
CD20 positive and viable cells (*10^4 cells)	956.2	10.7	7.0	385.4
CD20 positive and dead cells (%)	1.86	4.31	5.42	3.97
CD20 positive and dead cells (*10^4 cells)	18.6	0.6	2.1	16.5
CD20 negative cells (%)	2.52	14.84	76.42	3.38
CD20 negative cells (*10^4 cells)	25.2	2.0	29.3	14.1
Total cell number in fraction (*10^4 cells)	1000	13.3	38.4	416.0

As predicted, more than 95 % of cells in the suspension were CD20 positive and in a viable state (95.62 %), an additional 1.86 % was positive for the selected marker, but not viable. Collected fractions during load contained 80.84 % positive and viable cells which indicate there is a scope for the optimization of the loading conditions although only $1.33*10^5$ cells were present in this fraction (1.33 % of the applied cells). Options are further decreasing the linear flow rate or by pausing the flow when cell suspension reaches the top of the column in order to increase contact time of cells on the column. The increase of the flow rate for the removal of the weakly and non-specifically bound cells has a positive effect on the separation as it does not mechanically disturb the monomeric avidin – biotinylated antibody interaction, *i.e*. only 18.16 % of cells collected during the wash were detected as CD20 positive, which is equal to 0.7 % of all loaded CD20 positive cells. This indicates the developed technology is highly selective and could be applied for the negative selection of cells, *i.e.* the removal of not wanted cells from the suspension. In this case no elution step would be implemented.

The cells of choice were successfully eluted by the displacement of biotinylated antibody attached to the cells with free D-biotin present in the elution buffer, as 92.64 % were positive for the CD20 antigen and alive. A further 3.97 % of cells were CD20 positive but not in a viable condition. Eluted CD20 positive and viable cells represent 40.10 % of the injected CD20 positive cells or 39.60 % of specifically bound CD20 cells.

4.4 CONCLUDING REMARKS

The positive selection method using immobilized monomeric avidin packed bed was implemented for the selection of human B lymphocytes (CD20 positive cells). Two approaches were evaluated, namely binding biotinylated antibodies to the chromatographic support and *a priori* binding of antibodies to the cells. Not only the binding of biotinlyted antibody to cells rather to the chromatographic support proved to have positive impact on elution efficiency, binding of antibodies to the cells is the preferred way in the selection of cells using magnetic beads (Grützkau and Radbruch, 2010). Additionally it is more suitable for a user, as it is not limited to the products currently on the market and can use its own antibodies, antibody fragments or even aptamers.

In order to further improve elution efficiency and yields it might be worth reconsidering further decreasing the antibody concentration in the cell suspension to 0.1 µg/mL and/or loading linear flow rate, although it might have negative impact on the yields, binding and elution efficiency.

The immunophenotypic analysis of cells collected during the separation process indicated the developed affinity matrix is highly selective and could be therefore be applied for the removal of non-wanted cells (negative selection).

4.5 REFERENCES

Altman S.A., Randers L. and Rao G. 1993. Comparison of Trypan blue dye exclusion and fluorometric assays for mammalian cell viability determinations. *Biotechnology progress*, vol. 9, no. 6, pp. 671-674.

Berenson R.J., Bensinger W.I., Kalamasz D. and Martin P. 1986a. Elimination of Daudi lymphoblasts from human bone marrow using avidin- biotin immunoadsorption. *Blood*, vol. 67, no. 2, pp. 509-515.

Berenson R.J., Bensinger W.I. and Kalamasz D. 1986b. Positive selection of viable cell populations using avidin-biotin immunoadsorption. *Journal of immunological methods*, vol. 91, no. 1, pp. 11-19.

Cao X., Eisenthal R. and Hubble J. 2002. Detachment strategies for affinity-adsorbed cells. *Enzyme and microbial technology*, vol. 31, no. 1-2, pp. 153-160.

Gabay C., Ben-Bassat H., Schlesinger M. and Laskov R. 1999. Somatic mutations and intraclonal variations in the reaarnged Vkappa genes of B-non-Hodgkin's lymphoma cell lines. *European journal of haematology*, vol. 63, no. 3, pp. 180-191.

Ginaldi L., De Martinis M., Matutes E., Farahat N., Morilla R. and Catovsky D. 1998. Levels of expression of CD19 and CD20 in chronic B cell leukaemias. *Journal of clinical pathology*, vol. 51, no. 5, pp. 364-369.

Gravel R.A., Lam K.F., Mahuran D. and Kronis A. 1980. Purification of human liver propionyl-CoA carboxylase by carbo tetrachloride extraction and monomeric avidin affinity chromatography. *Archives of biochemistry and biophysics*, vol. 201, no. 2, pp. 669-673.

Grützkau A. and Radbruch A. 2010. Small but mighty: How the MACS®-Technology based on nanosized superparamagnetic particles has helped to analyze the immune system within the last 20 years. *Cytometry Part A*, vol. 77, no. 7, pp. 643-647.

Gu Y.J., Boonstra P.W., Graaff R., Rijnsburger A.A., Mungroop H. and van Oeveren W. 2000. Pressure drop, shear stress, and activation of leukocytes during cardiopulmonary bypass: A comparison between hollow fiber and flat sheet membrane oxygenators. *Artificial organs*, vol. 24, no. 1, pp. 43-48.

Henrikson K.P., Allen S.H.G. and Maloy W.L. 1979. An avidin monomer affinity column for the purification of biotin-containing enzymes. *Analytical biochemistry*, vol. 94, no. 2, pp. 366-370.

Jungbauer A. and Hahn R. 2004. Monoliths for fast bioseparation and bioconversion and their applications in biotechnology. *Journal of separation science*, vol. 27, no. 10-11, pp. 767-778.

Kohanski R.A. and Lane M.D. 1990. Monovalent avidin affinity columns. *Methods in enzymology*, vol. 184, pp. 194-200.

Kumar A., Plieva F.M., Galeav I.Y. and Mattiasson B. 2003. Affinity fractionation of lymphocytes using a monolithic cryogel. *Journal of Immunological methods*, vol. 283, no. 1-2, pp. 185-194.

Kuo S.C. and Lauffenburger D.A. 1993. Relationship between receptor/ligand binding affinity and adhesion strength. *Biophysical journal*, vol. 65, no. 5, pp. 2191-2200.

Lemarie C., Calmels B., Malenfant C., Arneodo V., Blaise D., Viret F., Bouabdallah R., Ladaique P., Viens P. and Chabannon C. 2005. Clinical experience with the delivery of thawed and washed autologous blood cells, with automated closed fluid management device: CytoMate. *Transfusion*, vol. 45, no. 5, pp. 737-742.

Lightfoot E.N. and Moscariello J.S. 2004. Bioseparations. *Biotechnology and bioengineering*, vol. 87, no. 3, pp. 259-273.

Magdeldin S. and Moser A. 2012. Affinity chromatography: Principles and applications. In: Magdeldin S., eds. *Affinity chromatography*. Rijeka: InTech, pp. 3-28.

Qureshi M.H. and Wong S.-L. 2002. Design, production, and characterization of a monomeric streptavidin and its application for affinity purification of biotinylated proteins. *Protein expression and purification*, vol. 25, no. 3, pp. 409-415.

5. GLASS BEAD CHROMATOGRAPHY VERSUS MACS® MICROBEADS: A FIRST PRINCIPLE COMPARISON

Abstract

Since the first applications of magnetic beads for cell separation they have been a popular choice and are now the first choice in the clinical applications and research. The goal of the experimental work presented in this chapter was to directly compare the developed affinity separation technology based on the immobilized monomeric avidin and MACS® Microbeads, the gold standard in the separation of human therapeutic cells. Results suggest that the developed chromatography method is a competitive and could be used for the purposes of regenerative medicine, as the achieved yields, purities and cell viabilities are comparable.

5.1 INTRODUCTION

Initial attempts to develop affinity chromatography separation for the selection of mammalian cells cover the magnetic separation of red blood cells and antibody-coated cells with iron-containing polymeric microspheres conjugated to lectines (Molday *et al*., 1977). A year later, separation of C-1300 neuroblastoma cells, 10 % of which expressed target ganglioside GM1 in their membranes, was published. The results were already promising, with researchers achieving a 99 % purity in only 6 minutes (Kronick *et al*., 1978), therefore, it is not surprising that by the 1985 it was already being frequently used for medical applications, such as tumour cell removal from bone marrow and cell sorting and screening for malarial parasites in blood. For these purposes heteroantisera or monoclonal antibodies as targeting agents were immobilized on magnetic beads of various size ranges and materials

(Kemsheadl and Ugelstad, 1985). The real breakthrough occurred in 1987, when Stefan Miltenyi invented cell sorting, shortly MACS®, few years later being granted with a patent and founding Miltenyi Biotec (Miltenyi *et al*., 1990; Miltenyi *et al*., 1991).

First magnetic particles were less than 0.5 µm in a diameter and with a particle surface modified by dextran. The selectivity of the separation was achieved by an avidin-biotin system, as to was considered to be the most versatile immunological detection system. Cells were at first labelled with biotinylated antibody, followed by staining with fluorescent avidin conjugate and completed with incubation with biotinylated microbeads. A steelwool column was inserted into the external magnetic field and cells were then applied onto column and eluted by removal of the column from the magnetic field (Miltenyi *et al*., 1990). Since then several improvements have been made and nowadays beads are suspension of colloids, ten times smaller than first beads (50 nm in the diameter) and the antibody is usually directly coupled onto the beads (Šafařik and Šafaříková, 1999). A column matrix is made up of spheres, which are between 250 and 500 µm in the diameter (Miltenyi Biotec MACS® Technology). Besides Miltenyi Biotec other magnetic beads are available, which can be roughly divided into micro- and nonobeads, for example Invitrogen (Carlsbad, USA) offers Dynal® microbeads, BD Biosciences (San Jose, USA) advertise nanobeads named IMAG® and EasySep®, nanobeads are manufactured by Stem Cell Technologies (Vancouver, Canada). All beads come with specially designed column and a separator (Grützkau and Radbruch, 2010).

No matter what beads are used, the separation process is usually performed in a batch mode and consists of three separation steps: (i) cells of interest are labelled with magnetic beads and applied on the column with the appropriate magnetic separator; (ii) column is washed several times in order to remove non-target cell population; and (iii) column is removed from the separator and cells are eluted by, for example, a plunger (Šafařik and Šafaříková, 1999). Miltenyi Biotech has also launched flow-through semi-automated, fully automated and robotic integrated magnetic separators, where magnetically labelled cells are pumped through the column and retained on it. After the removal of the magnetic field, cells are retrieved by the combination of flow and gentle vibration of the column (Šafařik and Šafaříková, 1999; Miltenyi Biotec MACS® Technology).

During the past 30 years magnetic particles have been established and accepted, with a plethora of applications in biology and biomedicine (Grützkau and Radbruch, 2010), stem cell separation is a bottleneck in stem cell therapy, as MACS® technology cannot meet purification needs for the purposes of cell therapy as it cannot provide highly pure and viable cells (Schriebl *et al*., 2010), even with optimized multistep protocols (Gonzáles-Gonzáles *et al*., 2011). The demand is enormous, as it was estimated that in 2009, in the USA alone, more than 100 million patients were treated by cell-based therapies and in the 2014 annual revenue in cell-based therapies (excluding cord blood banking) was predicated to be around 5 billion US dollars (Mason *et al*., 2011). Between 2007 and 2009, the average cost for the collection and processing of autologous peripheral blood stem cells together with a hospital treatment for a 100-day treatment in the USA was 99899 US dollars per patient (Majhail *et al*., 2013), because the isolation of CD34 positive cells includes apheresis, negative selection (depletion of non-target cells), followed by positive selection of cells of interest, which are present in small numbers (Riley *et al*., 2009).

In the past, magnetic separations have been as well combined with chromatographic approach. For the determination of which subclass of mice splenocytes able to metabolite benzo[a]pyrene (B(a)P), cells were initially separated by the density gradient centrifugation and immunomagnetic negative selection and then the metabolites were detected by high-pressure liquid chromatography (Ladics *et al*., 1992). Besides that, the enrichment of CD34 positive cells by magnetic beads were directly compared with chromatography separation. Magnetic separation was performed with Isolex 300i® magnetic separator in conjunction with Dynabeads® (Baxter Biotech) and for chromatography based separation CellPro® Ceprate SC system (Cell Pro Incorporation) (Stella *et al*., 1995; Johnsen *et al*., 1999). Initially was CellPro® developed for the depletion of T lymphocytes exploiting avidin-biotin approach. Native, tetrameric, avidin is conjugated to polyacrylamide beads packed into column and cells are passed through the column after the incubation in biotinylated monoclonal antibody solution (20 µg/mL) (Colter *et al*., 1996). Later on a positive selection was developed where elution is achieved by the agitation of the column (Johnsen *et al*., 1999). Both, magnetic beads or chromatography device did not perform to the required standard. While the purity achieved with magnetic beads was on average 86 % (for comparison only 49 % with affinity chromatography), the yield was poor using the both devices (40 % magnetic beads, 30 % chromatography). Additionally more than 50 % of depleted cells were positive for CD34. Authors suggested improvements of both devices in order to have a safe and sufficient product in clinical practice (Stella *et al*., 1995; Johnsen *et al*., 1999).

5.2 MATERIALS AND METHODS

5.2.1 MATERIALS

Medical grade nonporous borosilicate glass spheres GL-0179B5 (90-106 µm in diameter with 2.2 g/cm^3 density and 1.472 refractive index) were obtained from MO-SCI Specialty Products, L.L.C (Rolla, Missouri, USA).

Ethylenediaminetetraacetic acid, disodium salt dehydrate for electrophoresis (EDTA; Acros Organics), bovine serum albumin (BSA; cell culture grade, pH 7.0, lyophilised powder; Thermo Scientific HyClone), D(+)-biotin (Acros Organics; 98 % purity), 7-aminoactinomycin D (Molecular Probes®, Invitrogen; 7-AAD), streptavidin R-Phycoerythrin conjugate (Molecular Probes®, Invitrogen; SAPE; 1 mg/mL solution), RPMI-1640 liquid medium with 2.05 mM L-glutamine (Thermo Scientific HyClone; RPMI), foetal bovine serum (Thermo Scientific HyClone; FBS; standard filtered through three sequential 100 nm (0.1 µm) pore size rated filter) and Trypan blue (Molecular Probes®, Invitrogen; 0.4 % solution) were purchased through Fischer Scientific UK Ltd. (Loughborough, UK), as well as phosphate buffered saline (PBS buffer) in a tablet form. Each tablet prepares 100 mL of PBS buffer.

All solutions were prepared using water purified by a Millipore Elix Gulfstream Clinical 100 (Merck Millipore UK Ltd, Watford, UK) water purification system.

Sterilization of solutions and suitable materials was performed either by autoclaving at 121 °C for 30 min using ASB 300T autoclave (Astell Scientific, Sidcup, UK) or by filtering through through a 0.22 µm syringe filter (Merck Millipore UK Ltd, Watford, UK).

Rituximab (anti-CD20 monoclonal antibody) was purchased from Roche (Basel, Switzerland). Toledo ATCC® CRL2631™ continuous cell line (CD20 positive cell line (Gabay et al., 1999)) was purchased from LGC Standards

(Teddington, UK) and cell lines Jurkat E6.1, Bristol-8 and CCRF-HSB-2 were purchased from Health Protection Agency, Culture Collection (Salisbury, UK).

Tricorn 5/50 column and complementary Tricorn 5 coarse filter kit were supplied by GE Healthcare (Uppsala, Sweden).

CD20 MicroBeads (human) and LS columns for magnetic cell sorting were purchased from Miltenyi Biotec (Bergisch Gladbach, Germany), as well as CD20-PE (human, clone LT20) staining antibody for flow cytometry. MidiMACS separator, consisting of magnet and a stand, was generously lent for the use by Miltenyi Biotec UK Division.

5.2.2 METHODS

5.2.2.1 Preparation of affinity matrix

Glass beads were prepared, characterized and packed into Tricorn column to the bed height of 5.5 cm as described in Chapter 3 (Sections 3.2.2.1, 3.2.2.2, 3.2.2.5 and 3.2.2.6).

5.2.2.2 Chromatography-based cell enrichments

Chromatography-based separations were performed using the method detailed in this section. Rituximab antibody was biotinylated in advance and stored at 4 °C following the procedure from the Section 2.2.2.3.

Cell lines were cultured as described in the Section 2.2.2.5. Prior the use cell suspensions were collected, cells counted and their viability checked by Trypan blue exclusion method. Cells were then centrifuged at room temperature at 200 g_{av} for 5 min in a Heraeus Labofuge 400R centrifuge (Thermo Scientific, Fisher Scientific, Loughborough, UK). After completed centrifugation supernatant was decanted and pellet resuspended in 1 mL of PBS buffer. Just before the use suspensions were gently mixed by pipette and cell lines were combined if required. To the 5 mL of cell suspension ($4*10^7$ cells/mL; $2*10^8$ cells in total) in PBS buffer supplemented with 2 mM EDTA and 0.5 % BSA, required volume of antibody solution was added to the final concentration of 0.5 µg/mL. The suspension was then incubated on the 3-D rocking platform STR 9 (Stuart Scientific, Stone, UK) with shaking at 70 revs/min for 1 h at room temperature, followed by centrifugation at 200 g_{av} at room temperature for 5 min. Supernatant was decanted and the pellet resuspended in 10 mL of RPMI medium without supplements.

On the equilibrated column with PBS buffer as a running buffer, were injected $1*10^7$ cells through the 0.5 mL loop from the bottom to the top of the column at a loading flow rate of 30 cm/h for 10 min, followed by washing at 600 cm/h for 10 column volumes (CV; 10 mL) and elution with 2 mM D-biotin in PBS buffer at flow rate 600 cm/h. After 3 CV of elution buffer passed the column, the pump was stopped for 15 min. This was repeated at least 6 more times. Throughout the separation process fractions of 1 mL were collected. For the flow cytometry evaluation, fractions of each separation step were combined in order to have enough big samples for the analysis.

5.2.2.3 Immunophenotypic analysis of cell suspensions

Immunophenotypic analysis of cells was determined by flow cytometry using Guava easyCyte 8HT flow cytometer (Merck Millipore UK Ltd, Watford, UK) and data was analysed with InCyte software (Merck Millipore UK Ltd, Watford, UK) following the procedure from the Section 2.2.2.10.

5.2.2.4 MACS® enrichment of selected cell populations

MACS® experiments were performed in ice-cold PBS buffer supplemented with 0.5 % BSA and 2 mM EDTA. Each time $1*10^7$ cells were used for the separations. Cell suspensions were collected and centrifuged at room temperature at 200 g_{av} for 5 min and pellet resuspended in 80 µL of buffer, to which 20 µL of CD20 MicroBeads were added and incubated for 15 min at 4 °C in the dark. Then 10 µL of CD20-PE staining antibody was added and further incubated for 5 min. Wash was performed by addition of 2 mL of buffer and centrifuged at room temperature at 200 g_{av} for 5 min. Supernatant was decanted and pellet resuspended in 500 µL of buffer.

In the meantime, a LS column was mounted on the stand with a magnet and equilibrated by passing through 3 mL of buffer. Separations started by application of cells onto the column, labelled cells were retained on the column and passed cells were collected for further analysis. Then column was washed three times by 3 mL of buffer, each time column reservoir was emptied. Eluent was kept for flow cytometry analysis. The column was then removed from the stand and consequently magnetic field. In the reservoir 5 mL of buffer was pipetted and cells were eluted by the plunger supplied.

All the suspensions were then centrifuged at room temperature at 200 g_{av} for 5 min and pellet resuspended in 200 µL of buffer and 10 µL of 7-AAD viability dye was added. Cells were then analysed by flow cytometry following the same procedure as for the fluorescently labelled cells separated with affinity matrix.

5.3 RESULTS AND DISCUSSION

As MACS® technology cannot be directly comparable with the developed affinity approach, the experiments were performed by challenging both columns with the same number of cells – $1*10^7$ cells, as this is a recommended number of cells for the positive selection of CD20 cells with LS MACS® column by manufacturer (MACS Magnetic cell sorting).

Columns for the chromatography and magnetic cell separations are similar in size (Figure 5.1). The height of a packed bed column was fixed to 5.5 cm, while the height of the bead matrix in the LS column is 4 cm. The average glass bead is 98.43 µm in diameter, while beads packed in the LS column are in between 250 and 500 µm in diameter.

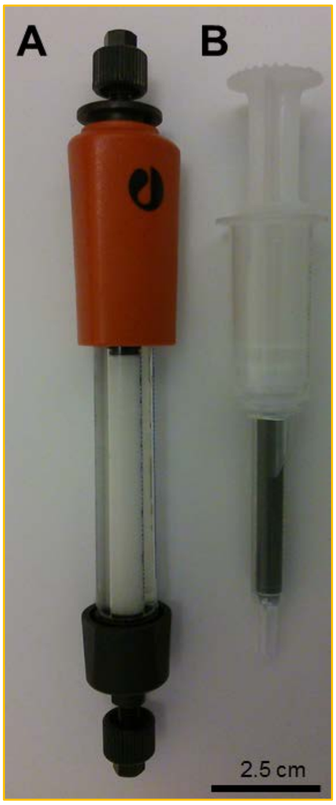

Figure 5.1: Comparison of chromatography and MACS® column. (A) Tricorn 5/50 column with adjustable adapter on the top packed with modified and functionalized glass beads. (B) MACS® LS column with the inserted plunger for the mechanical elution of cells of interest.

The performance of separation techniques was compared based on three separation challenges, using various feedstocks, namely (i) CD20 positive cell; (ii) 95 % of cells CD20 positive, remaining CD20 negative (CCRF-HSB-2 cell line); and (iii) mixture of cell with only 5 % CD20 positive cells. In all three cases the separation process (*e.g.* flow rates for chromatography and incubation times for the separation with magnetic beads) was the same. To reduce the impact of biological viability on the positive selection of CD20 cells, cells were synchronously taken from the same cell stock. Results are presented in the Table 5.1 below.

Table 5.1: Comparison of glass bead chromatography and MACS® system for the separation of human B lymphocytes

Challenge	Performance	MACS®	Chromatography
100 % CD20 positive cells	Elution efficiency (%)	20.14	40.37
	Cell purity (%)	99.5	96.7
	Cell viability (%)	99.6	95.7
	Yield (%)	15.25	39.50
95 % CD20 positive cells	Elution efficiency (%)	16.51	37.00
	Cell purity (%)	98.4	93.7
	Cell viability (%)	92.1	94.5
	Yield (%)	5.38	35.09
5 % CD20 positive cells	Elution efficiency (%)	32.39	38.82
	Cell purity (%)	28.8 (74.4*)	78.5
	Cell viability (%)	46.7 (90.8*)	95.5
	Yield (%)	32.29	30.93

*after 2nd separation step

The initial set of experiments with only CD20 positive cells, proved that the developed affinity separation method based on the monomeric avidin-biotin system could be used as an alternative to MACS®. Cell purity and viability in the elution fraction were slightly weaker, but the difference is less than 5 % which could be due to experimental error. On the other hand, when using a chromatographic approach, the elution efficiency was twice that observed with MACS®, additionally, the overall yield was better. This suggests affinity chromatography is a more efficient approach to positive cell separation.

Following this, CD20 positive cell lines were combined with 5 % of cells without CD20 antigens on the surface to further investigate the selectivity of both processes, although great differences were not expected as both approaches are based on the antibody interactions with the cell surface antigens. In terms of cell purity, MACS® performed slightly better, but this time the affinity beads used had a positive impact on the cell viability. Again, the differences in these two parameters are below 5 %. A new chromatographic approach was performed over magnetic beads. This time the elution efficiency was more than 2 times better, while the yield was 6.5 times better, suggesting that although to the avidin modified beads packed into column was nearly $1*10^6$ less cells specifically bound ($9.59*10^6$ *vs*. $8.61*10^6$ cells), almost 2 times more specifically bound cells are eluted ($1.67*10^6$ *vs*. $3.19*10^6$ cells).

To really challenge both matrices, the target CD20 population in the initial feedstock was further reduced to 5 %. It was expected that this would show the true value of the developed chromatographic system as the number of target cells, suitable for the therapeutic applications, in the cell suspensions is low, usually below the selected 5 % (Schriebl *et al*., 2010). Based on results, developed chromatography based separation has been ratified to be a step in the right direction. First of all, it was performed as a single step separation, while magnetic bead separation required a 2 step purification process, which was performed by reapplying the collected flow through and washing fractions to the new, fresh, LS column. Resulting in the overall, elution efficiency and yield of affinity based separations are being comparable to the results obtained with MACS®, but cell purity and viability were still slightly better even after the second MACS® purification. Finally $1.22*10^5$ CD20 positive cells (95.5 % viability) were collected in the elution fraction by chromatography and $1.20*10^5$ CD20 cells (90.8 % viability) in the second MACS® elution fraction. The difference between the both methods was only 2000 cells (1.6 %).

Unsurprisingly MACS® does not provide with a highly pure and viable cell suspensions isolated from feedstocks with initial low percentage of target cells after only one separation step. In one of the studies, performed with low cell target percentage cell sources, between 68.4 and 78.4 % purity was achieved (de Wynter *et al*., 1999). Significant improvement can be made by introducing a multi-stage process (Schriebl et al., 2010), as it was demonstrated above. Results presented in this chapter confirm chromatography requires less separation steps, especially when the initial cell population is complex and the starting percentage of cells is low.

The results from the monomeric avidin affinity separations are promising due to the fact that, based on the FDA recommendations, a safe CD34 positive cell dose in cell therapy should have a purity of at least 80 % and it is cost effective only when the process yield is at least 40 % (Johnsen *et al*., 1999).

In terms of costs, the estimate for each separation approach was made based on the online retail prices on 24th July 2014. The cost was calculated based on the material needed for a single purification of CD20 cells, sufficient for a single cell based treatment, from the heterogeneous cell population (5 % of the target population). The assumption was made that there are no differences between the required time for the separation, as chromatography based separation takes approximately 1.5 h less, but it requires preparation of beads and biotinylation of antibody. Comparing with MACS® technology, where beads and column are sold as ready to use kit, if beads for the affinity chromatography would be available on the market they would probably be already packed in the single use column, which would mean an advantage for the chromatography based separation. Additionally nowadays the most common antibodies against cell surface markers can be purchased biotinylated, which would spare the user approximately 30 minutes.

The initial cost of the required equipment was used for the cost evaluation, unless it is possible to rent it. In this case hourly rate is complied. Consumables (*e.g*. pipette tips and centrifuge tubes) and buffers were overlooked as similar amount is required for both separation processes. Additionally the cost of the use of flow cytometer for the evaluation of separated cells is left out as both approaches require it, with the only difference being the use of a fluorescently labelled marker.

Table 5.2: Evaluation of costs associated with affinity based chromatography and MACS® for the purification of 5 % target cells from the cell population, sufficient for a single dose of cell based treatment

Affinity based separation		MACS®	
Preparation of glass beads		**Separation**	
Glass beads	£1.50	Stand	£130.00
Avidin from egg white	£12.30	Separator	£427.00
D-Biotin	£0.06	LS column (2 pieces)	£21.20
Antibody biotinylation		CD20 MicroBeads	£4.11
Rituximab	£0.95	**Flow cytometry**	
D-biotin	£0.03	CD20-PE	£6.40
PD-10 columns (2 pieces)	£13.07	7-AAD viability dye	£0.53
Separation			
Äkta Pure (4 hour rental*)	£20.49		
Tricorn 5/50 column	£337.00		
Coarse 5/50 filter kit	£62.78		
D-biotin	£0.12		
Flow cytometry			
Streptavidin-PE	£3.18		
7-AAD viability dye	£0.53		
TOTAL COST	**£452.10**		**£589.24**

*based on the cost of 1 year lease

The simplified economical evaluation (Table 5.2) additionally confirms the adequacy of the newly developed monomeric avidin chromatographic separation technique, as it is the cost associated with the preparation of glass coverslips, the separation itself and evaluation performance, is comparable with the current leading technology for the cell separation for the purpose of cell therapy. Overall, the total cost for the affinity based separation is slightly lower.

The initial cost for the columns is greater for the affinity separation, but Tricorn columns are reusable and can be sterilized, while LS columns are single use. Additionally the coarse filters for the Tricorn column can be reused up to 10 times and one kit consists of 5 sets of bottom and top filters.

In terms of the cost of the antibody, which is the most crucial part for the success of the separation, as the selectivity is based on its reactivity with the surface antigens on the cells of interest, are expectedly antibodies conjugated with magnetic beads 4 times more expensive than biotinylated antibody for the developed packed bed chromatography. Flow cytometry of cells separated by MACS® requires as well an secondary antibody, which needs to bind to a different region on a cell in order to get a signal from the flow cytometric analysis. This additionally adds to the total cost of the separation technique.

In terms of equipment needed, for the liquid chromatography is required a chromatographic system, such as Äkta Pure, which was used for the experiments presented in this chapter. To reduce the cost, simpler liquid separation system can be used, as long as it allows set up described above. The biggest costs for MACS® technology are stand and magnetic separator. Both are reusable but especially magnetic separator cannot be substituted with less costly alternative as it is specially designed for LS columns.

5.4 CONCLUDING REMARKS

The direct comparison of the developed monomeric avidin based affinity system for the positive separation of human cells with MACS$^{®}$, magnetic affinity cell separation, currently the leading technology for the cell separation, has confirmed the adequacy of the newly developed system.

Throughout the evaluation glass bead chromatography outperformed magnetic beads in terms of the elution efficiency and yields and produced comparable results in the purity and the viability of purified cells. Challenging both columns with more heterogeneous cell population and with only 5 % target cells in it, resulted in promising results as for the similar purity and cell viability, MACS$^{®}$ system required 2 step purification, while the selectivity of affinity matrix requires only one. Additionally the simplified economic evaluation of both separation techniques was made and it can be concluded that the associated costs are similar.

It would be sensible to test both systems with different feedstocks, *e.g*. isolation of stem cells from the bone marrow or adipose tissue, and to perform the scale-up study in order to gain more purified cells of interest.

5.5 REFERENCES

Colter M., Jones M. and Heimfeld S. 1996. CD34+ progenitor cell selection: clinical transplantation, tumor cell purging, gene therapy, ex vivo expansion, and cord blood processing. *Journal of hematotherapy*, vol. 5, no. 2, pp. 179-184.

Gabay C., Ben-Bassat H., Schlesinger M. and Laskov R. 1999. Somatic mutations and intraclonal variations in the reaarnged Vkappa genes of B-non-Hodgkin's lymphoma cell lines. *European journal of haematology*, vol. 63, no. 3, pp. 180-191.

Gonzáles-Gonzáles M., Vázquez-Villegas P., García-Salinas C. and Rito-Palomares M. 2011. Current strategies and challenges for the purification of stem cells. *Journal of chemical technology and biotechnology*, vol. 87, no. 1, pp. 2-10.

Grützkau A. and Radbruch A. 2010. Small but mighty: how the MACS®-technology based on nanosized superparamagnetic particles has helped to analyze the immune system within the last 20 years. *Cytometry A*, vol. 77, no. 7, pp. 643-647.

Johnsen H.E., Hutchings M., Taaning E., Rasmussen T., Knudsen L.M., Hansen S.W., Andersen H., Gaarsdal E., Jensen L., Nikolajsen K., Kjaesgârd E. and Hansen N.E. 1999. Selective loss of progenitor subsets following clinical CD34+ cell enrichment by magnetic field, magnetic beads or chromatography separation. *Bone marrow transplantation*, vol. 24, no. 12, pp. 1329-1336.

Kemsheadl J.T. and Ugelstad J. 1985. Magnetic separation techniques: their application to medicine. *Molecular and cellular biochemistry*, vol. 67, no. 1, pp. 11-18.

Kronick P.L., Campbell G.L. and Joseph K. 1978. Magnetic microspheres prepared by redox polymerization used in a cell separation based on gangliosides. *Science*, vol. 200, no. 4345, pp. 1074-1076.

Ladics G.S., Kawabata T.T., Munson A.E. and White K.L. Jr. 1992. Evaluation of murine splenic cell type metabolism of benzo[a]pyrene and functionality in vitro following repeated in vivo exposure to benzo[a]pyrene. *Toxicology and applied pharmacology*, vol. 116, no. 2, pp. 258-266.

MACS Magnetic cell sorting. CD20 MicroBeads. Order No. 130-091-104 [online]. [viewed 07/01/2014]. Miltenyi Biotec*, Bergisch Gladbach, Germany*, pp. 1-3. Available from: http://www.miltenyibiotec.com/~/media/Images/Products/Import/0001100/IM0001149.ashx

Majhail N.S., Mau L.W., Denzen E.M. and Arneson T.J. 2013. Costs of autologous and allogeneic hematopoietic cell transplantation in the United States: a study using a large national private claims database. *Bone marrow transplantation*, vol. 48, no. 2, pp. 294-300.

Mason C., Brindley D.A., Culme-Seymour E.J. and Davie N.L. 2011. Cell therapy industry: Billion dollar global business with unlimited potential. *Regenerative medicine*, vol. 6, no. 3, pp. 265-272.

Miltenyi S., Mueller W., Weichel W. and Radbruch A. 1990. High gradient magnetic cell separation with MACS. *Cytometry*, vol. 11, no. 2, pp. 231-238.

Miltenyi S., Radbruch A., Weichel W., Mueller W., Goettlinger C. and Meyer K.L. 1991. Column for the magnetic separation of cells, cell aggregates and cellular constituents. DE Patent 3720844 C2 (Also published as DE Patent 3720844 A1).

Miltenyi Biotec MACS® Technology. The gold standard. Now and forever. [online]. [viewed 07/05/2014]. *Miltenyi Biotec, Bergisch Gladbach, Germany*, pp. 1-12. Available from: http://www.miltenyibiotec.com/~/media/Files/Navigation/Cell%20Separation/macs-technology-cell-isolation-brochure.ashx

Molday R.S., Yen S.P.S. and Rembaum A. 1977. Application of magnetic microspheres in labelling and separation of cells. *Nature*, vol. 268, no. 5619, pp. 437-438.

Riley J.L., June C.H. and Blazar B.R. 2009. Human T regulatory cell therapy: take a billion or so and call me in the morning. *Immunity*, vol. 30, no. 5, pp. 656-665.

Schriebl K., Lim S., Choo A., Tscheliessnig A. and Jungbauer A. 2010. Stem cell separation: a bottleneck in stem cell therapy. *Biotechnology journal*, vol. 5, no. 1, pp. 50-61.

Stella C.C., Cazzola M., De Fabritiis P., De Vincentiis A., Gianni A.M., Lanza F., Lauria F., Lemoli R.M., Tarella C., Zanon P. and Tura S. 1995. CD34-positive cells: biology and clinical relevance. *Haematologica*, vol. 80, no. 4, pp. 367-387.

Šafařik I. and Šafaříková M. 1999. Use of magnetic techniques for the isolation of cells. Journal of chromatography B, vol. 722, no. 1-2, pp. 33-53.

de Wynter E.A., Ryder D., Lanza F., Nadali G., Johnsen H., Denning-Kendall P., Thing-Mortensen B., Silvestri F. and Testa N.G. 1999. Multicentre European study comparing selection techniques for the isolation of CD34+ cells. *Bone marrow transplantation*, vol. 23, no. 11, pp. 1191-1196.

6. CONCLUSIONS AND FUTURE WORK RECOMMENDATIONS

6.1 CONCLUSIONS

Research of adult stem cells has been slow, largely because challenges associated with the maintenance of pure stem cell culture over long period of time, especially as these cells are low in the number in their original sources. It is believed that although the use of adult stem and progenitor cells is currently limited, their future utilization in tissue specific regenerative therapies shows a great potential, especially as they can be used in autologous therapies, thus avoiding any immune rejections (Hipp and Atala, 2008).

The goal of the work presented in this thesis was to develop a new affinity matrix for the separation of human (therapeutic) cells. The feasibility of the developed separation technology has been proven in this work by successful transfer from static tests on glass coverslips, through initial studies under flow with glass hollow capillary tubes, to the application on non-porous glass coverslips. The positive cell selection method was successful developed and optimized. Based on the results, the affinity method is comparable with MACS™ technology, currently the number one choice in the research, as well as in the clinical applications.

The development and optimization of the biocompatible surface chemistry was performed on glass coverslips. Consistent manufacture of affinity supports was achieved by layer-by-layer deposition of (3-aminopropyl)triethoxysilane and oxidized dextran, followed by the cleavage of native avidin from egg white into its subunits under controlled conditions. The selectivity of so modified glass coverslips was obtained by the use of biotinylated monoclonal antibodies specific for the cell surface antigens. Cells were recovered from the support by the competitive elution with 2 mM D-biotin. This approach proved to be highly selective on a small scale and has the additional advantage of not promoting non-specific cell attachment.

The first attempts of the chromatographic separation of cells were performed with human red blood cells. Although they might not be representative model for the majority of human cells due to their size and shape, they are visible to the naked eye; therefore there was no need for the additional labelling, which might interfere with the selection assay, in order to track them online throughout the experiment.

After the partial optimization of the chromatographic method, white blood cells, *i.e*. B and T lymphocytes from human cell lines, were introduced as they are more similar to the CD34+ progenitor cells, the most popular target population in the positive cell selection (Tomlinson *et al*., 2012).

The ideal separation conditions were set as loading at 30 cm/h or 60 cm/h (depending on the location of the biotinylated antibody – on the cell or immobilized on the support), washing non-specific cells and elution was performed at 600 cm/h. The elution efficiency was significantly improved once sequential pause of the flow during the elution was introduced and allowed D-biotin to displace biotinylated antibody and consequently elute cells.

The goal of the final study was the direct comparison between the developed technology on the packed bed affinity column and MACS®. Both devices were synchronously challenged with the same number and origin of cells. Although there is still a scope for the improvement of the developed affinity approach to the positive selection, the packed bed chromatography was a competitive product and it even performed better than magnetic beads in terms of elution efficiency and yields.

6.2 FUTURE WORK RECOMMENDATIONS

Clinical devices for cell separation exist, but there is still room for the improvement of the technology before the procedure results in a sufficient and safe product in clinical practice (Johnsen *et al*., 1999). Due to the current techniques, FACS, MACS® and density gradient centrifugation, having limitations such us low selectivity, low scalability and contaminations risks (Diogo *et al*., 2012). As the low-cost alternative selection method we propose the developed affinity chromatography method.

There are many areas highlighted in this work that would be interesting for further study. The most promising are listed and shortly described below.

6.2.1 THE SELECTION OF THE CHROMATOGRAPHIC SUPPORT

The selected format of packed bed of spherical particles is not the ideal affinity chromatographic support format, but it is preferred choice in the separations as it can currently be made with the highest degree of uniformity (Billen and Desmet, 2007). As the transport in packed bed columns is based on the diffusivity, it would be interesting to test convective media, such as cryogels and polymeric monoliths. The separation should be faster and the productivity higher (Jungbauer and Hahn, 2004) which should result in a positive impact on cell viability. This is important as one of the biggest issues during the method development was the duration of the separation process and its negative impact on cell viability. Another alternative chromatographic support suitable for the positive selection of cells with the developed monomeric avidin-biotin system are membranes.

6.2.2 OPTIMIZATION OF THE SURFACE MODIFICATION AND FUNCTIONALIZATION

In order to reduce the cost of the chromatographic support manufacturing, it would be interesting to attempt to collect and recycle avidin from the immobilization procedure with, *e.g*. size exclusion chromatography. Furthermore it might be worth reconsidering the production on a larger scale and, if possible, under flow conditions, especially if the chromatographic support of choice are monolithic columns.

6.2.3 SCALE-UP

Currently, single dose for cells for the therapy consists in between of $1*10^7$ and $4*10^7$ cells (Perin et al., 2003), therefore, for the transfer of the technology into clinics, there is a need to investigate the scale-up of the developed technology. This can be done either by the scale up of the existing chromatographic matrix using Tricorn™ columns or by using a different support. In both cases the characteristics of the affinity matrix need to be carefully chosen in order to allow efficient mass transport and to not expose cells to a large pressure drop in the column and consequently a too big shear stress.

6.2.4 THE SELECTION OF AFFINITY LIGANDS

In this study purely monoclonal antibodies were used as selection markers, but there are limitations connected with its use as the specific marker for the cells of interest might not be known, although new markers are being described rapidly (Hipp and Atala, 2008; Diogo *et al*., 2012). But both, FACS and MACS® are based on monoclonal antibodies as the selection tool for the efficient separation. Aptamers, in laboratory engineered ligands, could be used as an alternative, although they are not yet widely accepted in the connection with FACS and MACS®. As the developed chromatographic support allows both, use of the immobilized ligands on the separation matrix, and labelling cells with them, this is an additional bonus. Any ligand of choice can be used, as long as it is in advance biotinylated, which is a simple and fast procedure and usually does not interfere with the function of the biotinylated molecule (Cole *et al*., 1987; Cronan *et al*., 2000; Elia, 2008).

6.2.5 THE EVALUATION OF THE SELECTIVITY AND EFFICIENCY OF THE DEVELOPED AFFINITY METHOD WITH VARIOUS FEEDSTOCKS

Due to the limited resources, the method development was performed with red blood cells from cord blood and B and T lymphocytes from the continuous cell lines. To further evaluate the adequacy of the positive selection the method should be tested with various feedstocks, *e.g*. peripheral blood, bone marrow, cord blood and adipose tissue. These samples are more complex in terms of the cell diversity and in addition, cells of interest (*e.g*. CD34+ cells) are present in low numbers (Hipp and Atala, 2008). This will really challenge the developed support and consequently show the true value of this approach for the cell separation.

6.2.6 ADDITIONAL ASSESSMENT OF CELLS AFTER COMPLETED SEPARATION

The additional evaluation of the function (*e.g*. white blood cells take part in the immune response) and origin of cells after completed separation process can be done by their transplant *in vivo* into immunodeficient mice models. Using this approach additional data would be generated to demonstrate if the developed selection method does not have negative impact on cells and subsequently confirm its adequacy for the use in the clinical and medical research applications.

6.2.7 CLOSED SYSTEM SEPARATION

For the translation of stem cells and stem cell-derived products to the clinics and drug discovery it is necessary to retain sterility of cells during separation (Diogo *et al*., 2012). Developed chemistry is resistant to the sterilization with antibiotics, but not to the autoclave sterilization. In order to avoid contamination of cells during the processing, is essential the use of sterile techniques in sterile closed environment. This can be achieved either by placing the chromatographic system in the biological safety cabinet or, even better, the direct integration of separation technique with stem cell bioreactor culture.

6.3 REFERENCES

Billen J. and Desmet G. 2007. Understanding and design of existing and future chromatographic support formats. *Journal of chromatography A*, vol. 1168, no. 1-2, pp. 73-99.

Cole S.R., Ashman L.K. and Ey P.L. 1987. Biotinylation: An alternative to radioiodination for the identification of cell surface antigens in immunoprecipitates. *Molecular immunology*, vol. 24, no. 7, pp. 699-705.

Cronan J.E. Jr. and Reed K.E. 2000. Biotinylation of proteins *in vivo*: A useful posttranslational modification for protein analysis. *Methods in enzymology*, vol. 326, pp. 440-458.

Diogo M.M., da Silva C.L and Cabral J.M.S. 2012. Separation technologies for stem cell bioprocessing. *Biotechnology and bioengineering*, vol. 109, no. 11, pp. 2699-2709.

Elia G. 2008. Biotinylation reagents for the study of cell surface proteins. *Proteomics*, vol. 8, no. 19, pp. 4012-4024.

Hipp J. and Atala A. 2008. Sources of stem cells for regenerative medicine. *Stem Cell reviews and reports*, vol. 3, no. 1, pp. 3-11.

Johnsen H.E., Hutchings M., Taaning E., Rasmussen T., Knudsen L.M., Hansen S.W., Andersen H., Gaarsdal E., Jensen L., Nikolajsen K., Kjaesgârd E. and Hansen N.E. 1999. Selective loss of progenitor subsets following clinical CD34+ cell enrichment by magnetic field, magnetic beads or chromatography separation. *Bone marrow transplantation*, vol. 24, no. 12, pp. 1329-1336.

Jungbauer A. and Hahn R. 2004. Monoliths for fast bioseparation and bioconversion and their applications in biotechnology. *Journal of separation science*, vol. 27, no. 10-11, pp. 767-778.

Perin E.C., Geng Y.J. and Willerson J.T. 2003. Adult stem cell therapy in perspective. *Circulation*, vol. 107, no. 7, pp. 935-938.

Tomlinson M.J., Tomlinson S., Yang X.B. and Kirkham J. 2012. Cell separation: Terminology and practical considerations. *Journal of tissue engineering*, vol. 4, pp.1-14, doi: 10.1177/2041731412472690.

7. APPENDICES

APPENDIX A: STANDARD CURVE FOR TNBS (PICRYLSULFONIC ACID) ASSAY

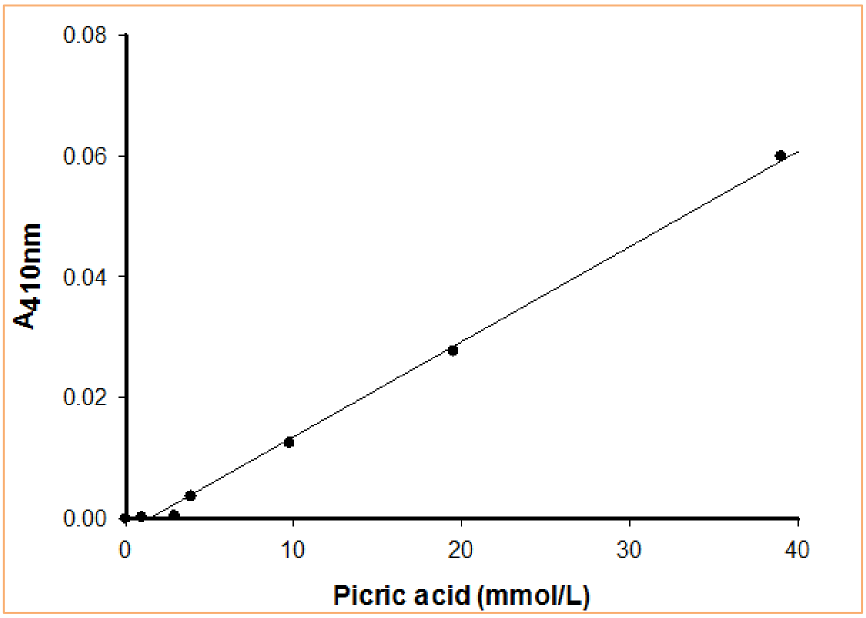

Figure App. A: An example of standard curve for TNBS assay. The absorbance of standard, picric acid in 1 M NaOH (mmol/L), was measured at 410 nm wavelength. Black circles represent measured data and a line statistical evaluation of the data using a nonlinear regression.

The data analysis was performed with SigmaPlot 12.0 software (Systat Software, Inc., San Jose, California, USA) and the report is summarized below. As the R^2 is above 0.95 and P value for a is below 0.05, are results statistically significant, therefore the model can be used for the determination of picric acid in the slurries.

Nonlinear Regression
Equation: Polynomial, Linear
f = y0+a*x

R	**Rsqr**	**Adj Rsqr**	**Standard Error of Estimate**
0.9982	0.9964	0.9956	0.0015

	Coefficient	**Std. Error**	**t**	**P**
y0	-0.0022	0.0007	-2.9818	0.0307
a	0.0016	4.2557E-005	36.9521	<0.0001

APPENDIX B: STANDARD CURVE FOR BCA (BICINCHONINIC ACID) PROTEIN ASSAY

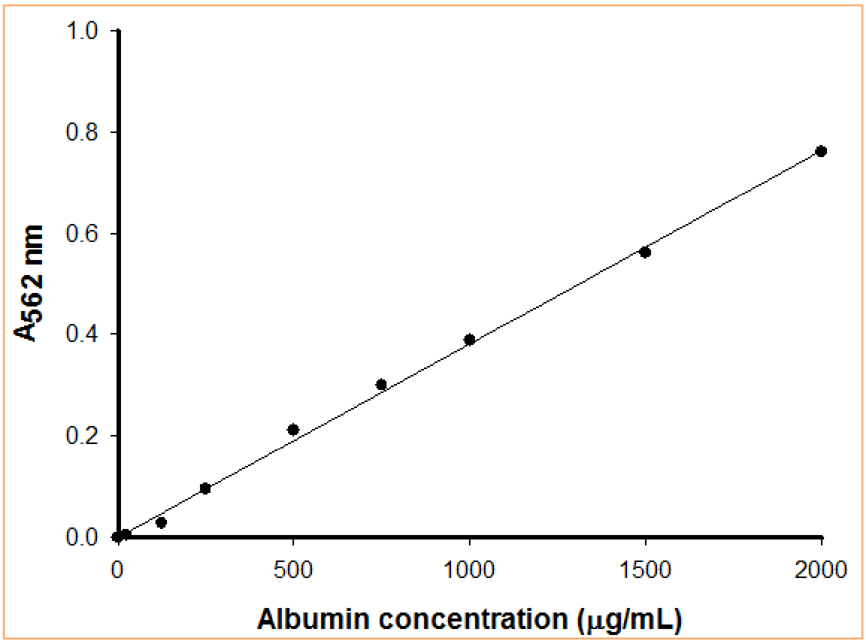

Figure App. B: An example of standard curve for BCA assay. Concentration of standard albumin (µg/mL) is plotted on the x-axis and absorbance at 562 nm on the y-axis. Black circles represent measured data and a line statistical evaluation of the data using a nonlinear regression.

The model is statistically significant (R^2 is above 95 % and P value for the coefficient a is below 0.05), as it can be seen from the software report section below.

```
Nonlinear Regression
Equation: Polynomial, Linear
f = y0+a*x

R       Rsqr    Adj Rsqr        Standard Error of Estimate
0.9990  0.9979  0.9976          0.0131
        Coefficient     Std. Error      t               P
y0      -7.5849E-005    0.0063          -0.0121         0.9907
a       0.0004          6.5931E-006     57.8992         <0.0001
```

APPENDIX C: STANDARD CURVE FOR THE DETERMINATION OF FREE BIOTIN

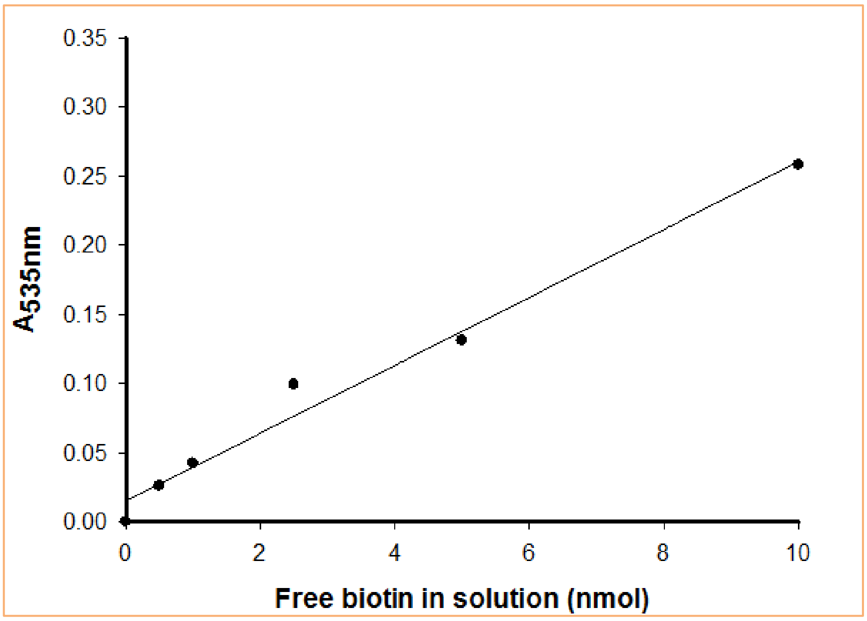

Figure App. C: An example of standard curve for the determination of free biotin in the experimental slurries. Concentration of standard biotin (nmol) is plotted on the x-axis and absorbance at 535 nm on the y-axis. Black circles represent measured data and a line statistical evaluation of the data using a nonlinear regression.

The statistical model used for the determination of free biotin in the samples is statistically significant , as R^2 is aboce 0.95 and P value for the coefficient a in the used equation is less than 0.05.

Nonlinear Regression
Equation: Polynomial, Linear
f = y0+a*x

R	**Rsqr**	**Adj Rsqr**	**Standard Error of Estimate**
0.9910	0.9821	0.9776	0.0141

	Coefficient	**Std. Error**	**t**	**P**
y0	0.0149	0.0078	1.9086	0.1290
a	0.0246	0.0017	14.8072	0.0001

APPENDIX D: MEDICAL GRADE BOROSILICATE GLASS SPHERES “GL-0179” DATA SHEET

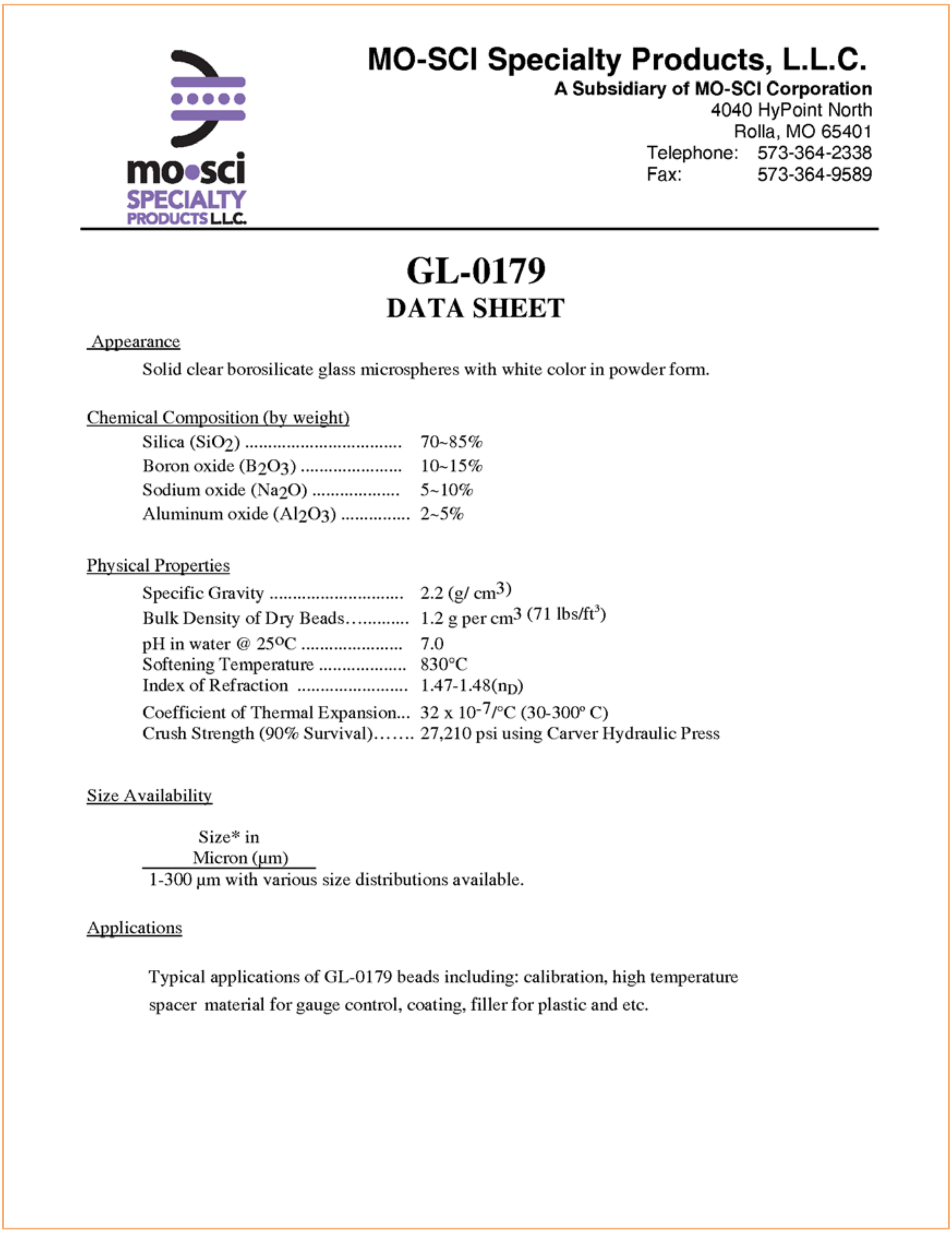

MO-SCI Specialty Products, L.L.C.
A Subsidiary of MO-SCI Corporation
4040 HyPoint North
Rolla, MO 65401
Telephone: 573-364-2338
Fax: 573-364-9589

mo•sci SPECIALTY PRODUCTS L.L.C.

GL-0179
DATA SHEET

Appearance

Solid clear borosilicate glass microspheres with white color in powder form.

Chemical Composition (by weight)

Silica (SiO_2)	70~85%
Boron oxide (B_2O_3)	10~15%
Sodium oxide (Na_2O)	5~10%
Aluminum oxide (Al_2O_3)	2~5%

Physical Properties

Specific Gravity	2.2 (g/ cm^3)
Bulk Density of Dry Beads	1.2 g per cm^3 (71 lbs/ft^3)
pH in water @ 25°C	7.0
Softening Temperature	830°C
Index of Refraction	1.47-1.48(n_D)
Coefficient of Thermal Expansion	32×10^{-7}/°C (30-300° C)
Crush Strength (90% Survival)	27,210 psi using Carver Hydraulic Press

Size Availability

Size* in Micron (µm)
1-300 µm with various size distributions available.

Applications

Typical applications of GL-0179 beads including: calibration, high temperature spacer material for gauge control, coating, filler for plastic and etc.

APPENDIX E: GLASS BEADS SIZE DISTRIBUTION – ANALYSIS REPORT

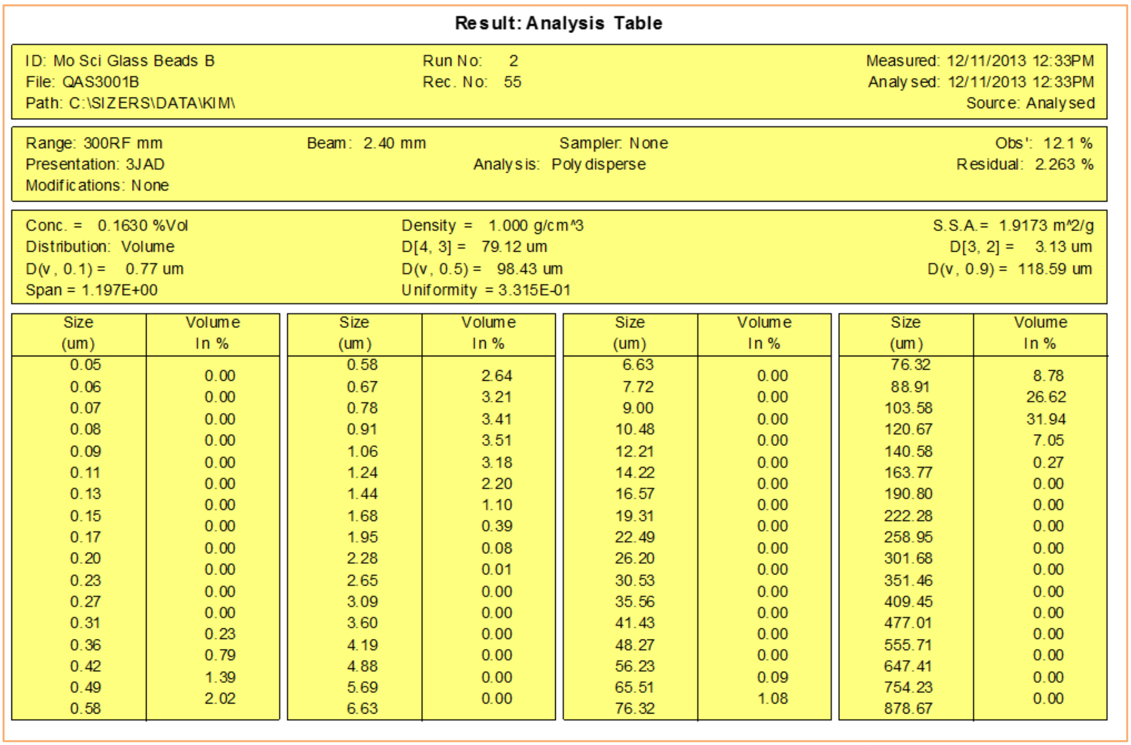

Result: Analysis Table

ID: Mo Sci Glass Beads B
File: QAS3001B
Path: C:\SIZERS\DATA\KIM\
Run No: 2
Rec. No: 55
Measured: 12/11/2013 12:33PM
Analysed: 12/11/2013 12:33PM
Source: Analysed

Range: 300RF mm
Presentation: 3JAD
Modifications: None
Beam: 2.40 mm
Sampler: None
Analysis: Polydisperse
Obs': 12.1 %
Residual: 2.263 %

Conc. = 0.1630 %Vol
Distribution: Volume
D(v, 0.1) = 0.77 um
Span = 1.197E+00
Density = 1.000 g/cm^3
D[4, 3] = 79.12 um
D(v, 0.5) = 98.43 um
Uniformity = 3.315E-01
S.S.A.= 1.9173 m^2/g
D[3, 2] = 3.13 um
D(v, 0.9) = 118.59 um

Size (um)	Volume In %	Size (um)	Volume In %	Size (um)	Volume In %	Size (um)	Volume In %
0.05	0.00	0.58	2.64	6.63	0.00	76.32	8.78
0.06	0.00	0.67	3.21	7.72	0.00	88.91	26.62
0.07	0.00	0.78	3.41	9.00	0.00	103.58	31.94
0.08	0.00	0.91	3.51	10.48	0.00	120.67	7.05
0.09	0.00	1.06	3.18	12.21	0.00	140.58	0.27
0.11	0.00	1.24	2.20	14.22	0.00	163.77	0.00
0.13	0.00	1.44	1.10	16.57	0.00	190.80	0.00
0.15	0.00	1.68	0.39	19.31	0.00	222.28	0.00
0.17	0.00	1.95	0.08	22.49	0.00	258.95	0.00
0.20	0.00	2.28	0.01	26.20	0.00	301.68	0.00
0.23	0.00	2.65	0.00	30.53	0.00	351.46	0.00
0.27	0.00	3.09	0.00	35.56	0.00	409.45	0.00
0.31	0.23	3.60	0.00	41.43	0.00	477.01	0.00
0.36	0.79	4.19	0.00	48.27	0.00	555.71	0.00
0.42	1.39	4.88	0.00	56.23	0.00	647.41	0.00
0.49	2.02	5.69	0.00	65.51	0.09	754.23	0.00
0.58		6.63		76.32	1.08	878.67	0.00

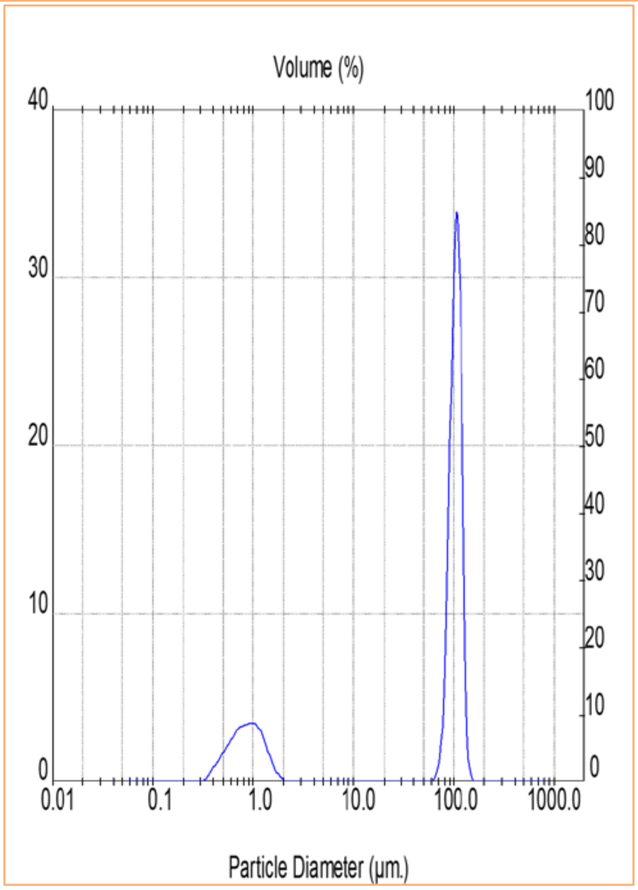

APPENDIX F: CERTIFICATE OF ANALYSIS FOR AVIDIN, EGG WHITE

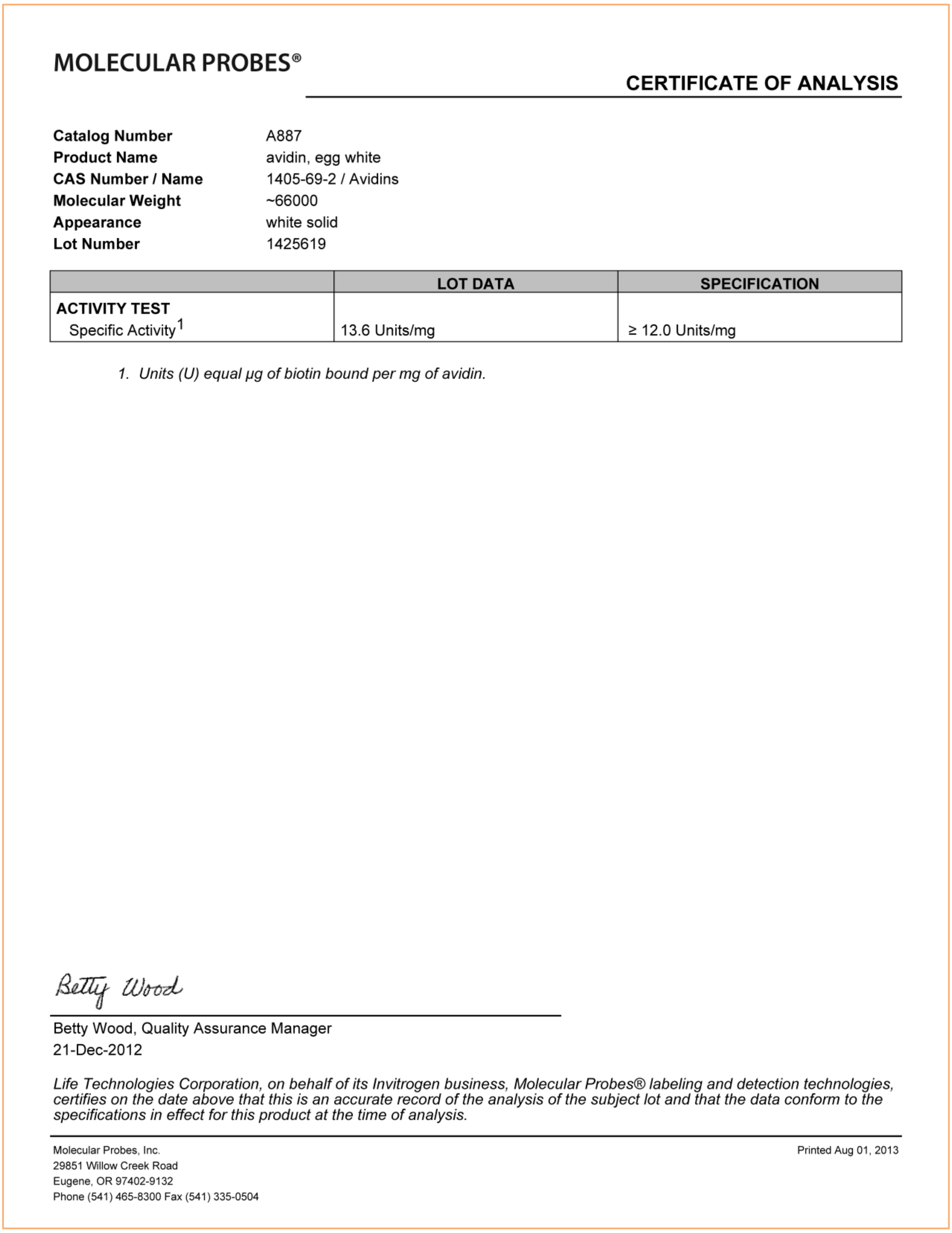

MOLECULAR PROBES®

CERTIFICATE OF ANALYSIS

Catalog Number	A887
Product Name	avidin, egg white
CAS Number / Name	1405-69-2 / Avidins
Molecular Weight	~66000
Appearance	white solid
Lot Number	1425619

	LOT DATA	SPECIFICATION
ACTIVITY TEST Specific Activity[1]	13.6 Units/mg	≥ 12.0 Units/mg

1. *Units (U) equal μg of biotin bound per mg of avidin.*

Betty Wood

Betty Wood, Quality Assurance Manager
21-Dec-2012

Life Technologies Corporation, on behalf of its Invitrogen business, Molecular Probes® labeling and detection technologies, certifies on the date above that this is an accurate record of the analysis of the subject lot and that the data conform to the specifications in effect for this product at the time of analysis.

Molecular Probes, Inc.
29851 Willow Creek Road
Eugene, OR 97402-9132
Phone (541) 465-8300 Fax (541) 335-0504

Printed Aug 01, 2013

APPENDIX G: PUBLICATIONS

Šutar T., Goodyear O., Podgornik A., Thomas O.R.T., Cobbold M. and Theodosiou E. Tailored surfaces for the affinity selection of human cells (poster presentation). *PREP 2015 — 25th International Symposium on Preparative and Process Chromatography*, July 2012, Boston, Massachusetts, USA.

Müller C., **Šutar T**., Thomas O.R.T. and Theodosiou E. Development and critical evaluation of a glass bead based chromatography system for the selection of human cells (poster presentation). *10th European Symposium on Biochemical Engineering Sciences and 6th International Forum on Industrial Bioprocesses in collaboration with ACS*, September 2014, Lille, France.

Müller C., **Šutar T**., Thomas O.R.T. and Theodosiou E. Development of low-cost chromatographic alternatives to magnetic affinity cell sorting (MACS®) (poster presentation). *Scale-up and manufacturing of cell-based therapies IV*, January 2014, San Diego, California, USA

The following two papers are in the preparation and will be submitted to the Journal of Chromatography B:

(i) Development and critical evaluation of tailored glass surfaces for the selection of human cells

(ii) Glass bead chromatography: a low-cost alternative to magnetic affinity cell sorting.